AD-A047 238 ROME AIR DEVELOPMENT CENTER GRIFFISS AFB N Y F/G 20/14
VLF/LF REFLECTIVITY OF THE POLAR IONOSPHERE, 2 JANUARY-30 APRIL--ETC(U)
JUL 77 J E RASMUSSEN, J P TURTLE
UNCLASSIFIED RADC-TR-77-251 NL

1 OF 1
ADA047 238

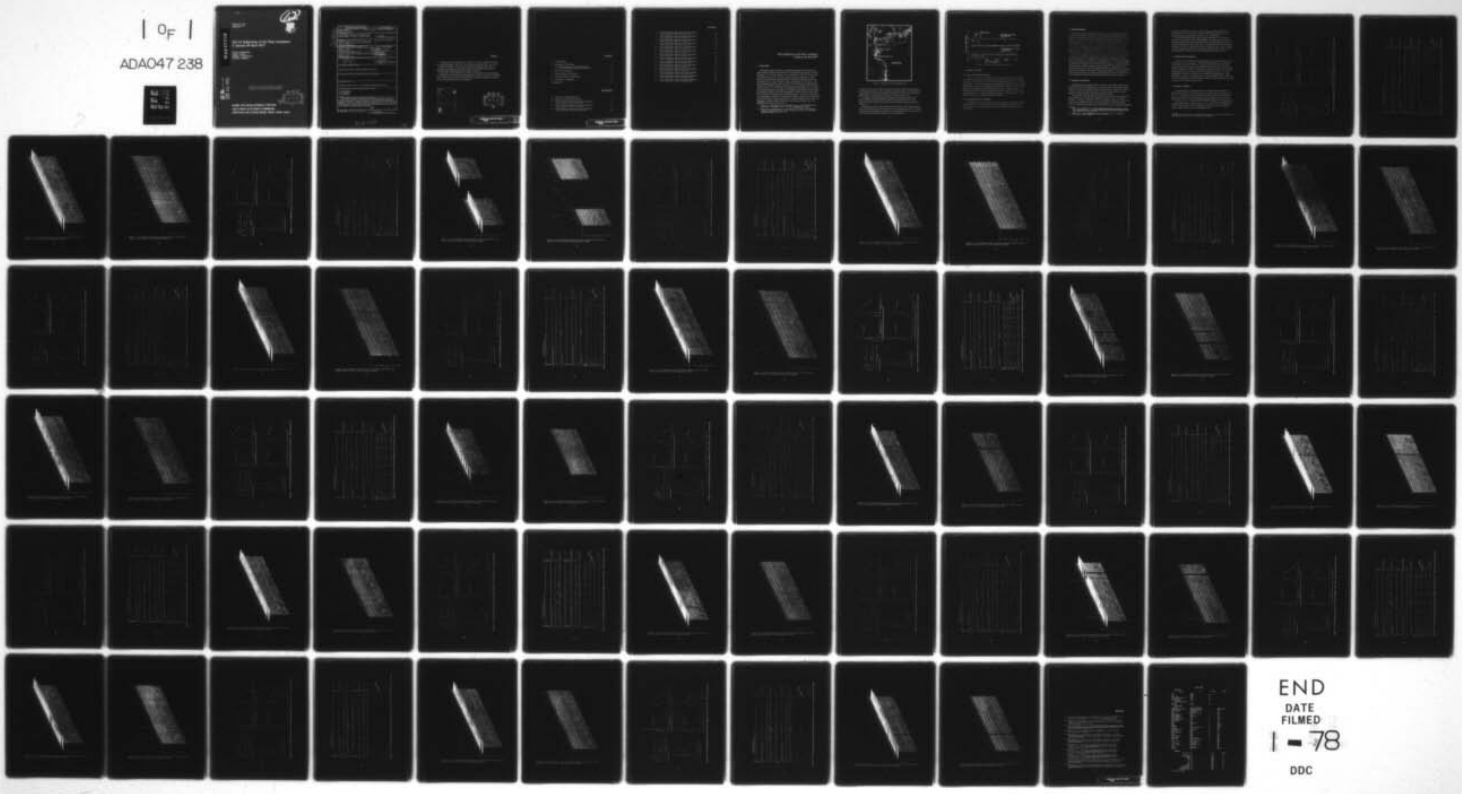

END
DATE FILMED
1-78
DDC

RADC-TR-77-251
IN-HOUSE REPORT
JULY 1977

VLF/LF Reflectivity of the Polar Ionosphere 2 January-30 April 1977

JOHN E. RASMUSSEN
JOHN P. TURTLE
ROBERT P. PAGLIARULO
WAYNE I. KLEMETTI

ROME AIR DEVELOPMENT CENTER
AIR FORCE SYSTEMS COMMAND
GRIFFISS AIR FORCE BASE, NEW YORK 13441

SECURITY CLASSIFICATION OF THIS PAGE (When Data Entered)

REPORT DOCUMENTATION PAGE

READ INSTRUCTIONS BEFORE COMPLETING FORM

(14) 1. REPORT NUMBER: RADC-TR-77-251

2. GOVT ACCESSION NO.

3. RECIPIENT'S CATALOG NUMBER

(6) 4. TITLE (and Subtitle): VLF/LF REFLECTIVITY OF THE POLAR IONOSPHERE, 2 January – 30 April 1977

5. TYPE OF REPORT & PERIOD COVERED: In-House

6. PERFORMING ORG. REPORT NUMBER

(10) 7. AUTHOR(s): John E. Rasmussen, Wayne I. Klemetti*, John P. Turtle, Robert P. Pagliarulo

8. CONTRACT OR GRANT NUMBER(s)

9. PERFORMING ORGANIZATION NAME AND ADDRESS: Deputy for Electronic Technology (RADC/ETEE), Hanscom AFB, Massachusetts 01731

10. PROGRAM ELEMENT, PROJECT, TASK AREA & WORK UNIT NUMBERS: 62702F, 46001605 (16) (17) 16

11. CONTROLLING OFFICE NAME AND ADDRESS: Deputy for Electronic Technology (RADC/ETEE), Hanscom AFB, Massachusetts 01731

12. REPORT DATE: (11) July 1977

13. NUMBER OF PAGES: 81

14. MONITORING AGENCY NAME & ADDRESS (if different from Controlling Office): (12) 81p.

15. SECURITY CLASS. (of this report): Unclassified

15a. DECLASSIFICATION/DOWNGRADING SCHEDULE

16. DISTRIBUTION STATEMENT (of this Report)

Approved for public release; distribution unlimited.

17. DISTRIBUTION STATEMENT (of the abstract entered in Block 20, if different from Report)

18. SUPPLEMENTARY NOTES

*Barkley & Dexter Labs., Inc., Fitchburg, Massachusetts 01420

19. KEY WORDS (Continue on reverse side if necessary and identify by block number)

VLF propagation
LF propagation
Low ionosphere

20. ABSTRACT (Continue on reverse side if necessary and identify by block number)

This report provides a summary of high latitude ionospheric reflectivity as observed by the USAF high resolution VLF/LF ionosounder operating in northern Greenland. Ionospheric reflectivity parameters, including reflection heights and coefficients, are presented as a function of time of day. VLF long path propagation measurements, along with magnetometer and riometer data, are presented as supplementary information.

DD FORM 1 JAN 73 1473 EDITION OF 1 NOV 65 IS OBSOLETE

Unclassified

SECURITY CLASSIFICATION OF THIS PAGE (When Data Entered)

309 050

LB

Preface

The authors thank in particular Dr. Edward A. Lewis for valuable discussions on preparing this paper, Sgt. Gary L. Schroeder for data preparation, Mr. Royce C. Kahler of Barkley & Dexter Labs for help with the equipment that made the measurements possible, and Mr. Bjarne Ebbesen of the Danish Meteorological Institute for the outstanding operation at Qanaq, Greenland.

Appreciation is also extended to the Danish Commission for Scientific Research in Greenland for allowing these measurements to be conducted and to Jorgen Taagholt and V. Neble Jensen of the Danish Meteorological Institute's Ionospheric Laboratory for their continued cooperation in this program.

Contents

Illustrations

VLF/LF Reflectivity of the Polar Ionosphere 2 January—30 April 1977

1. INTRODUCTION

This paper provides a summary of high latitude ionospheric reflectivity, as observed by the USAF's high resolution VLF/LF ionosounder operating in northern Greenland.[1,2] As shown in Figure 1, the transmitter is located at Thule Air Base, Greenland (76° 33'N. Lat., 68° 40'W. Long.), and the receiving site is 106 km north at the Danish Meteorological Institute's Ionospheric Observatory in Qanaq, Greenland (77° 24'N. Lat., 69° 20'W. Long., Geomagnetic Lat. 89° 06'N.). The ionosounding transmissions consist of a series of extremely short (approximately 100 μ sec) VLF pulses, precisely controlled in time, and radiated from a 130 meter vertical antenna. At the receiving site, orthogonal loop antennas are used to separate the two polarization components of the ionospherically reflected skywave signal. One antenna, oriented in the plane of propagation, is used to sense the groundwave and the "parallel" component of the downcoming skywave. The second loop, nulled on the groundwave, senses the "perpendicular" skywave component. The signal from each of the antennas is digitally averaged to improve the signal-to-noise ratio of the individual received waveforms before they are recorded on magnetic tape. An

(Received for publication 28 July 1977)

1. Lewis, E.A., Rasmussen, J.E., and Kossey, P.A. (1973) Measurements of ionospheric reflectivity from 6 to 35 kHz, J. Geophys. Res. 78:19.

2. Kossey, P.A., Rasmussen, J.E., and Lewis, E.A. (1974) VLF pulse ionosounder measurements of the reflection properties of the lower ionosphere, Akademie Verlaq, COSPAR, July.

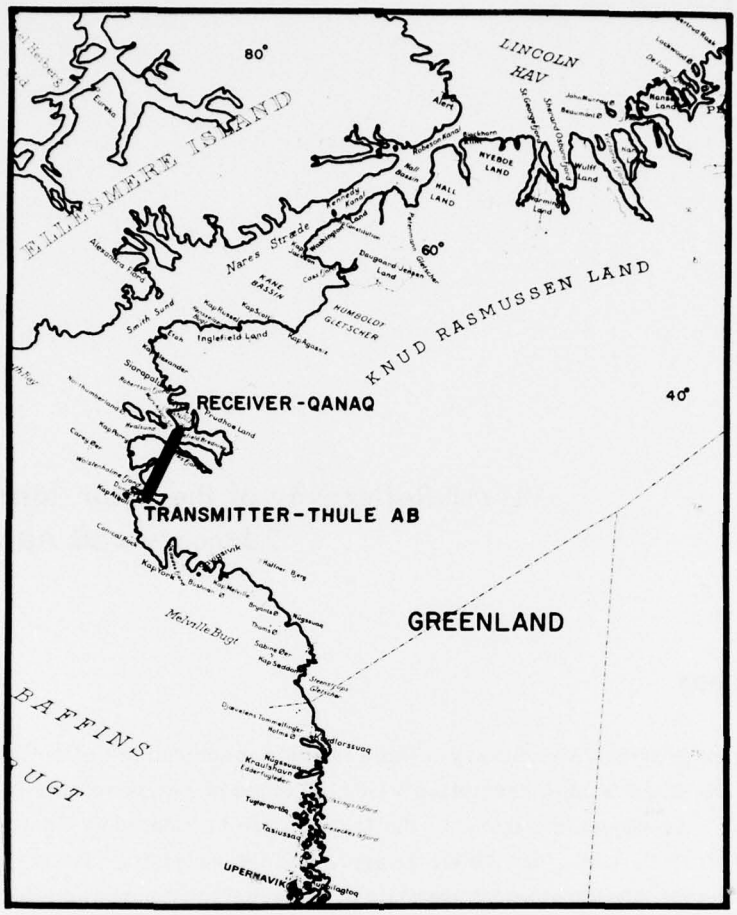

Figure 1. Geometry of the Propagation Path

example of the observed waveforms is given in Figure 2, where the parallel waveform (Figure 2a) consists of (1) a groundwave propagated pulse, (2) a quiet interval containing low level, off path groundwave reflections, followed by (3) the first-hop skywave signal. The perpendicular waveform is shown in Figure 2b.

Ionospheric reflection parameters are derived by computer (AFGL's CDC 6600) processing of the ground and ionospherically reflected waveforms with allowance made for factors such as ground conductivity and antenna patterns (see Section 4).

Although the data are recorded about once per minute, for this paper the waveforms are averaged into two-hour time blocks with the exception of the three-dimensional waveform presentations (Section 2.2). The resulting information is presented in a weekly format (Figures 3 through 19) as described below.

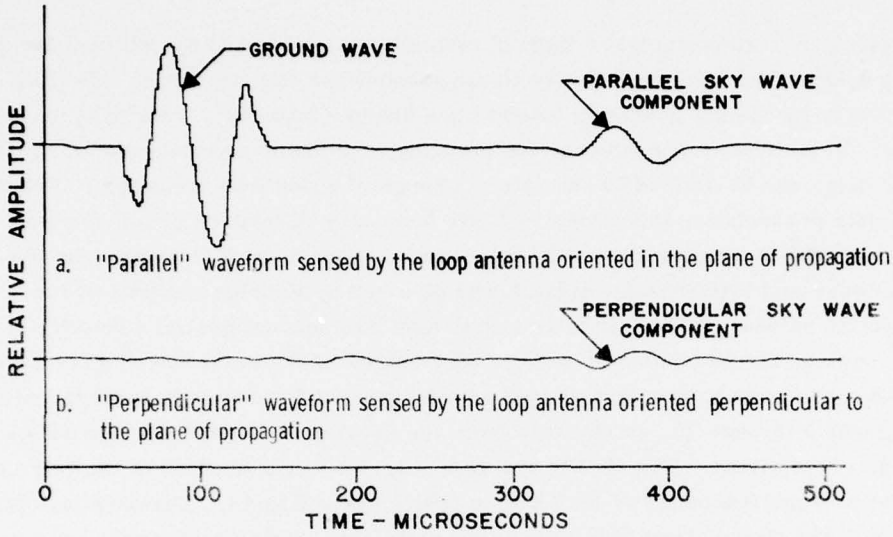

Figure 2. Example of the Observed Waveforms

2. OBSERVED WAVEFORMS

2.1 Weekly Example of Individual Waveforms

In part A of Figures 3 through 19 a set of averaged parallel and perpendicular waveforms is presented for the time block centered near local noon of the indicated day. Each of these waveforms is comprised of 256 digitally averaged points spaced 2 μsec apart. In part B of the figures, the groundwave Fourier amplitudes are shown as a function of frequency. Although the data presented in parts C through L of the figures are generally limited to frequencies in the first, or principal, lobe of the spectrum, information at higher frequencies can be used when sufficient signal-to-noise conditions exist. There is, however, a frequency range around each spectral null where insufficient signal exists for measurements.

2.2 Three-Dimensional Waveform Presentation

A three-dimensional display of the recorded $\parallel$ waveforms covering each weekly period is shown in Part R of each figure and the corresponding $\perp$ waveforms are shown in Part S. For these plots the data has been averaged into fifteen minute time blocks.

3. REFLECTION HEIGHTS

The group mirror height (GMH) of reflection was obtained by determining the group delay of the skywave relative to the groundwave and attributing this time difference, by simple geometry (assuming a sharply bounded mirror-like ionosphere) to a difference in propagation distance. As discussed in Lewis et al,[1] the group delay can be defined as the rate of change of phase with frequency. For the GMH data presented in this paper, a finite frequency difference of 1.0 kHz was used, and the corresponding phase difference as a function of frequency for the groundwave and both skywave signals was obtained by Fourier analysis of the respective pulses. The GMH calculations took into account ground conductivity (10^{-3} mho/meter is assumed), and the corrections of Wait and Howe[3] were applied.

Group mirror heights are plotted as a function of frequency in parts C and D of Figures 3 through 19, as obtained from the parallel and perpendicular waveforms, respectively. The GMH's are also presented as a function of time-of-day for the average frequency of 16.5 kHz in figure parts E and I. The parallel GMH's in part E are shown along with an average reflection height for reference purposes. Each point of the reference height is a weekly average, by time block, for the 7-day period indicated. The corresponding perpendicular GMH's, part I of the figures, are also shown with the weekly average for comparison. Part G gives the average, by time block, for the daily parallel GMH data of part E, and part K gives the corresponding perpendicular GMH averages from the daily data of part I.

4. REFLECTION COEFFICIENTS

Assuming that the ionosphere acts as a "mirror" at the GMH, plane wave reflection coefficients[4] were obtained by comparing the ratio of the skywave Fourier amplitude at a specific frequency to that of the groundwave, taking into account the antenna patterns, wave spreading, earth curvature, ground conductivity, path lengths, and antenna patterns including ground image effects.

The reflection coefficient $_{||}R_{||}$ was obtained from analysis of the parallel skywave component and is plotted as a function of frequency in part C of Figures 3 through 19. The $_{||}R_{||}$ coefficient for 16 kHz is plotted as a function of time-of-day in part F along with the average of the indicated week for reference purposes. From the perpendicular skywave pulse, the coefficient $_{||}R_{\perp}$ was obtained and appears

3. Wait, J.R., and Howe, H.H. (1956) Amplitude and Phase Curves for Ground-Wave Propagation in the Band 200 Cycles per Second to 500 Kilocycles, Nat. Bur. Stand. U.S. Circ. No. 574.

4. Budden, K.G. (1961) Radio Waves in the Ionosphere, p. 85, Cambridge University Press, London.

as a function of frequency in part D. The 16 kHz $\|R_\perp$ is shown along with its reference in part J. Parts H and L present the average, by time block, of the daily $\|R_\|$ and $\|R_\perp$ data presented in parts F and J, respectively.

For certain coefficient data points, plotted as asterisks (*), the reflection coefficient appears without a corresponding GMH. For these particular data, only the skywave-groundwave ratios could be obtained as the skywaves were too weak to provide reliable group delay information. The reflection coefficients were therefore estimated using a nominal GMH of 80 km in the calculations. These estimated coefficient values are included in the averages presented in parts H and L, but the assumed heights are not used in the GMH averages shown in parts G and K.

5. SUPPLEMENTARY INFORMATION

For purposes of comparison and interpretation, certain supplementary data are presented in Figures 3 through 19. Part M of the figures shows the magnitude of the horizontal component of the polar magnetic field observed with a three-axis fluxgate magnetometer, and part N presents 30-MHz riometer data, an indicator of D-region particle precipitation. Figure parts P and Q give the received VLF phase and amplitude from the 18.6 kHz station NLK (transmitter location: Jim Creek, Washington), as observed at Thule AB over a 3900-km propagation path. These supplementary data were recorded at 30-sec intervals by RADC/ETEE at Thule AB; the curves represent the average of 10-min periods. The solar zenith angle is given in part O for the indicated mid-week date.

6. ADDITIONAL COMMENTS

It is noted that the transmitter power was occasionally unstable during the period between day 93 and day 103 as indicated in parts R and S of Figures 17 and 18. As the ionospheric reflection height and reflection coefficient calculations are based on comparisons between the groundwave and skywaves, which are equally influenced by the power variation, these data remain unaffected through this period.

This report is one of a series.[5, 6, 7, 8, 9, 10, 11] Comments and suggestions for improving its usefulness should be addressed to the VLF/ULF Techniques Branch (ETEE), Electromagnetic Sciences Division, Deputy for Electronic Technology (RADC/ETEE), Hanscom AFB, Massachusetts 01731.

(Because of the large number of references cited above, they will not be listed here. See Reference Page No. 81, for References 5 through 11.

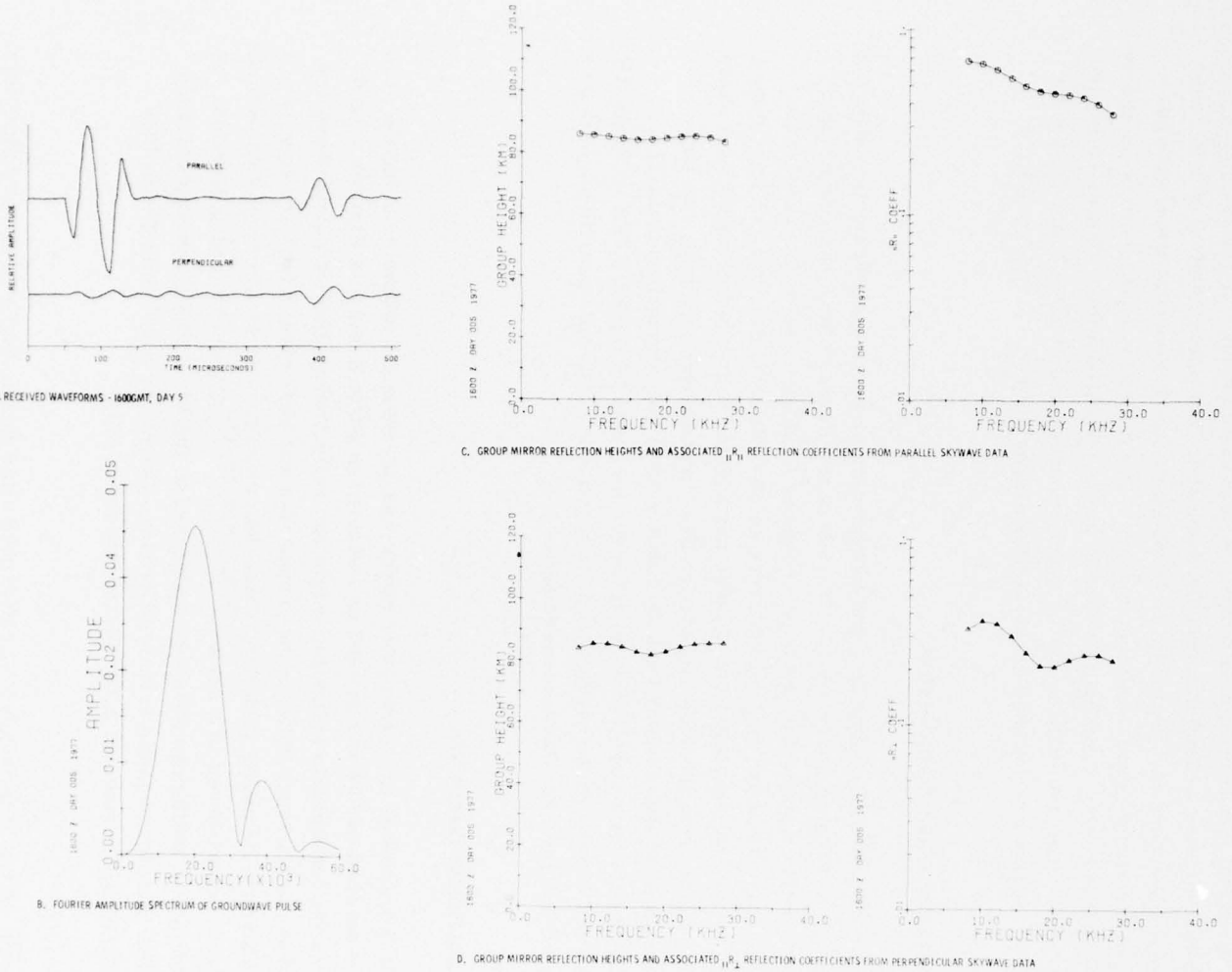

Figure 3. VLF/LF Reflectivity Data for the Polar Ionosphere, DAY 2 (2 Jan) – DAY 8 (8 Jan) 1977

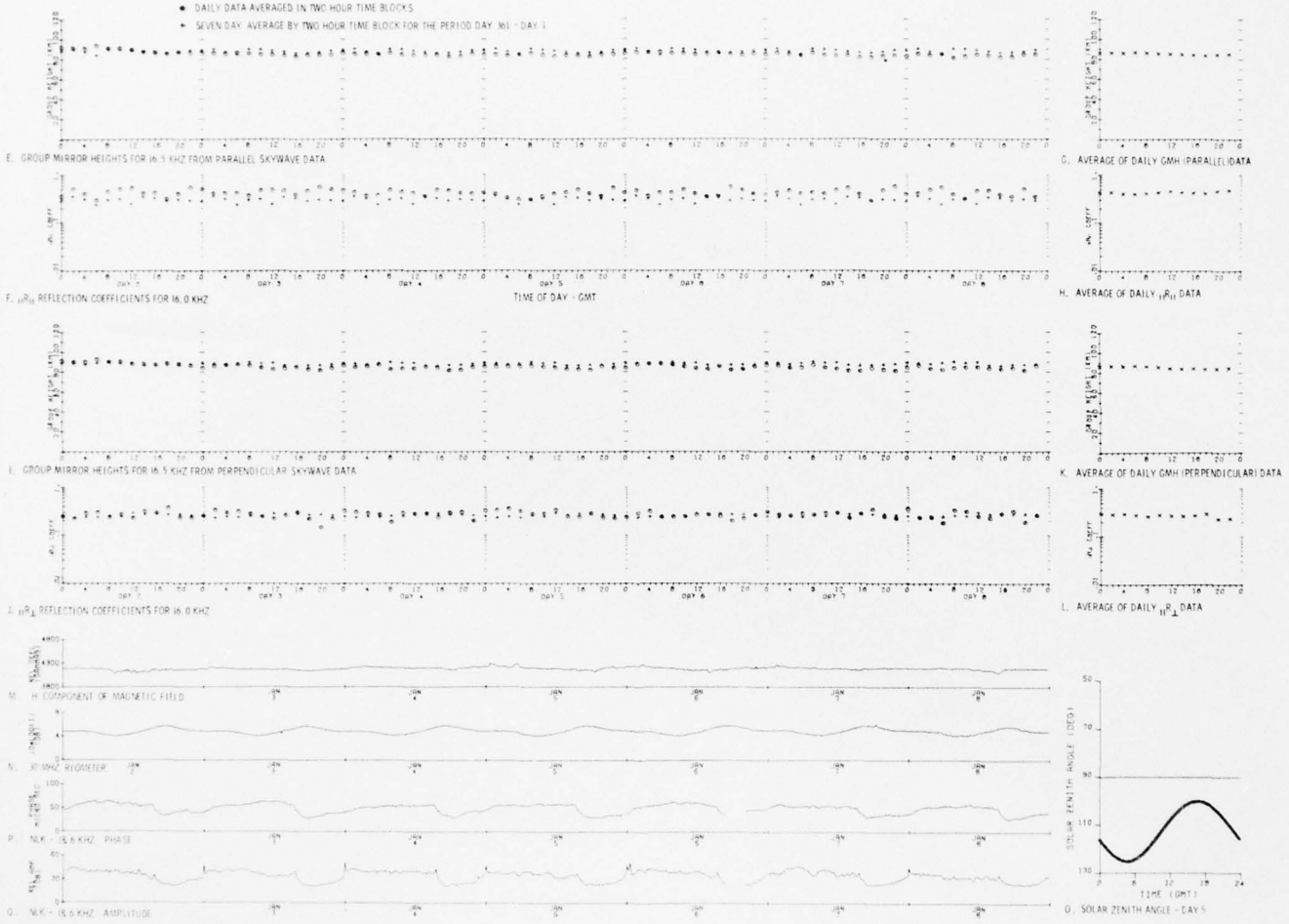

Figure 3. VLF/LF Reflectivity Data for the Polar Ionosphere, DAY 2 (2 Jan) – DAY 8 (8 Jan) 1977 (Cont)

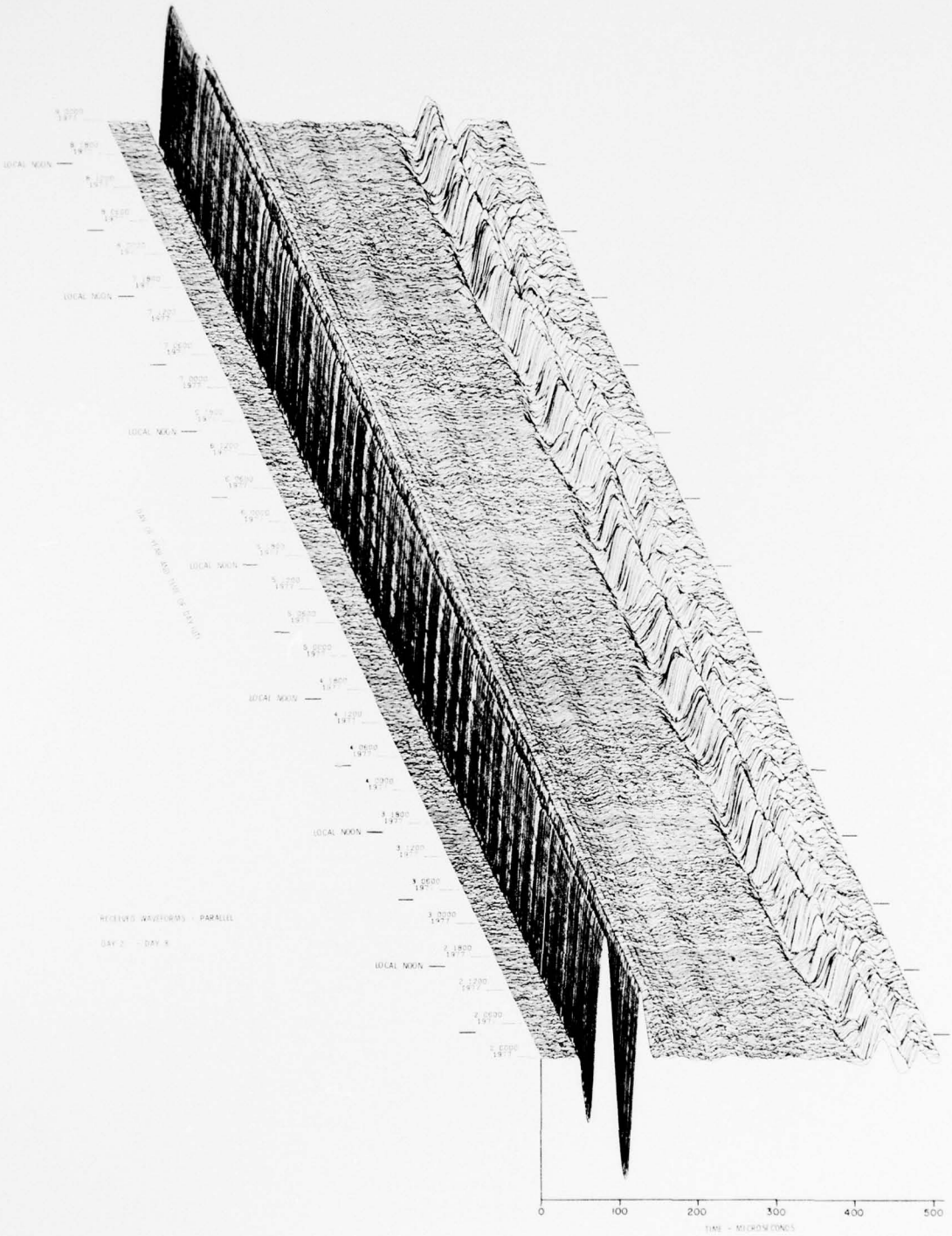

Figure 3. VLF/LF Reflectivity Data for the Polar Ionosphere, DAY 2 (2 Jan) — DAY 8 (8 Jan) 1977 (Cont). Part R, ||Waveform Display

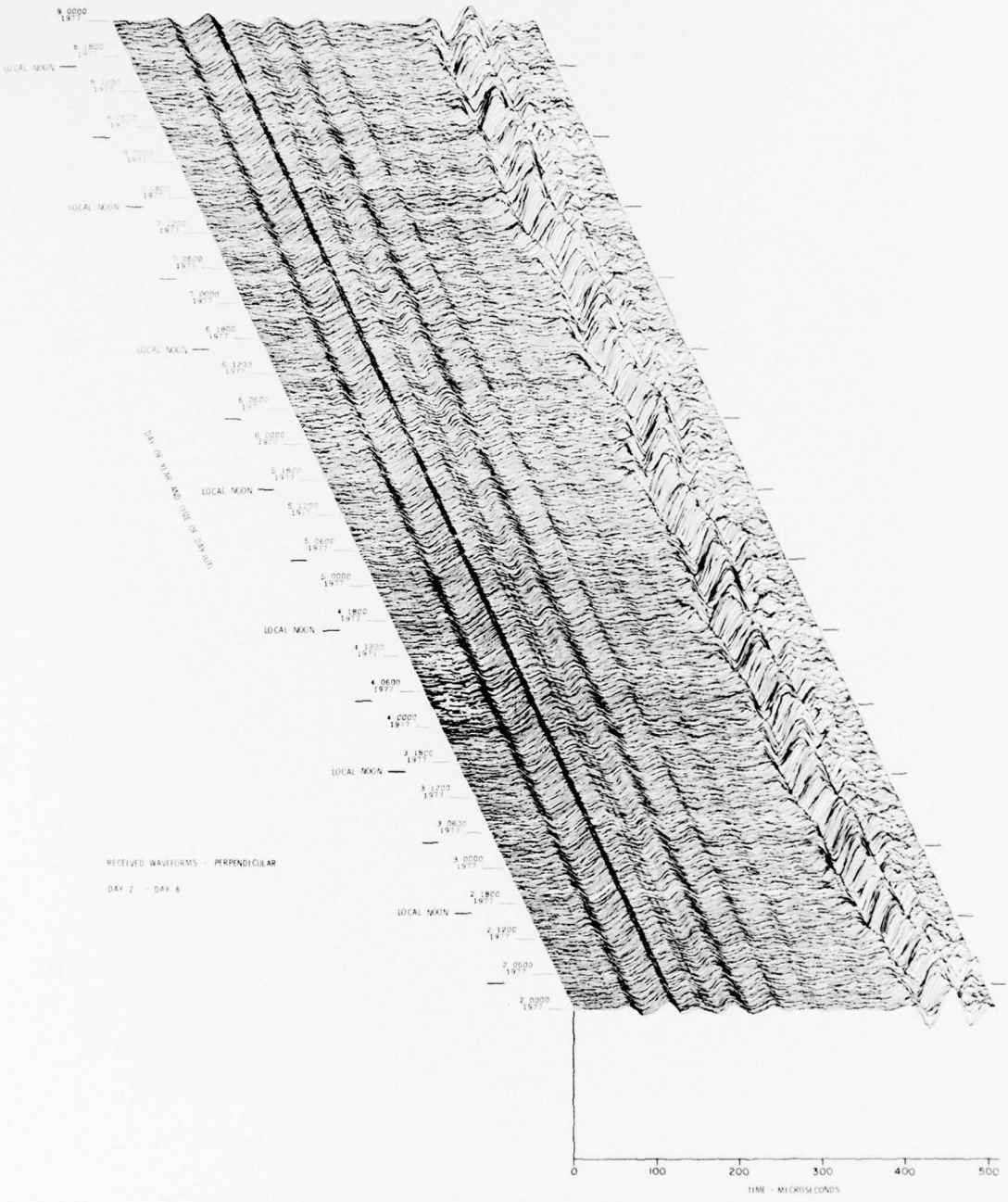

Figure 3. VLF/LF Reflectivity Data for the Polar Ionosphere, DAY 2 (2 Jan) – DAY 8 (8 Jan) 1977 (Cont). Part S, ⊥ Waveform Display

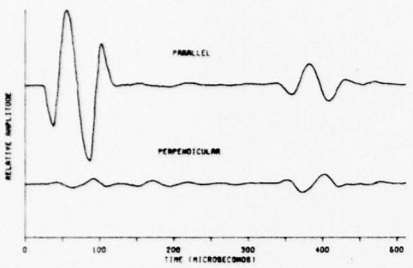

A. RECEIVED WAVEFORMS - 1600GMT, DAY 14

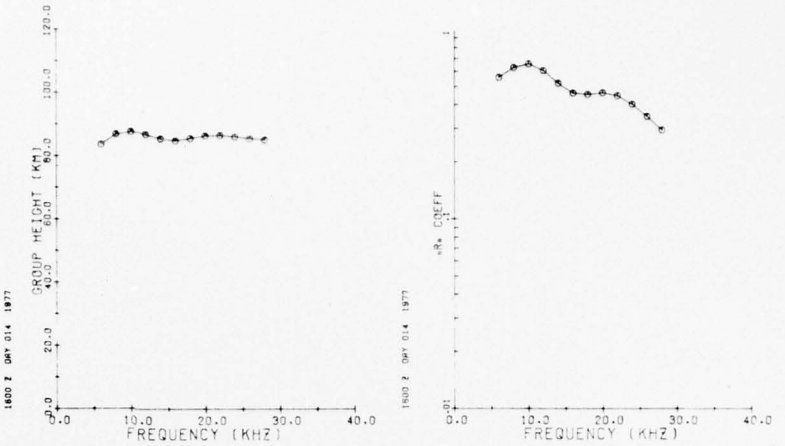

C. GROUP MIRROR REFLECTION HEIGHTS AND ASSOCIATED $_{\parallel}R_{\parallel}$ REFLECTION COEFFICIENTS FROM PARALLEL SKYWAVE DATA

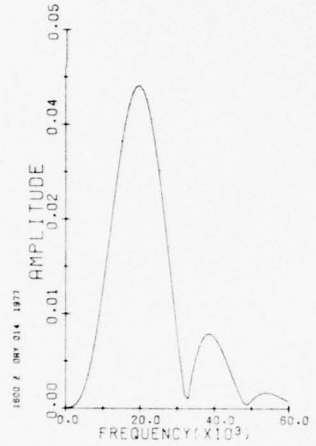

B. FOURIER AMPLITUDE SPECTRUM OF GROUNDWAVE PULSE

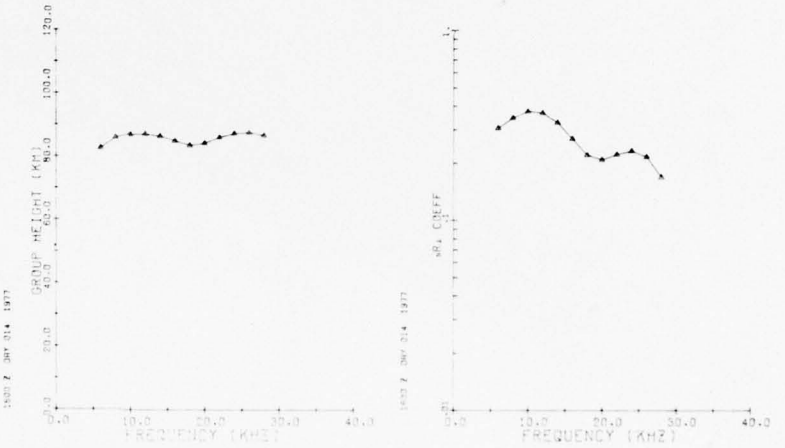

D. GROUP MIRROR REFLECTION HEIGHTS AND ASSOCIATED $_{\perp}R_{\perp}$ REFLECTION COEFFICIENTS FROM PERPENDICULAR SKYWAVE DATA

Figure 4. VLF/LF Reflectivity Data for the Polar Ionosphere, DAY 9 (9 Jan) – DAY 15 (15 Jan) 1977

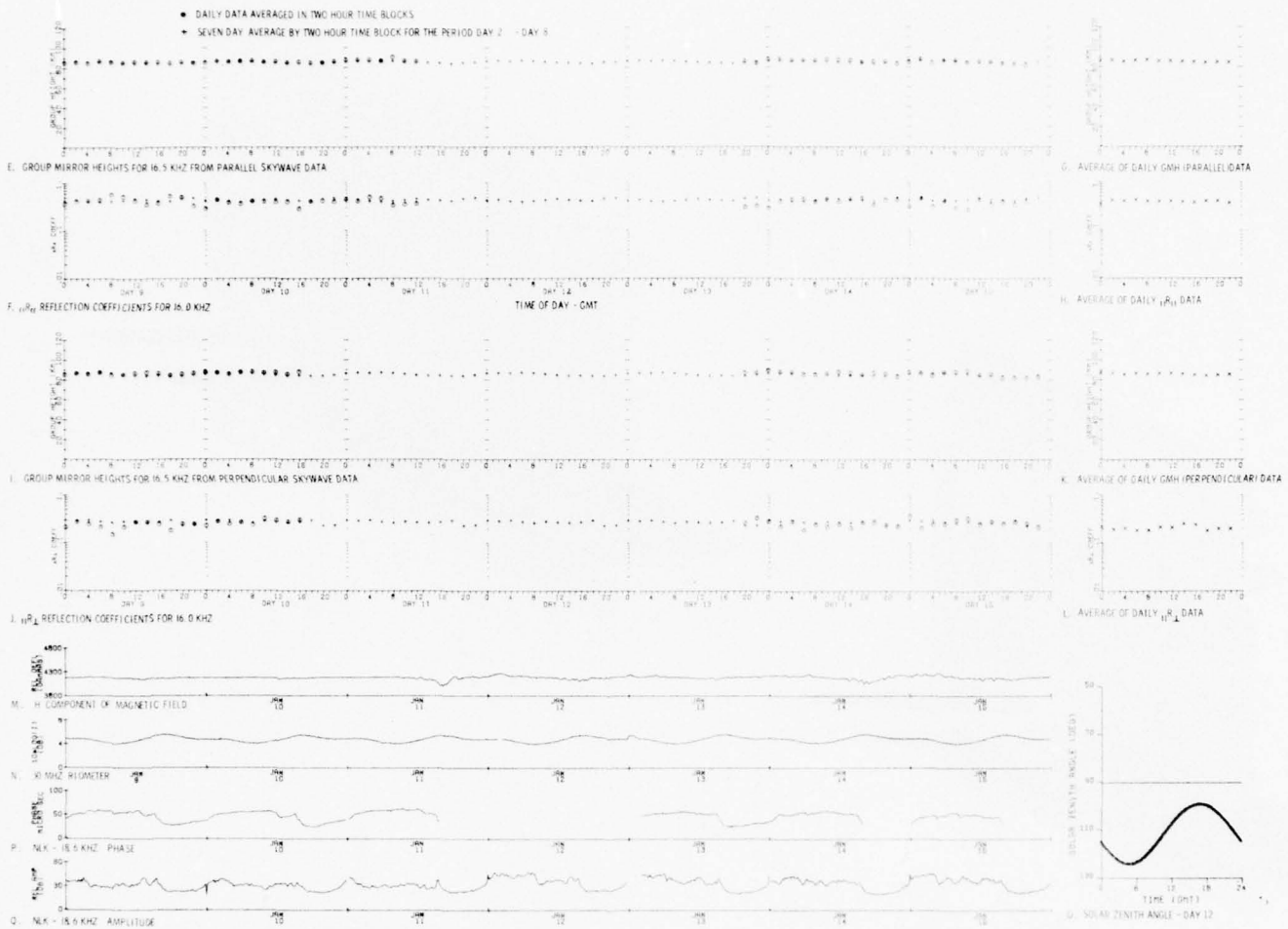

Figure 4. VLF/LF Reflectivity Data for the Polar Ionosphere, DAY 9 (9 Jan) – DAY 15 (15 Jan) 1977 (Cont)

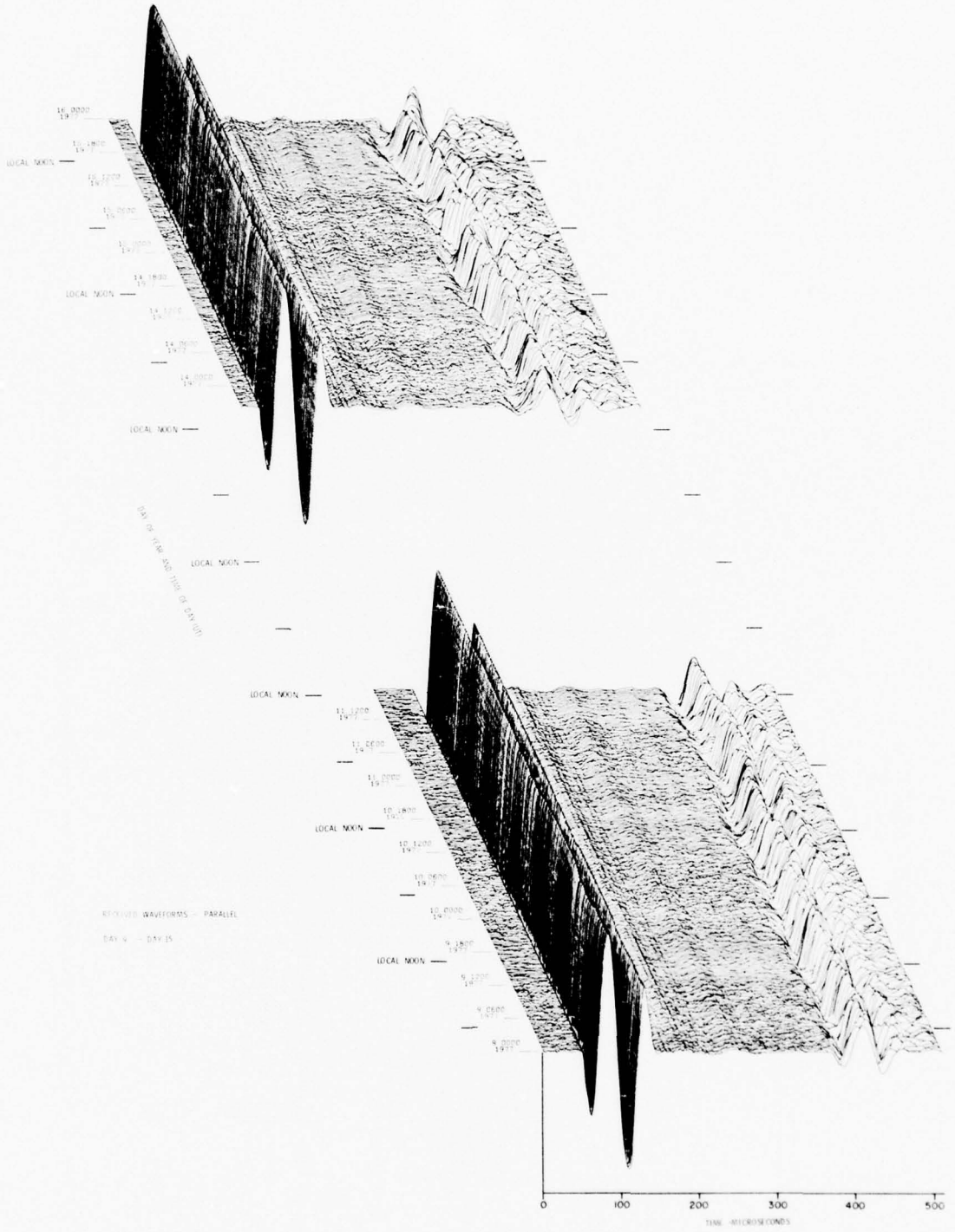

Figure 4. VLF/LF Reflectivity Data for the Polar Ionosphere, DAY 9 (9 Jan) — DAY 15 (15 Jan) 1977 (Cont). Part R, ||Waveform Display

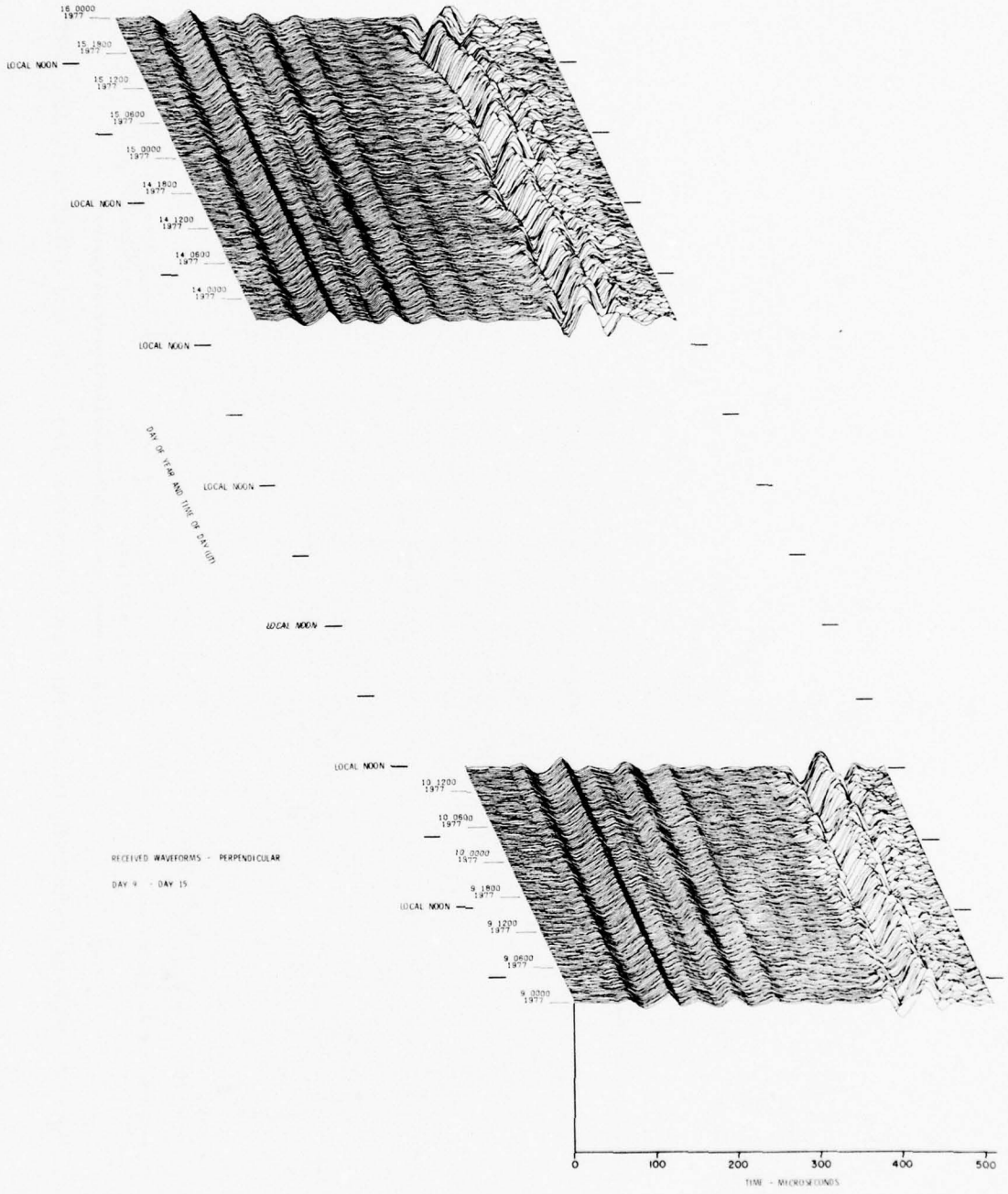

Figure 4. VLF/LF Reflectivity Data for the Polar Ionosphere, DAY 9 (9 Jan) – DAY 15 (15 Jan) 1977 (Cont). Part S, ⊥Waveform Display

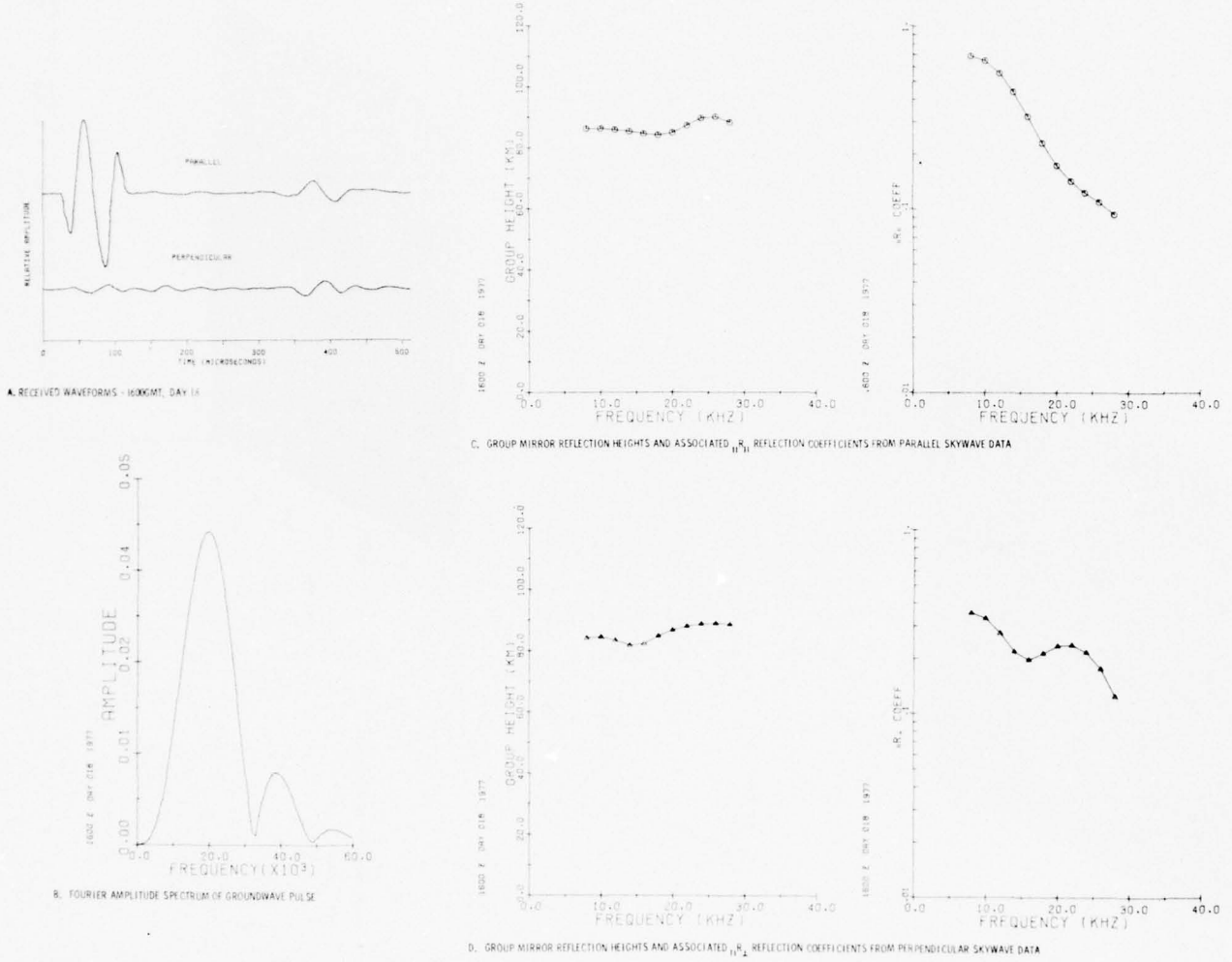

Figure 5. VLF/LF Reflectivity Data for the Polar Ionosphere, DAY 16 (16 Jan) -- DAY 22 (22 Jan) 1977

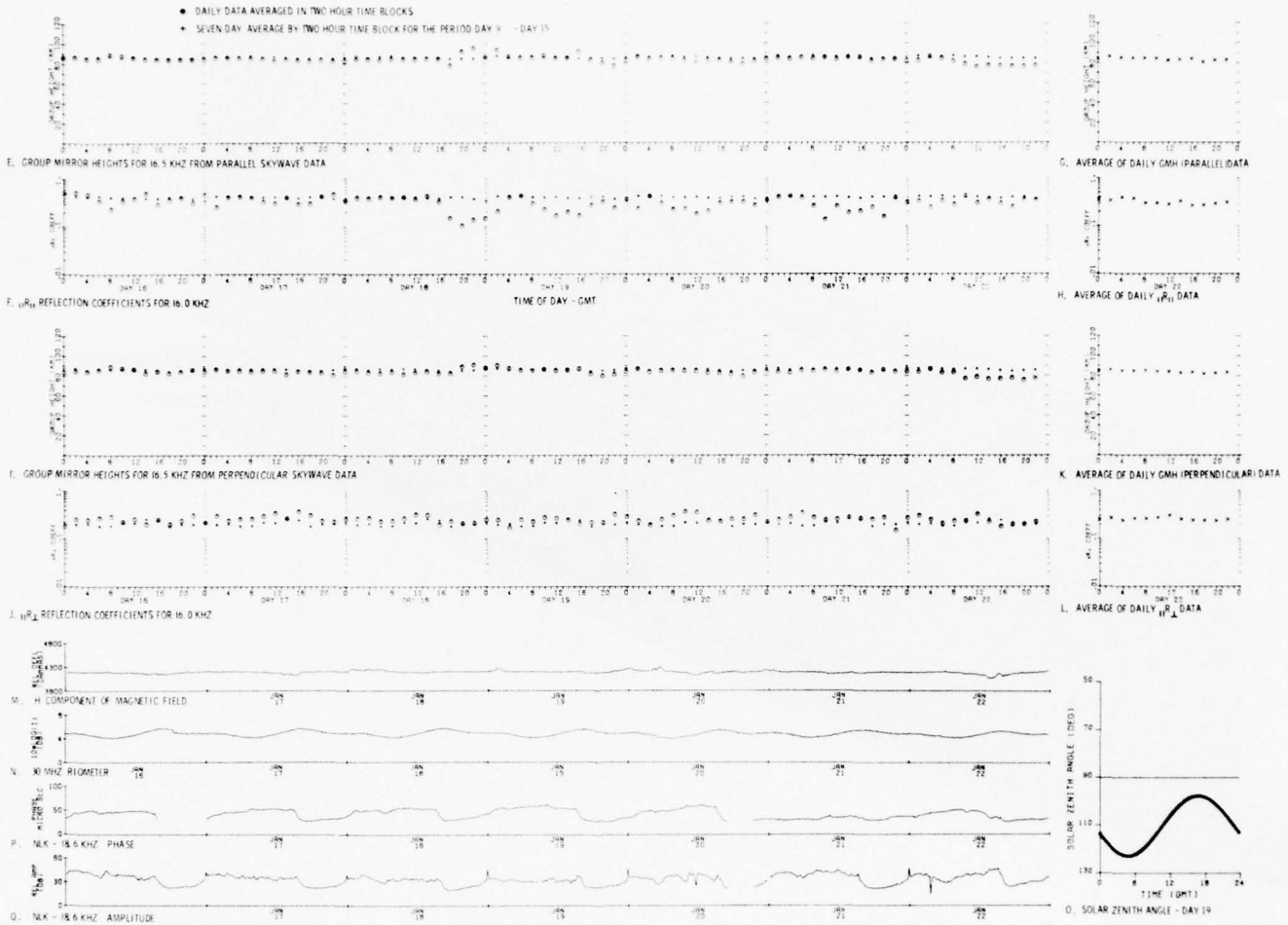

Figure 5. VLF/LF Reflectivity Data for the Polar Ionosphere, DAY 16 (16 Jan) – DAY 22 (22 Jan) 1977 (Cont)

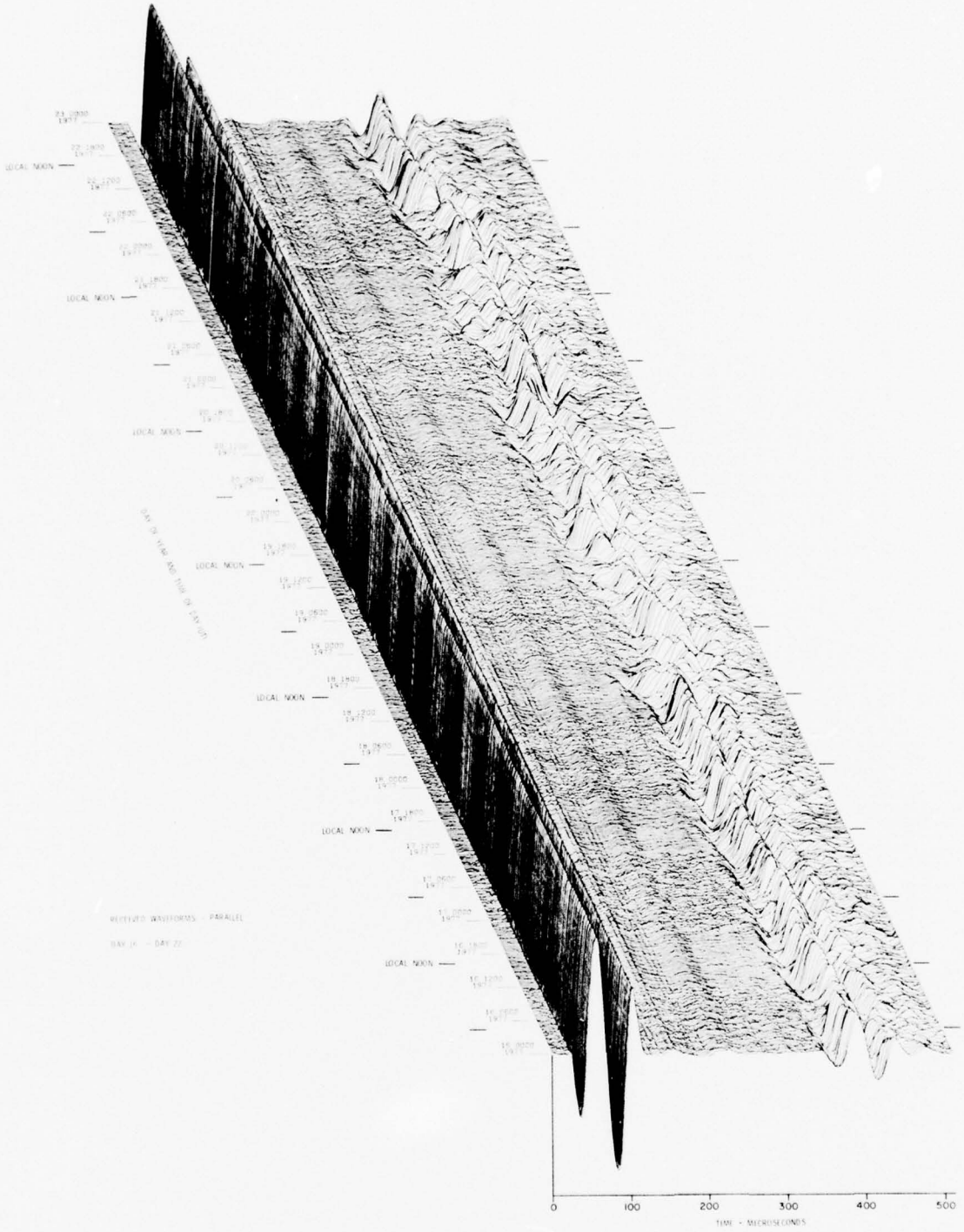

Figure 5. VLF/LF Reflectivity Data for the Polar Ionosphere, DAY 16 (16 Jan) – DAY 22 (22 Jan) 1977 (Cont). Part R, ‖Waveform Display

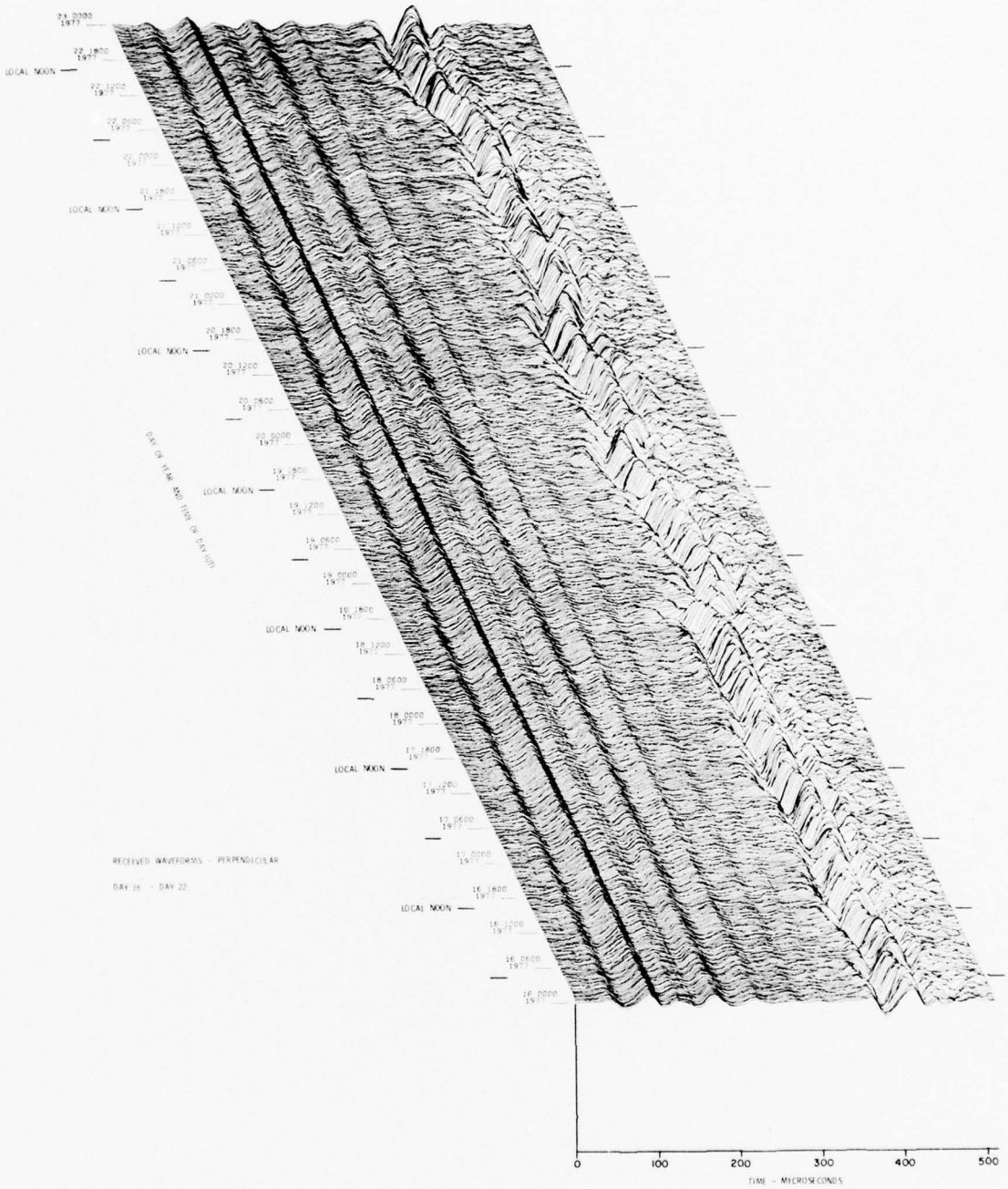

Figure 5. VLF/LF Reflectivity Data for the Polar Ionosphere, DAY 16 (16 Jan) — DAY 22 (22 Jan) 1977 (Cont). Part S, ⊥Waveform Display

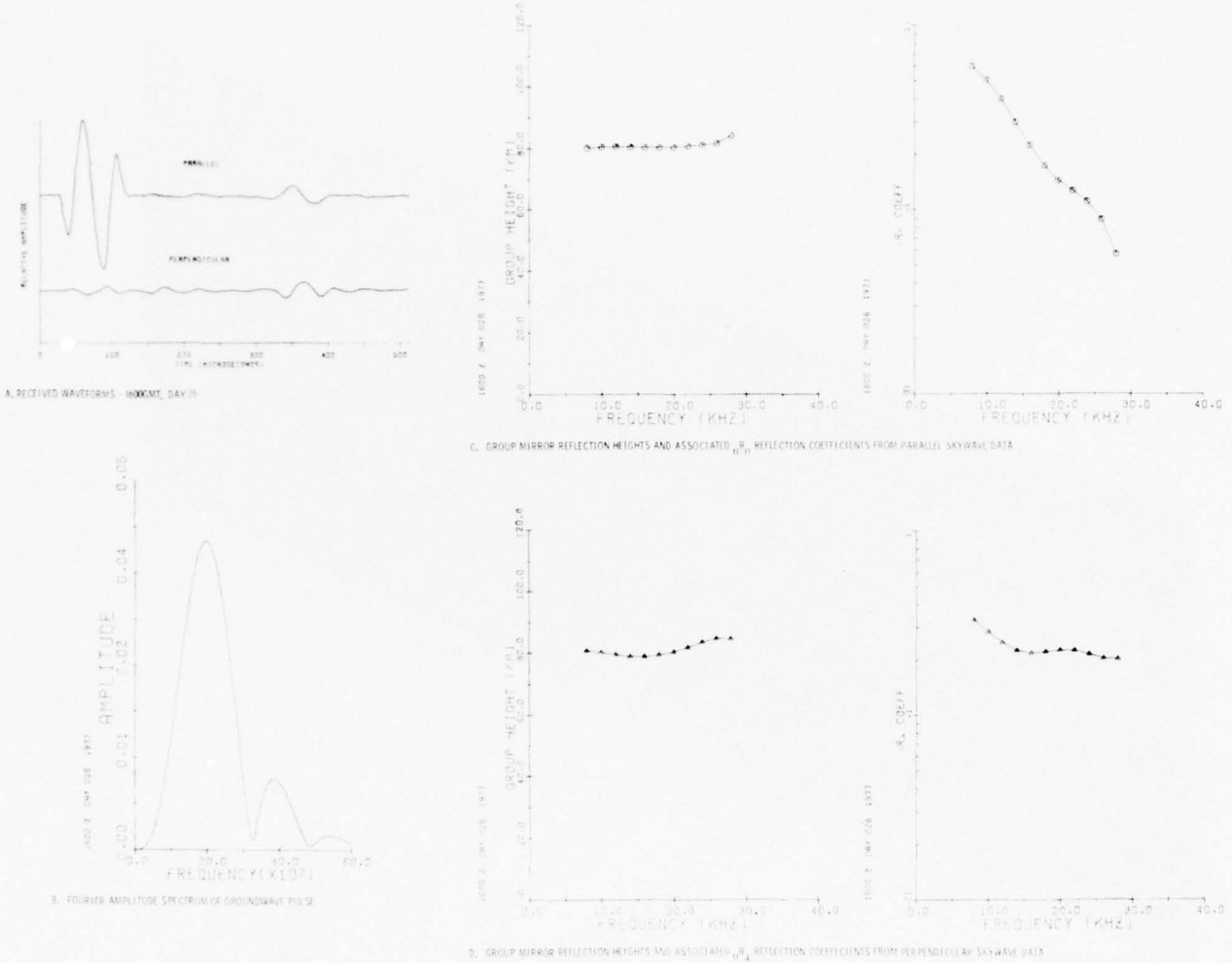

Figure 6. VLF/LF Reflectivity Data for the Polar Ionosphere, DAY 23 (23 Jan) -- DAY 29 (29 Jan) 1977

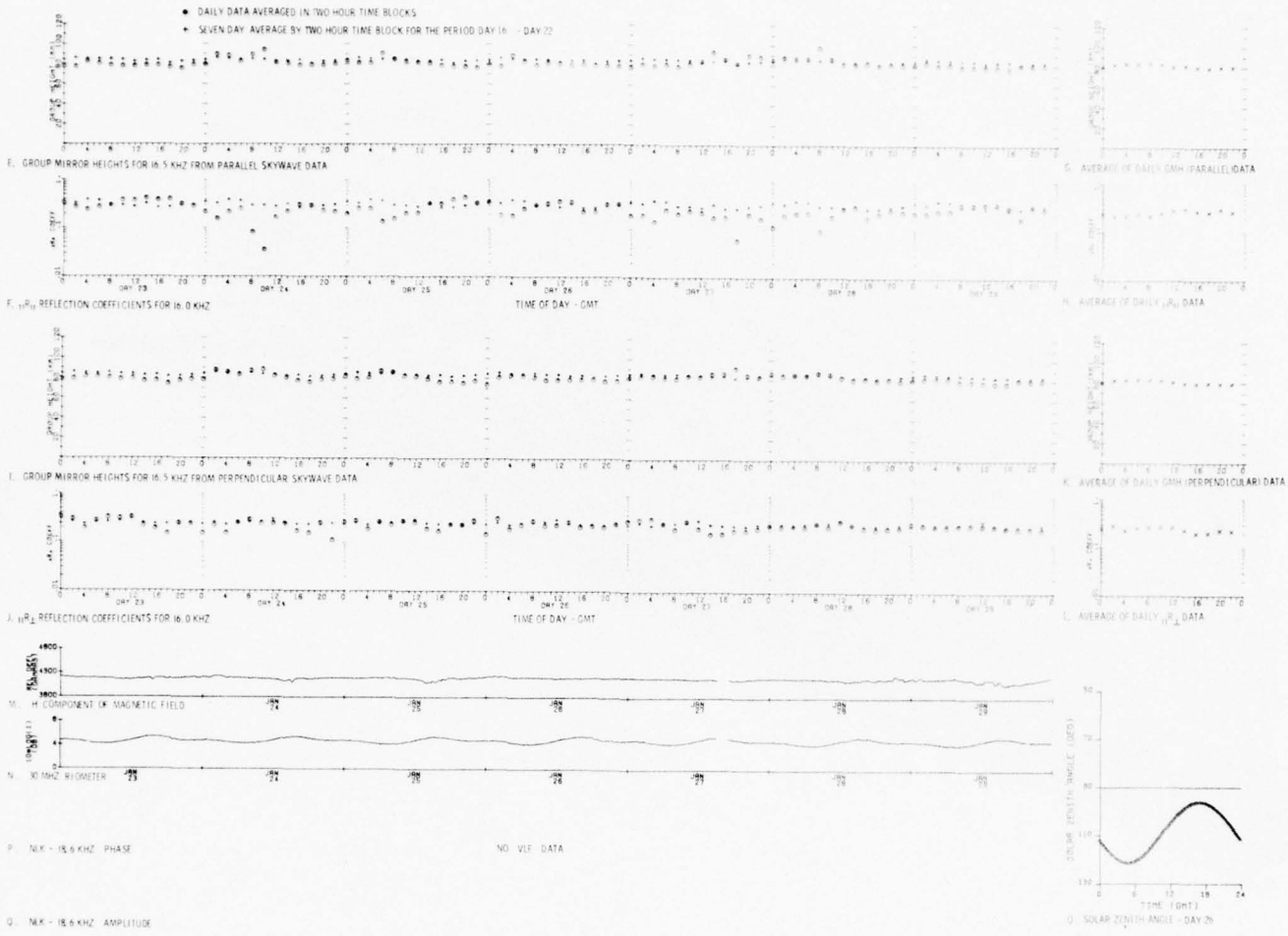

Figure 6. VLF/LF Reflectivity Data for the Polar Ionosphere, DAY 23 (23 Jan) — DAY 29 (29 Jan) 1977 (Cont)

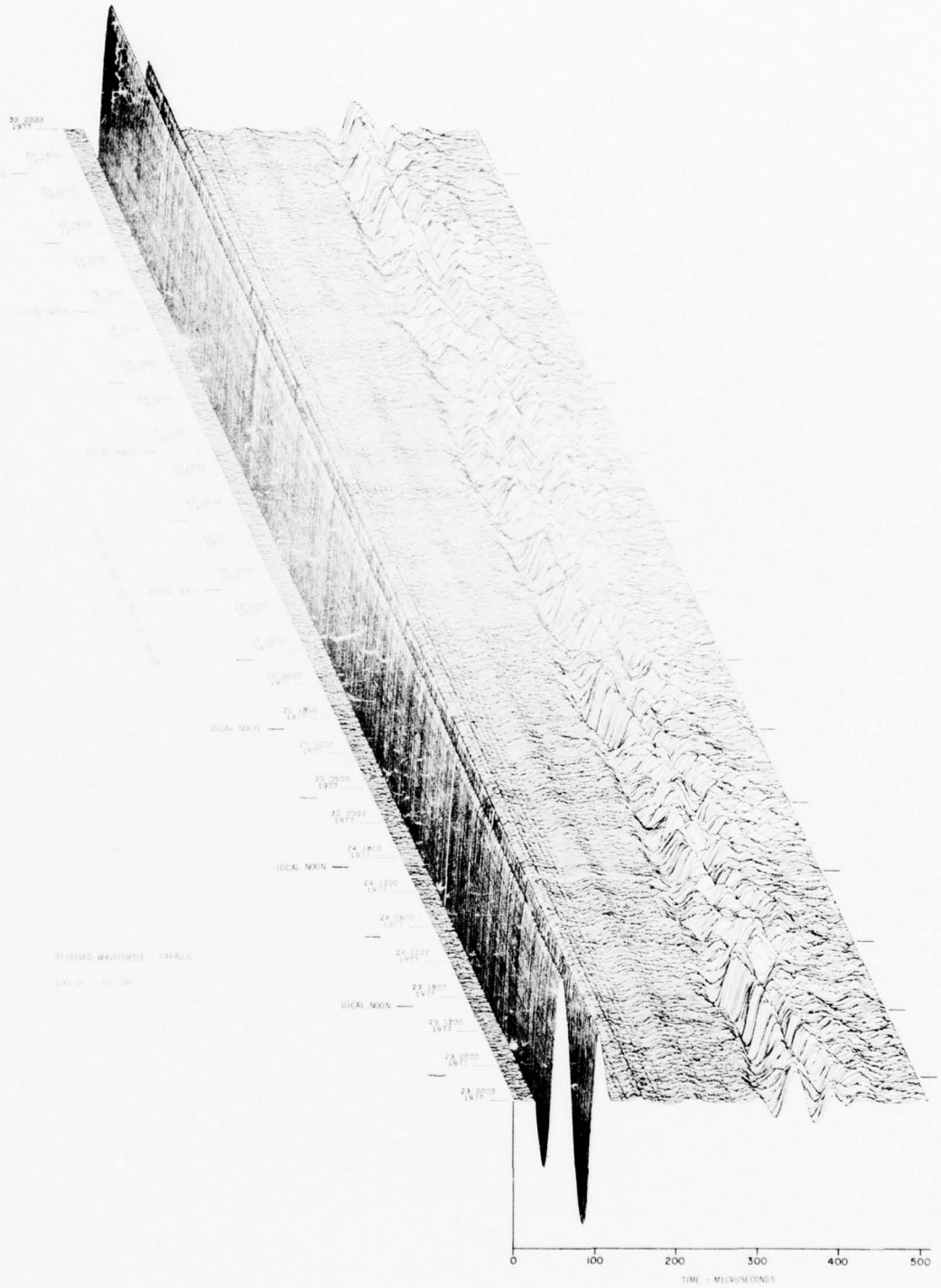

Figure 6. VLF/LF Reflectivity Data for the Polar Ionosphere, DAY 23 (23 Jan) — DAY 29 (29 Jan) 1977 (Cont). Part R, ||Waveform Display

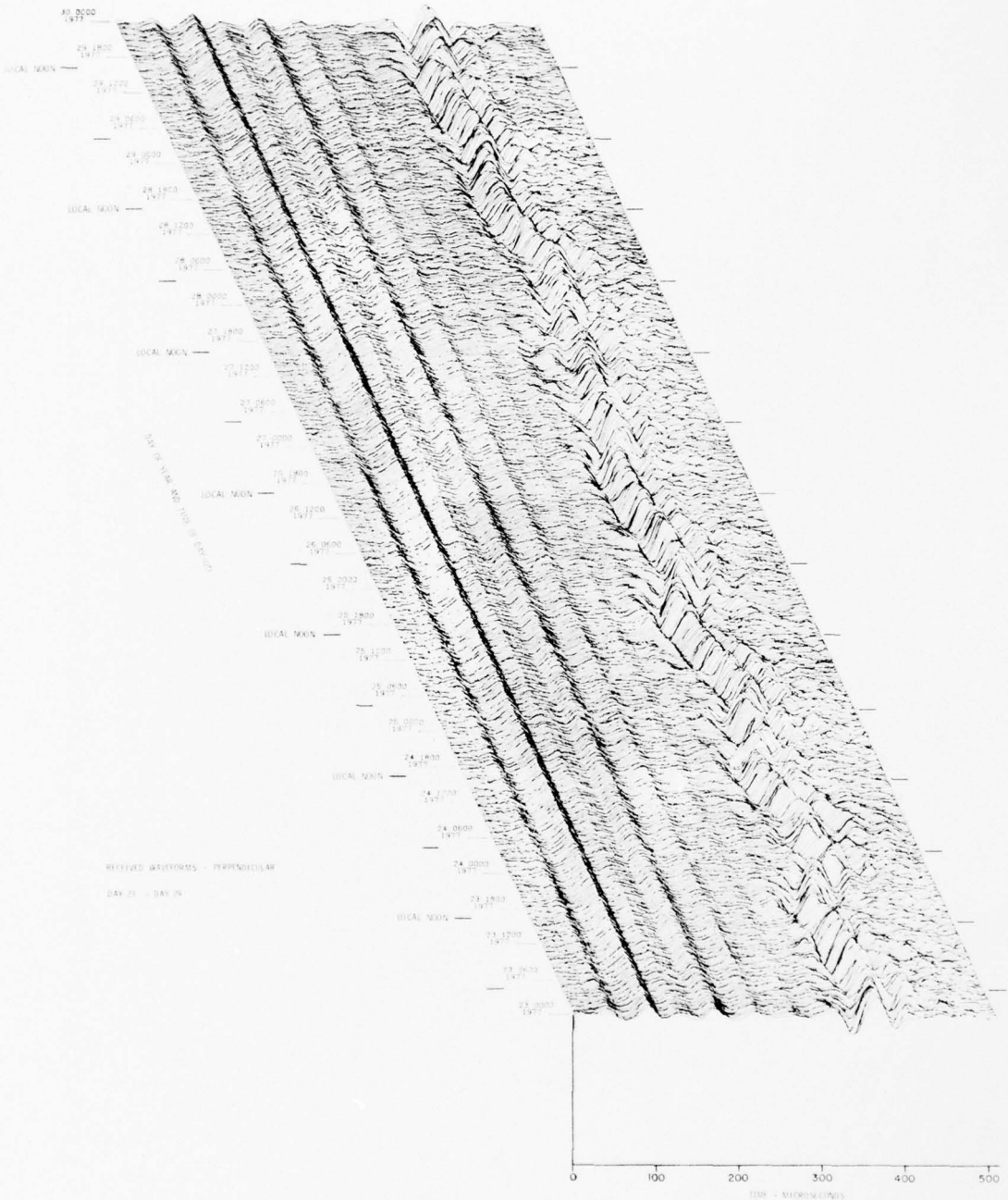

Figure 6. VLF/LF Reflectivity Data for the Polar Ionosphere, DAY 23 (23 Jan) – DAY 29 (29 Jan) 1977 (Cont). Part S, ⊥Waveform Display

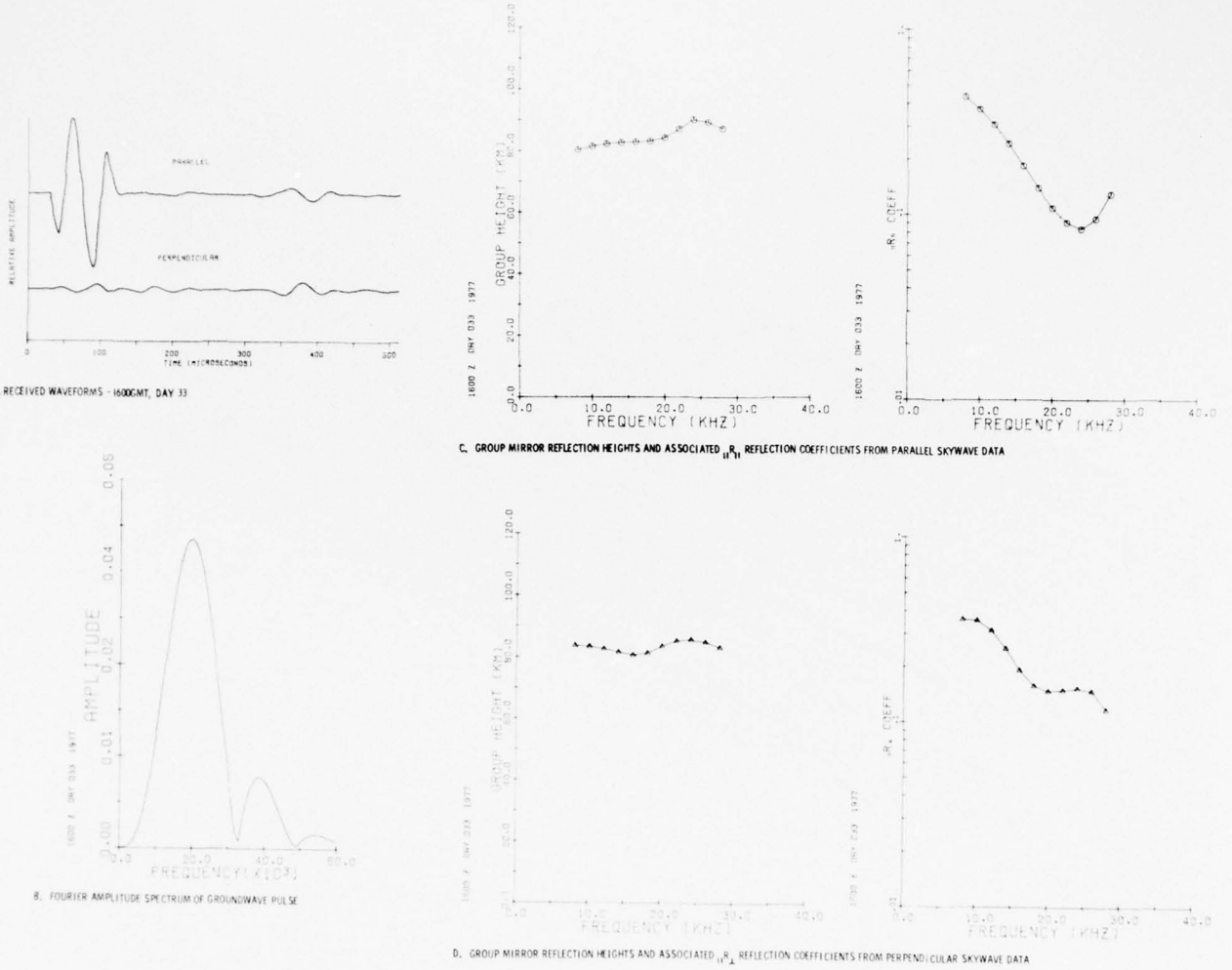

Figure 7. VLF/LF Reflectivity Data for the Polar Ionosphere, DAY 30 (30 Jan) – DAY 36 (5 Feb) 1977

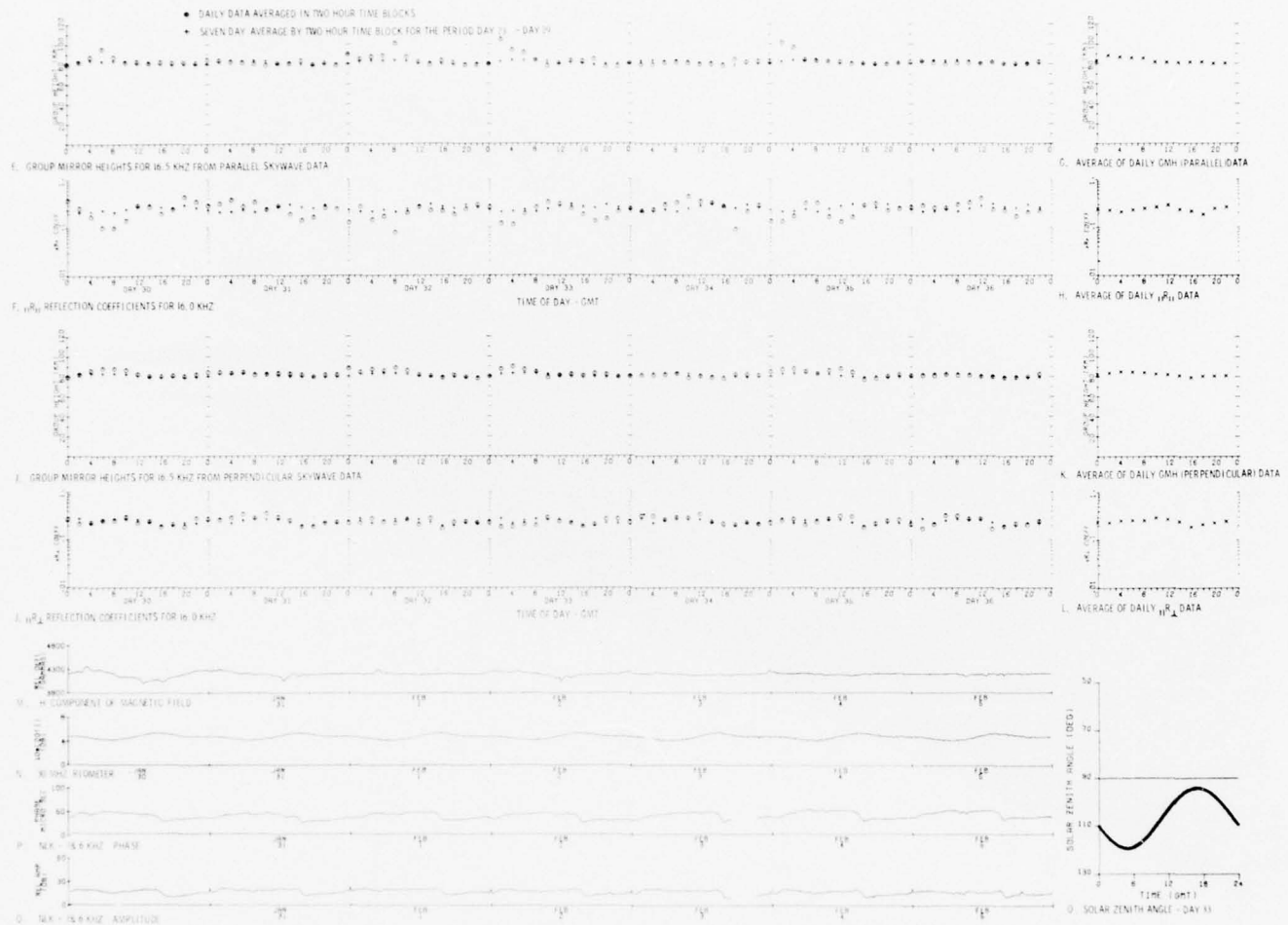

Figure 7. VLF/LF Reflectivity Data for the Polar Ionosphere, DAY 39 (30 Jan) -- DAY 36 (5 Feb) 1977 (Cont)

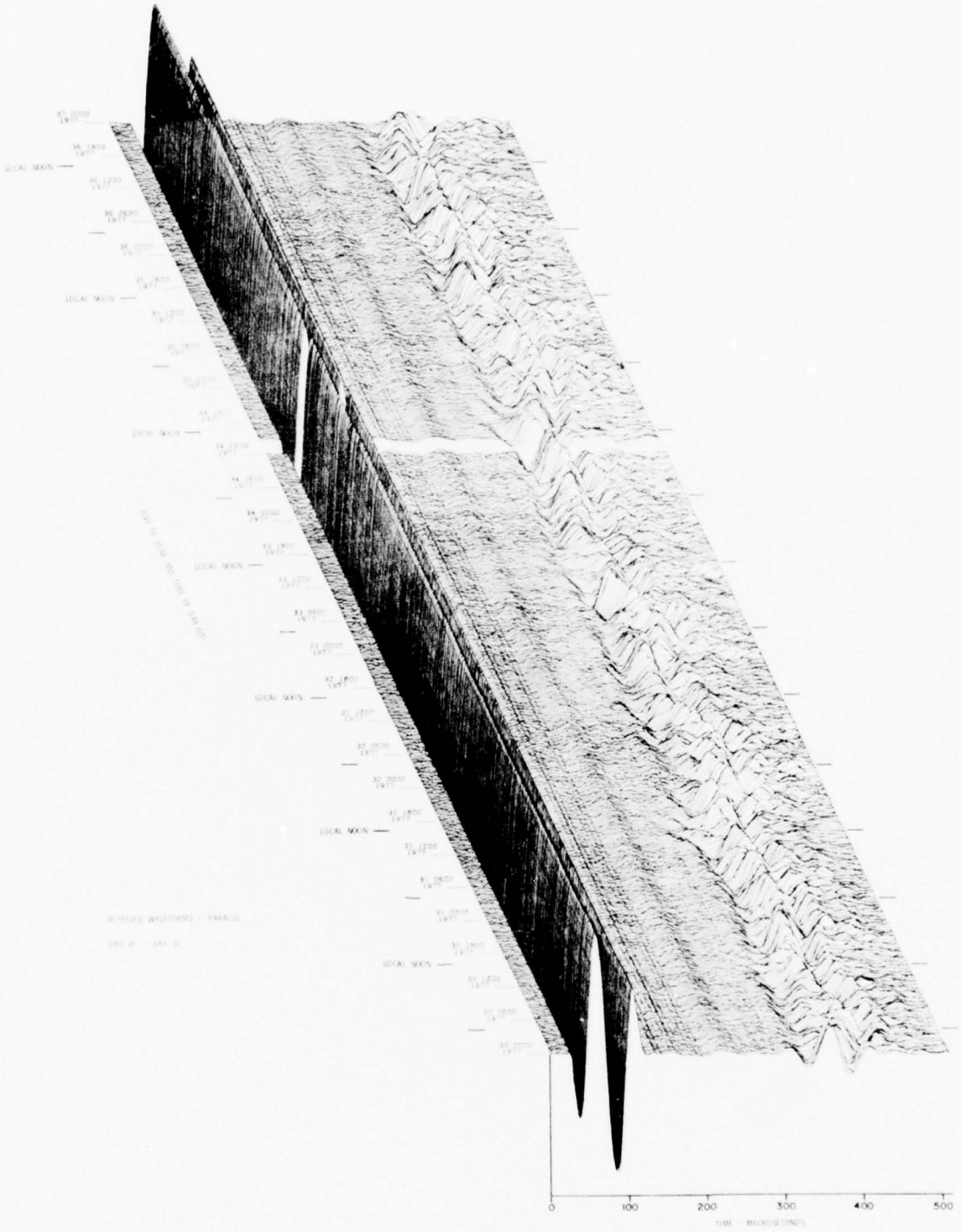

Figure 7. VLF/LF Reflectivity Data for the Polar Ionosphere, DAY 30 (30 Jan) — DAY 36 (5 Feb) 1977 (Cont). Part R, || Waveform Display

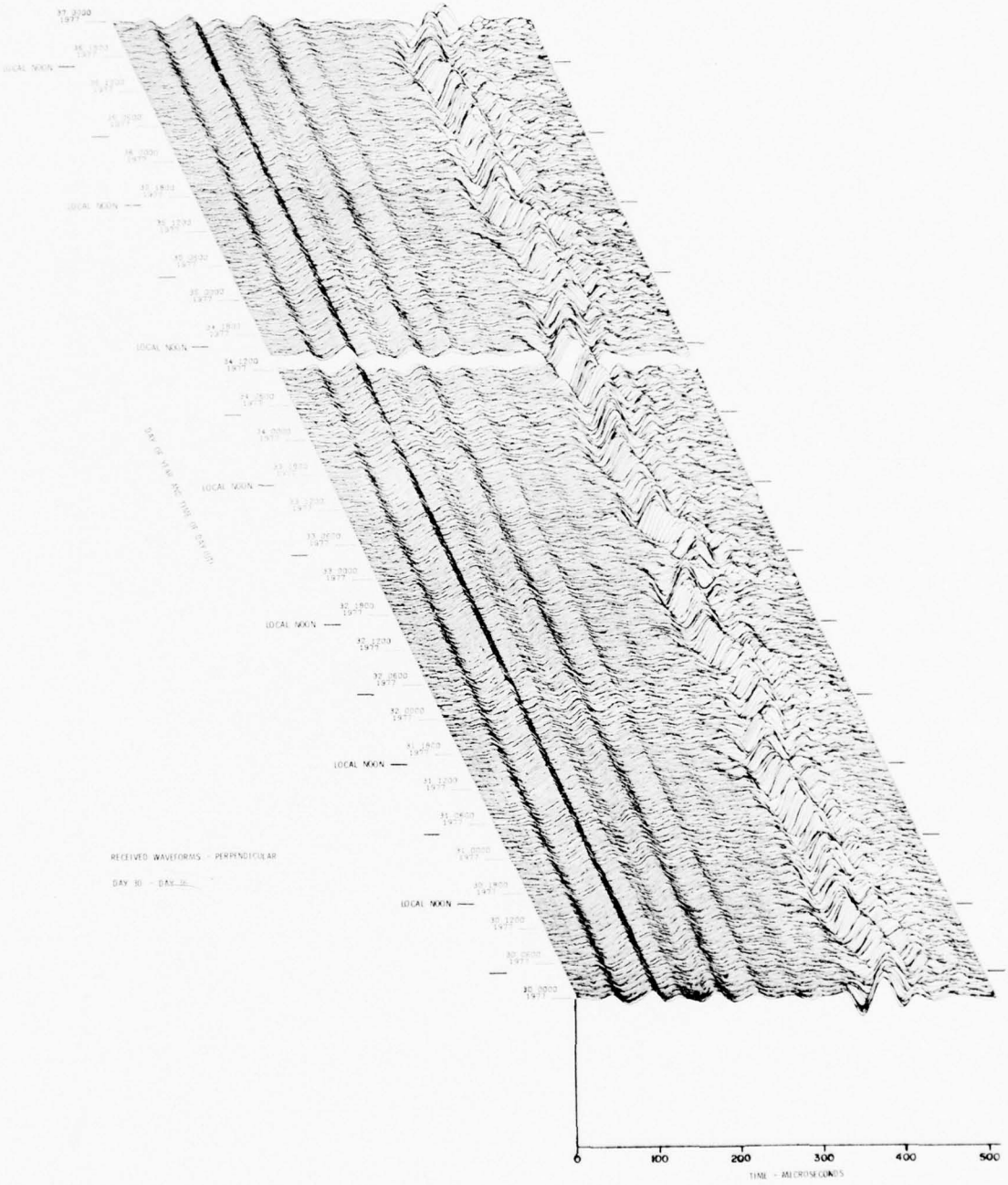

Figure 7. VLF/LF Reflectivity Data for the Polar Ionosphere, DAY 30 (30 Jan) — DAY 36 (5 Feb) 1977 (Cont). Part S, ⊥Waveform Display

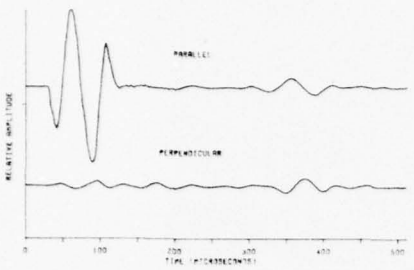

A. RECEIVED WAVEFORMS - 1600GMT, DAY 40

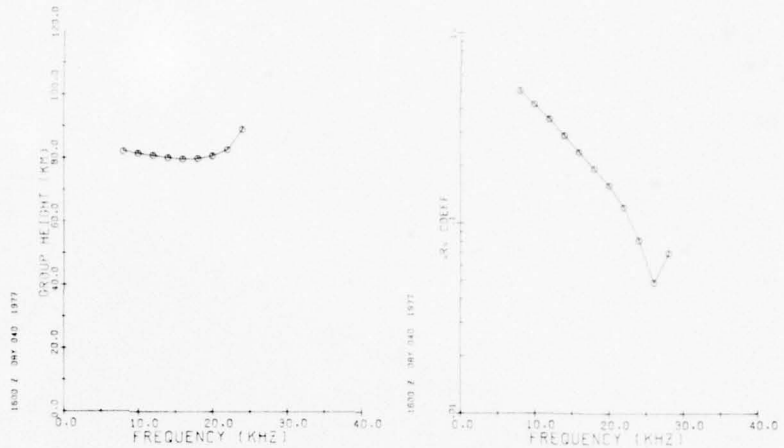

C. GROUP MIRROR REFLECTION HEIGHTS AND ASSOCIATED $_{\parallel}R_{\parallel}$ REFLECTION COEFFICIENTS FROM PARALLEL SKYWAVE DATA

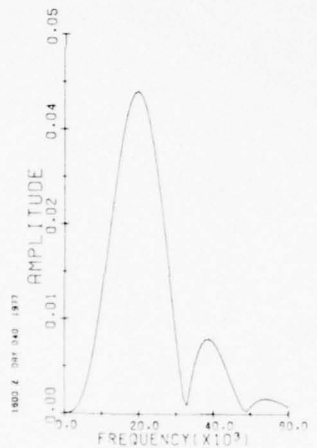

B. FOURIER AMPLITUDE SPECTRUM OF GROUNDWAVE PULSE

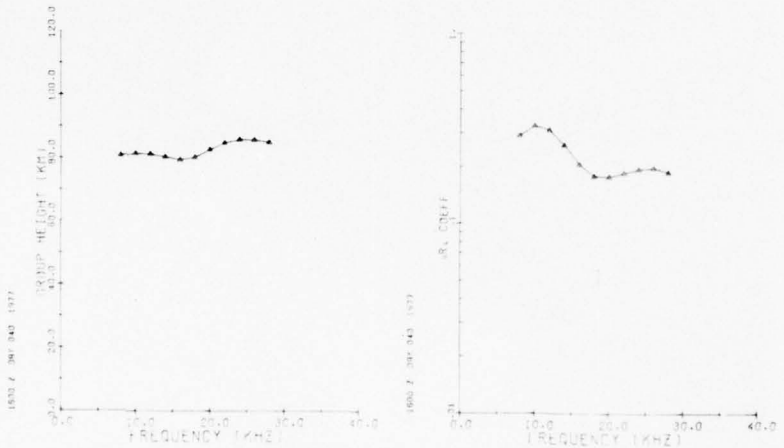

D. GROUP MIRROR REFLECTION HEIGHTS AND ASSOCIATED $_{\perp}R_{\perp}$ REFLECTION COEFFICIENTS FROM PERPENDICULAR SKYWAVE DATA

Figure 8. VLF/LF Reflectivity Data for the Polar Ionosphere, DAY 37 (6 Feb) – DAY 43 (12 Feb) 1977

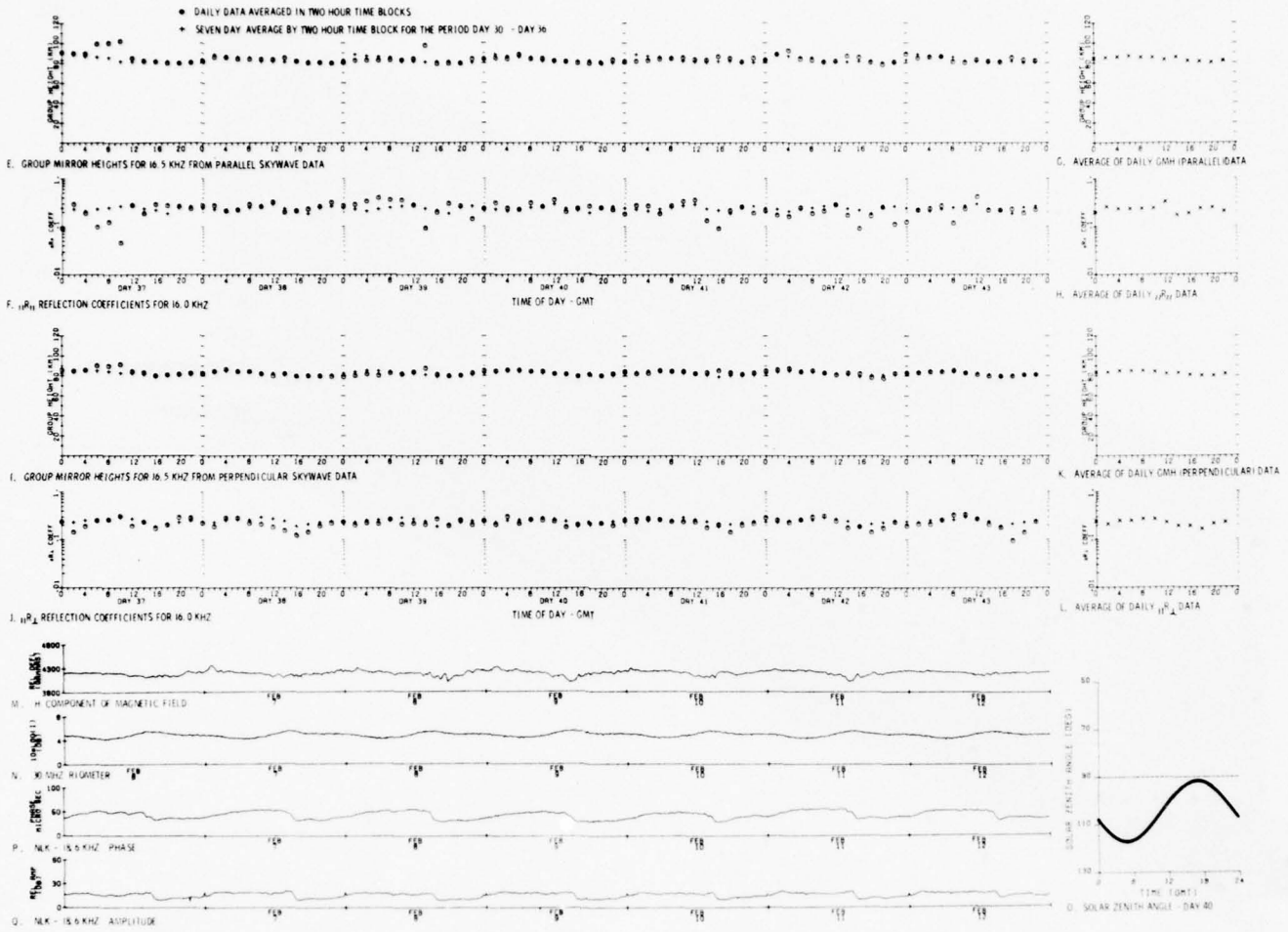

Figure 8. VLF/LF Reflectivity Data for the Polar Ionosphere, DAY 37 (6 Feb) – DAY 43 (12 Feb) 1977 (Cont)

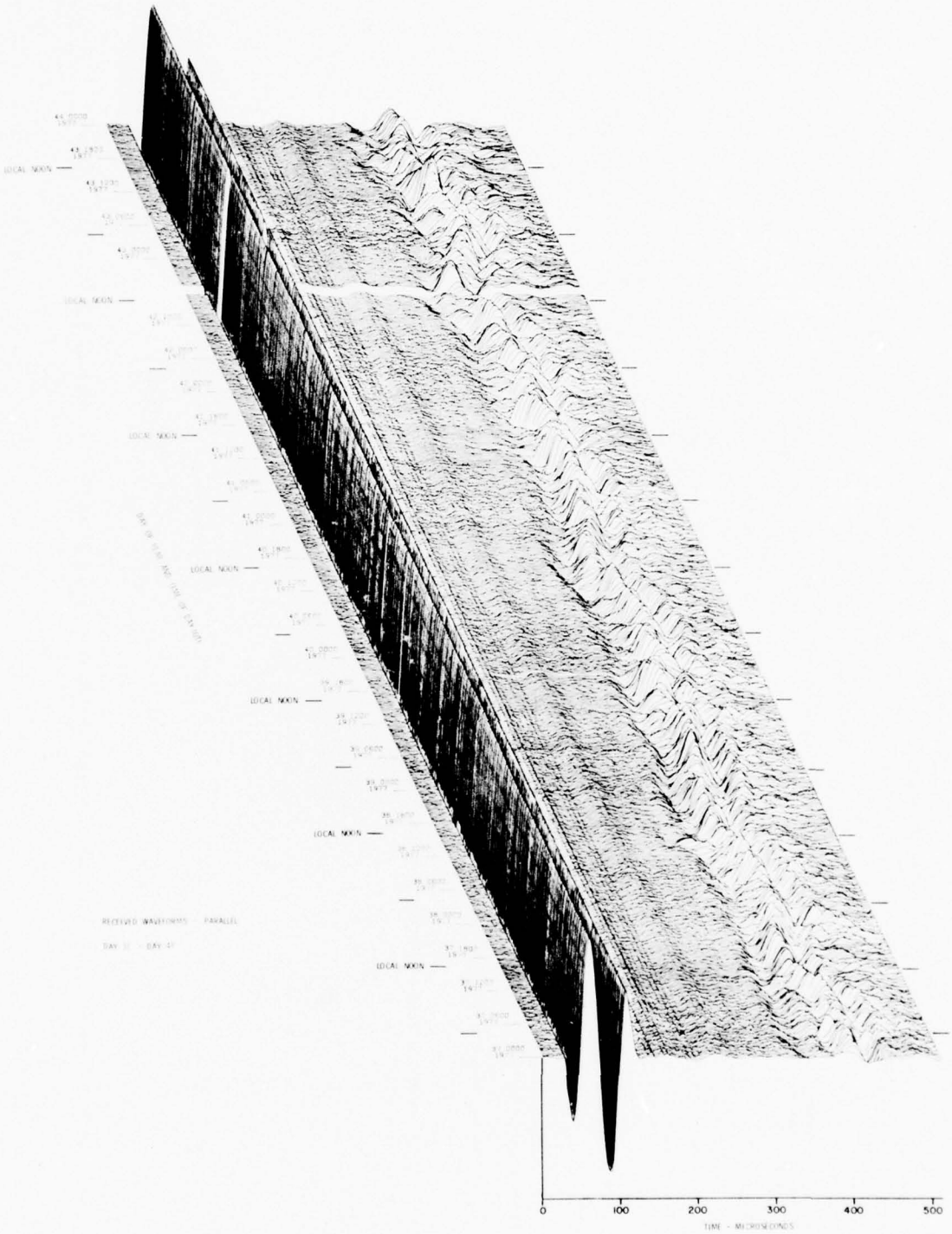

Figure 8. VLF/LF Reflectivity Data for the Polar Ionosphere, DAY 37 (6 Feb) – DAY 43 (12 Feb) 1977 (Cont). Part R, ||Waveform Display

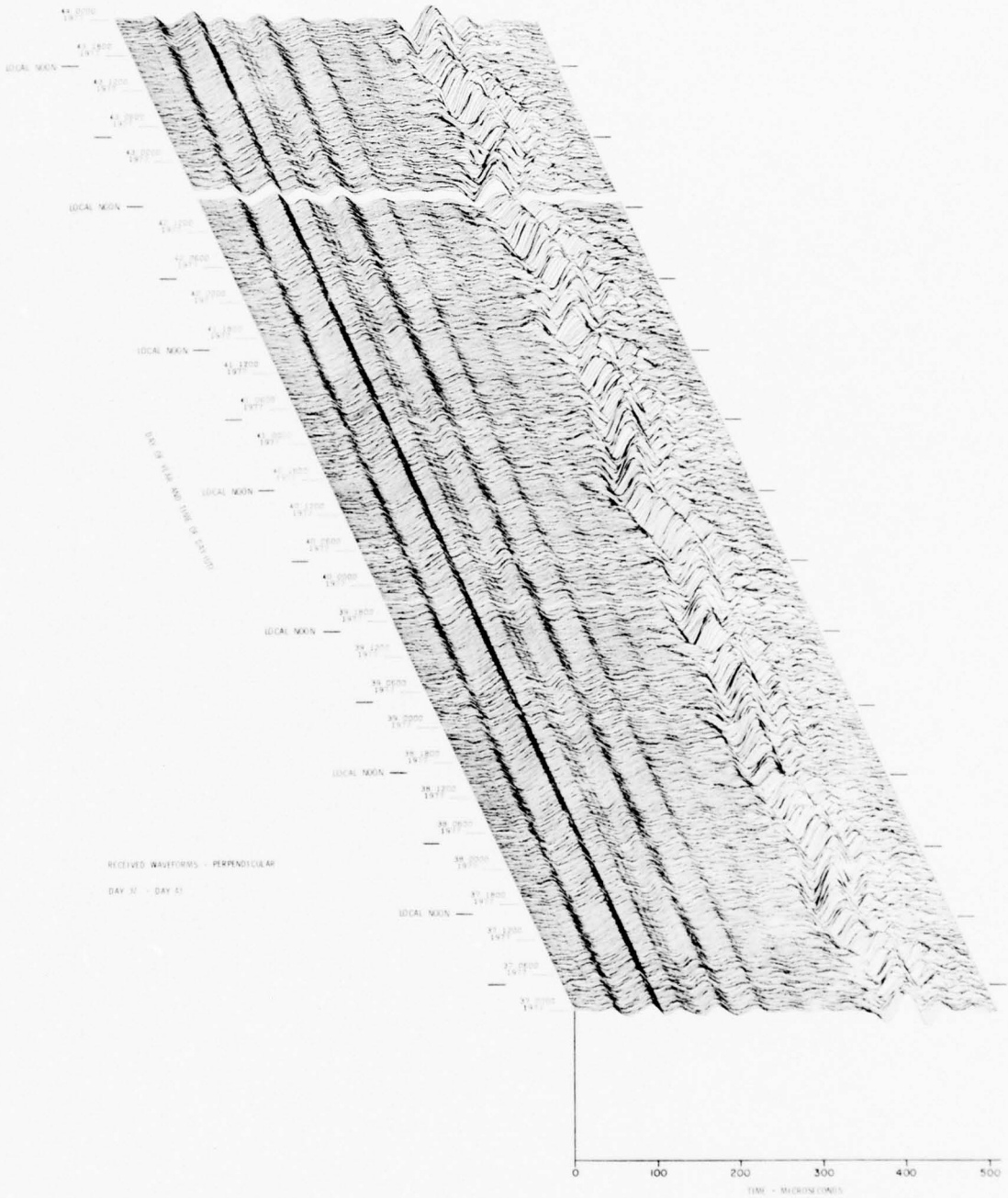

Figure 8. VLF/LF Reflectivity Data for the Polar Ionosphere, DAY 37 (6 Feb) – DAY 43 (12 Feb) 1977 (Cont). Part S, ⊥Waveform Display

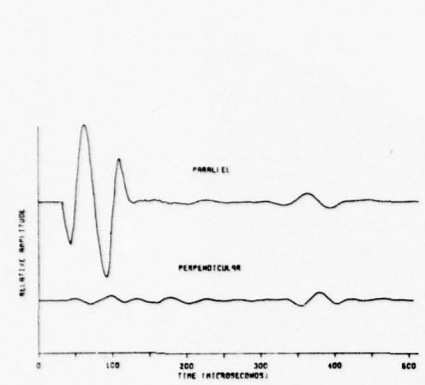

A. RECEIVED WAVEFORMS - 1600GMT, DAY 47

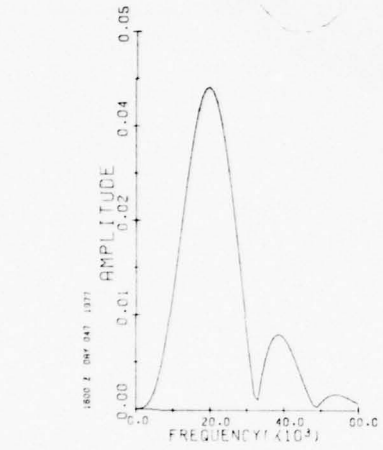

B. FOURIER AMPLITUDE SPECTRUM OF GROUNDWAVE PULSE

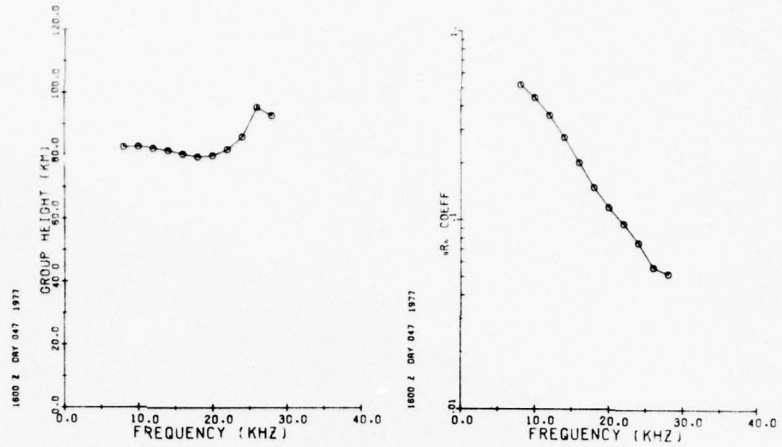

C. GROUP MIRROR REFLECTION HEIGHTS AND ASSOCIATED $_{\parallel}R_{\parallel}$ REFLECTION COEFFICIENTS FROM PARALLEL SKYWAVE DATA

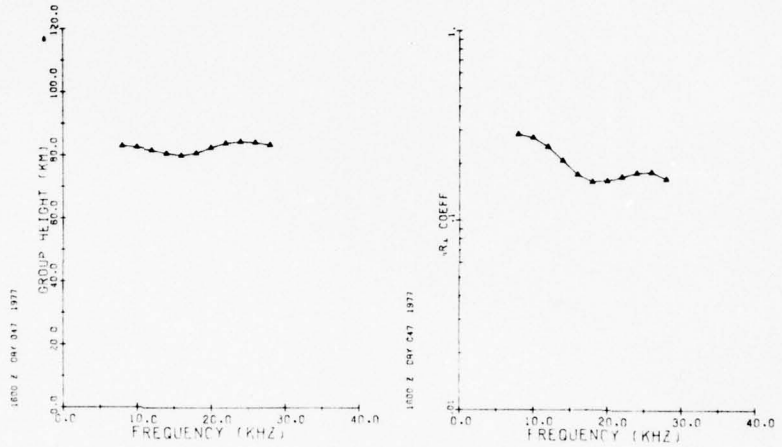

D. GROUP MIRROR REFLECTION HEIGHTS AND ASSOCIATED $_{\parallel}R_{\perp}$ REFLECTION COEFFICIENTS FROM PERPENDICULAR SKYWAVE DATA

Figure 9. VLF/LF Reflectivity Data for the Polar Ionosphere, DAY 44 (13 Feb) — DAY 50 (19 Feb) 1977

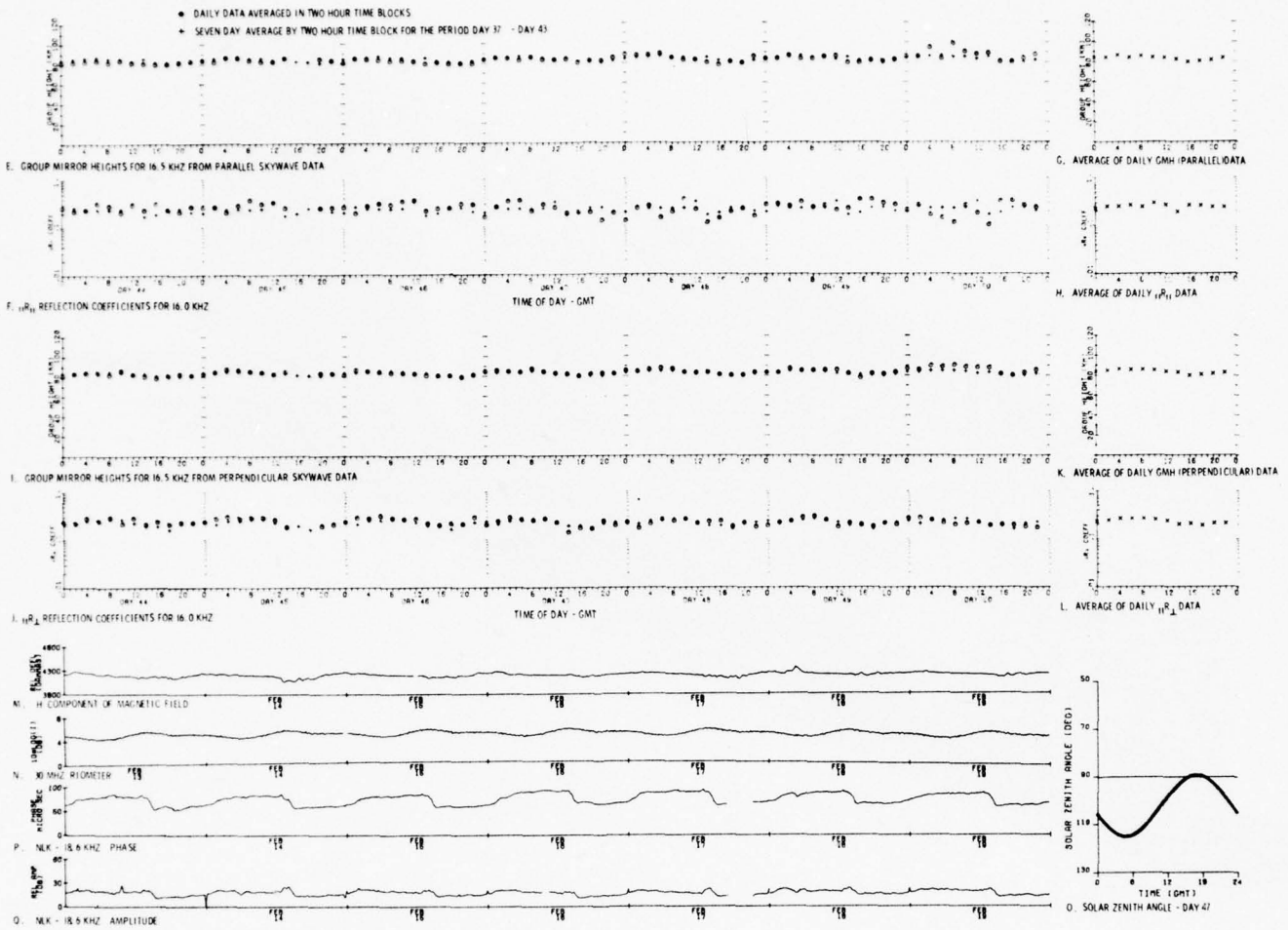

Figure 9. VLF/LF Reflectivity Data for the Polar Ionosphere, DAY 44 (13 Feb) — DAY 50 (19 Feb) 1977 (Cont)

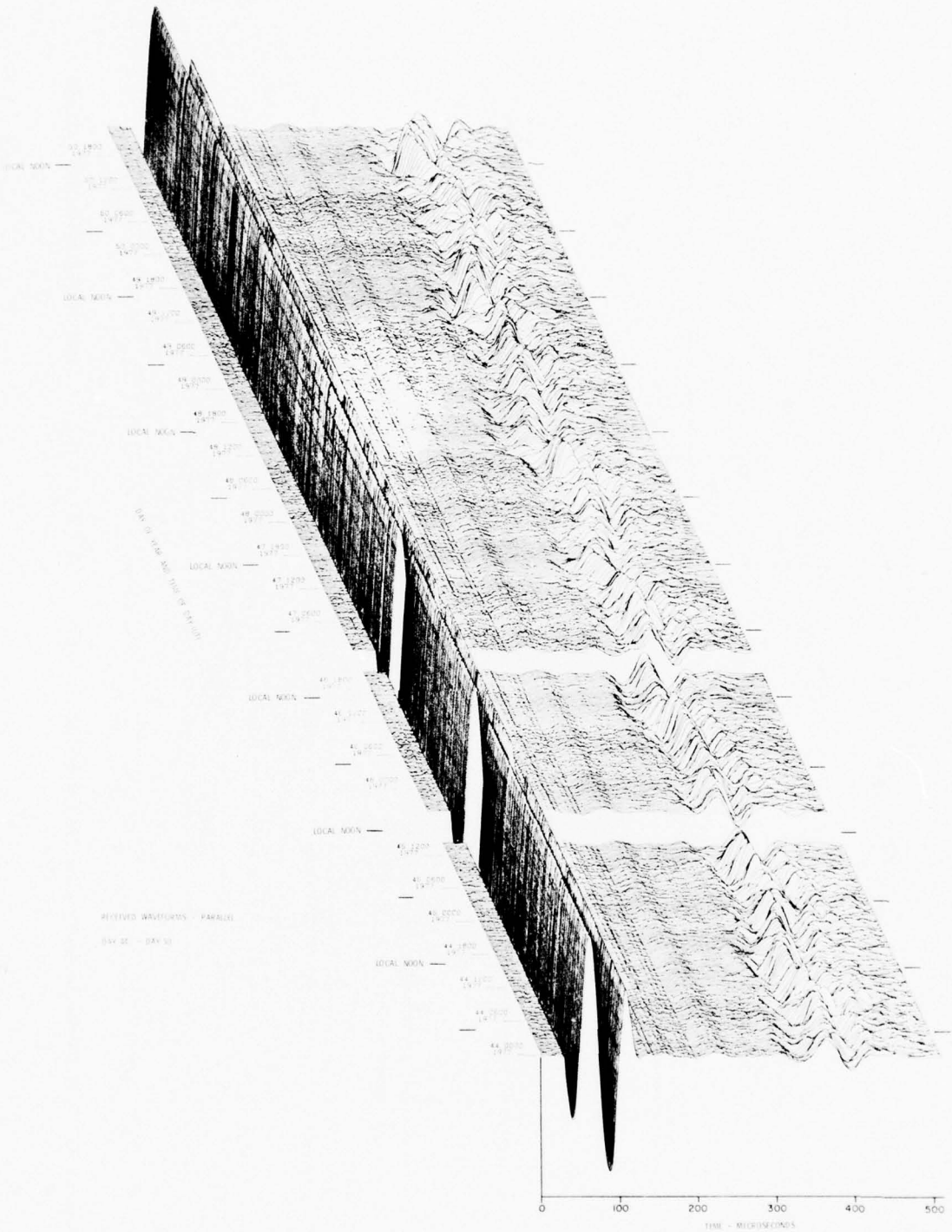

Figure 9. VLF/LF Reflectivity Data for the Polar Ionosphere, DAY 44 (13 Feb) — DAY 50 (19 Feb) 1977 (Cont). Part R, || Waveform Display

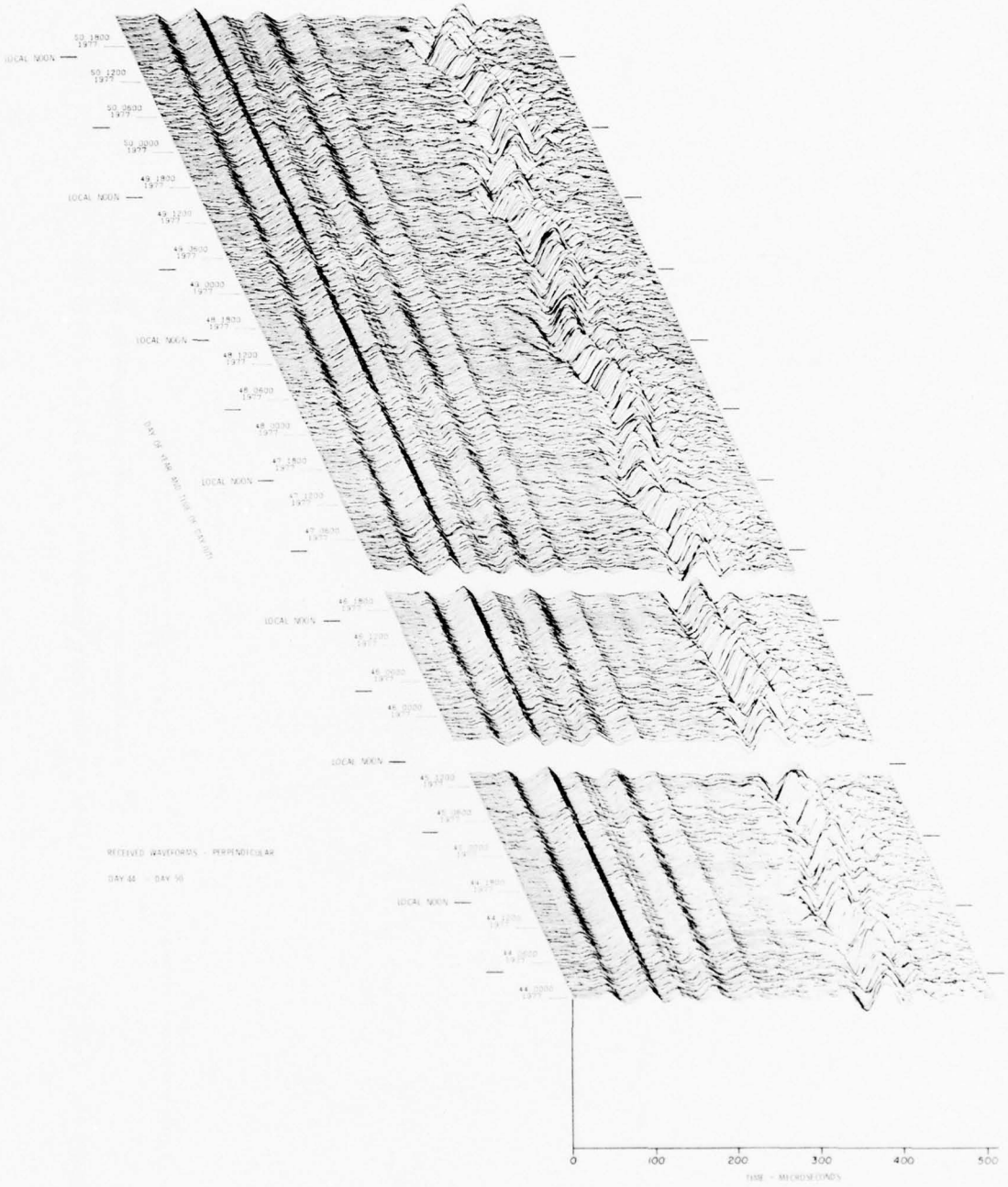

Figure 9. VLF/LF Reflectivity Data for the Polar Ionosphere, DAY 44 (13 Feb) – DAY 50 (19 Feb) 1977 (Cont). Part S, ⊥Waveform Display

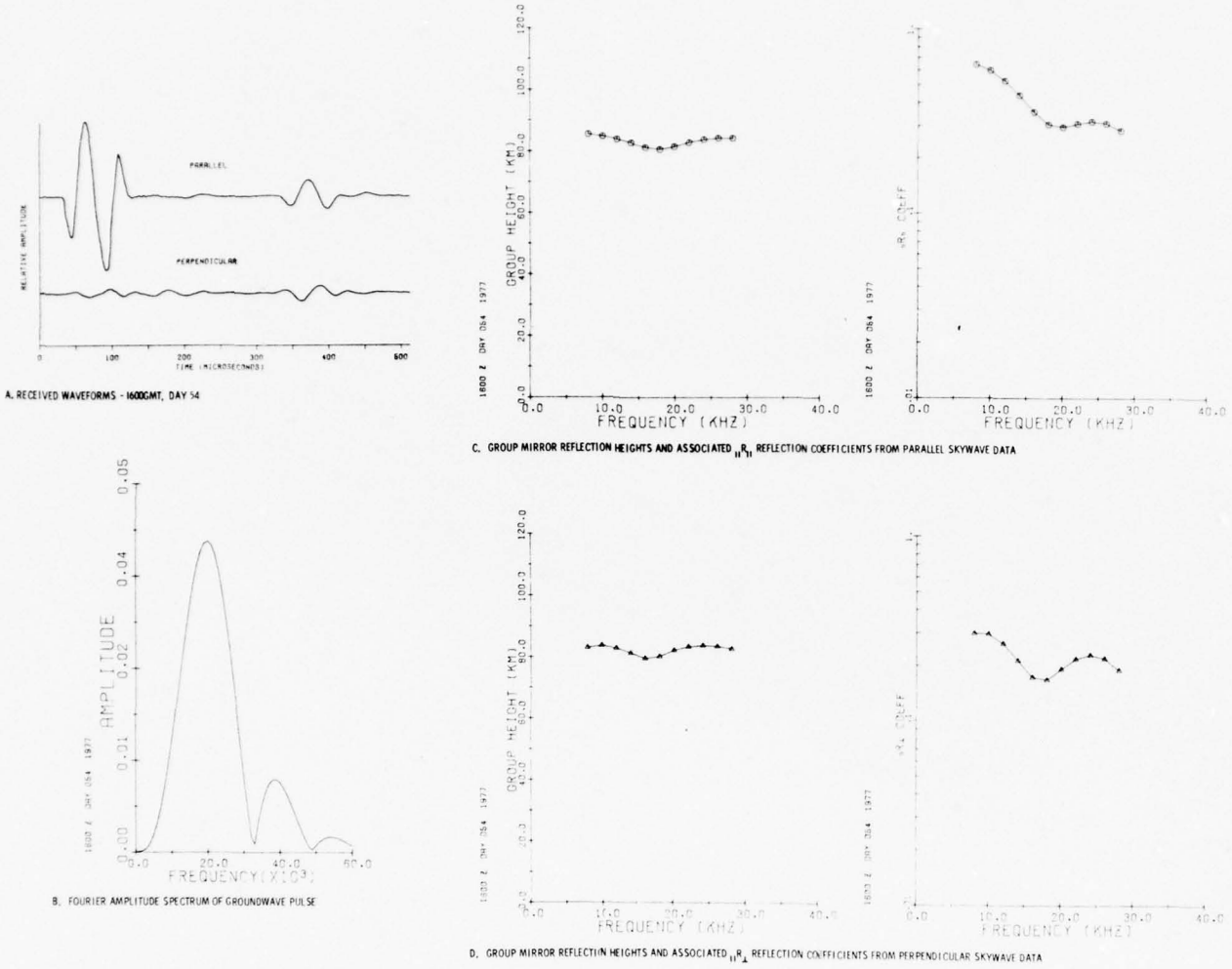

Figure 10. VLF/LF Reflectivity Data for the Polar Ionosphere, DAY 51 (20 Feb) — DAY 57 (26 Feb) 1977

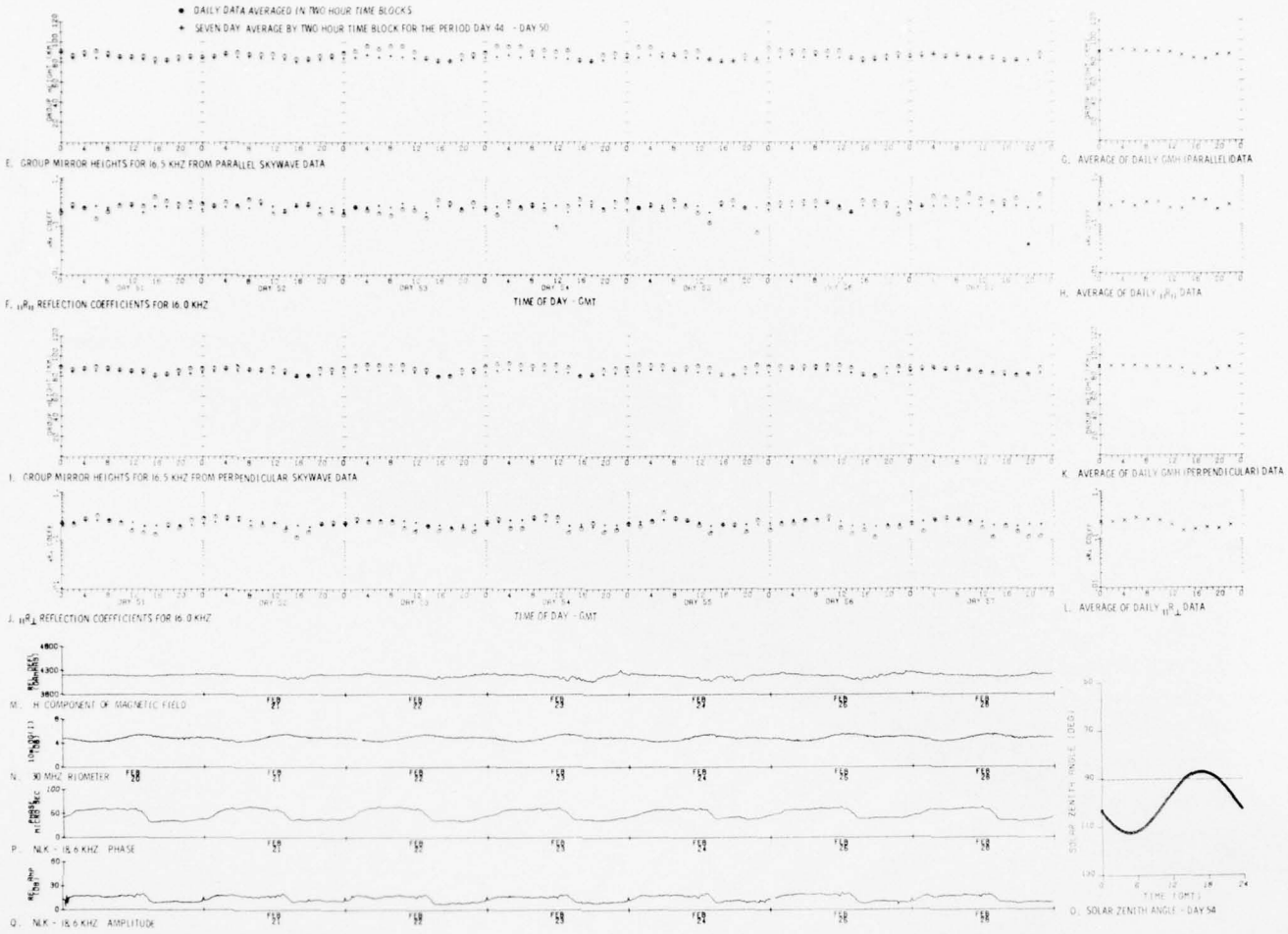

Figure 10. VLF/LF Reflectivity Data for the Polar Ionosphere, DAY 51 (20 Feb) – DAY 57 (26 Feb(1977 (Cont)

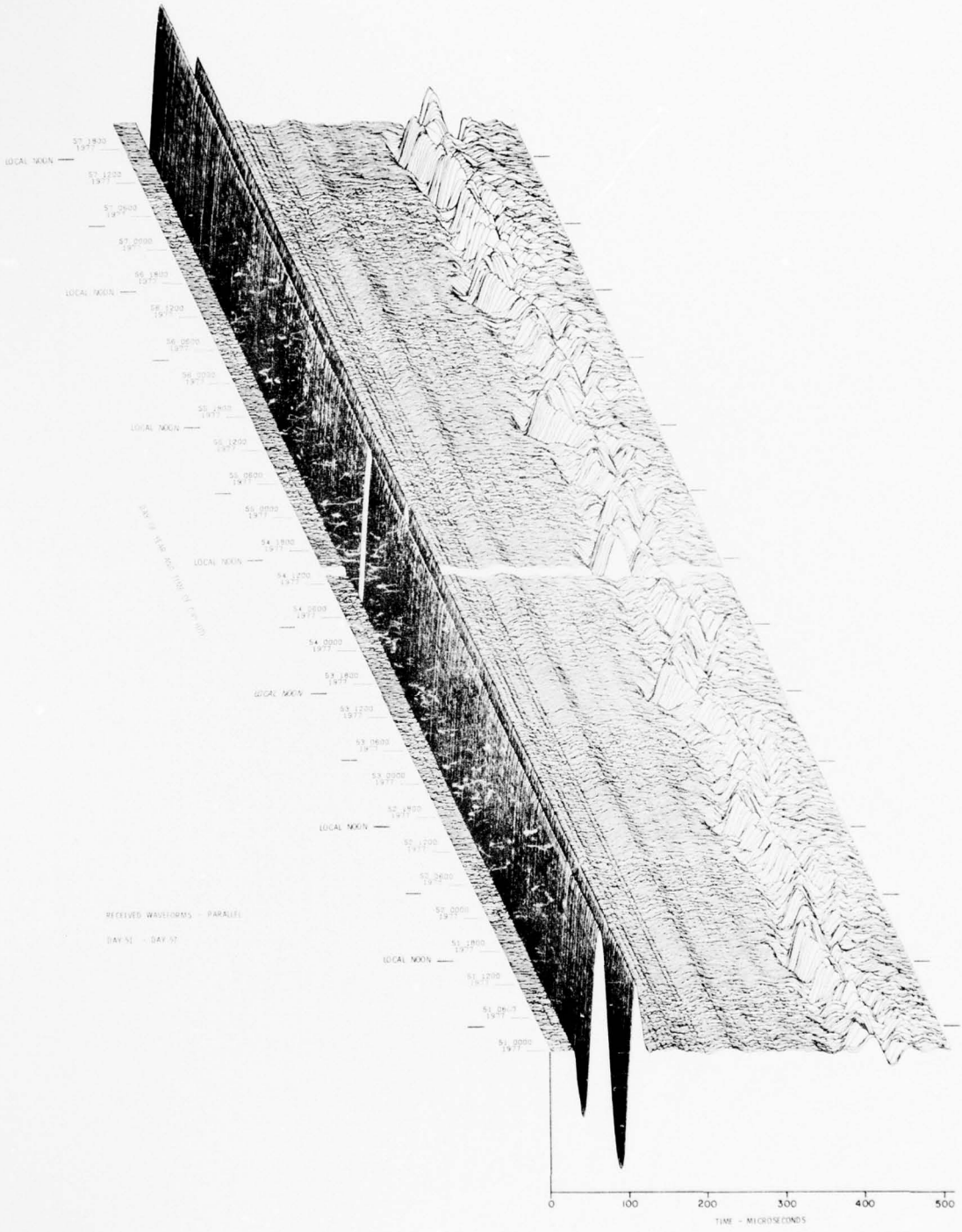

Figure 10. VLF/LF Reflectivity Data for the Polar Ionosphere, DAY 51 (20 Feb) – DAY 57 (26 Feb) 1977 (Cont). Part R, || Waveform Display

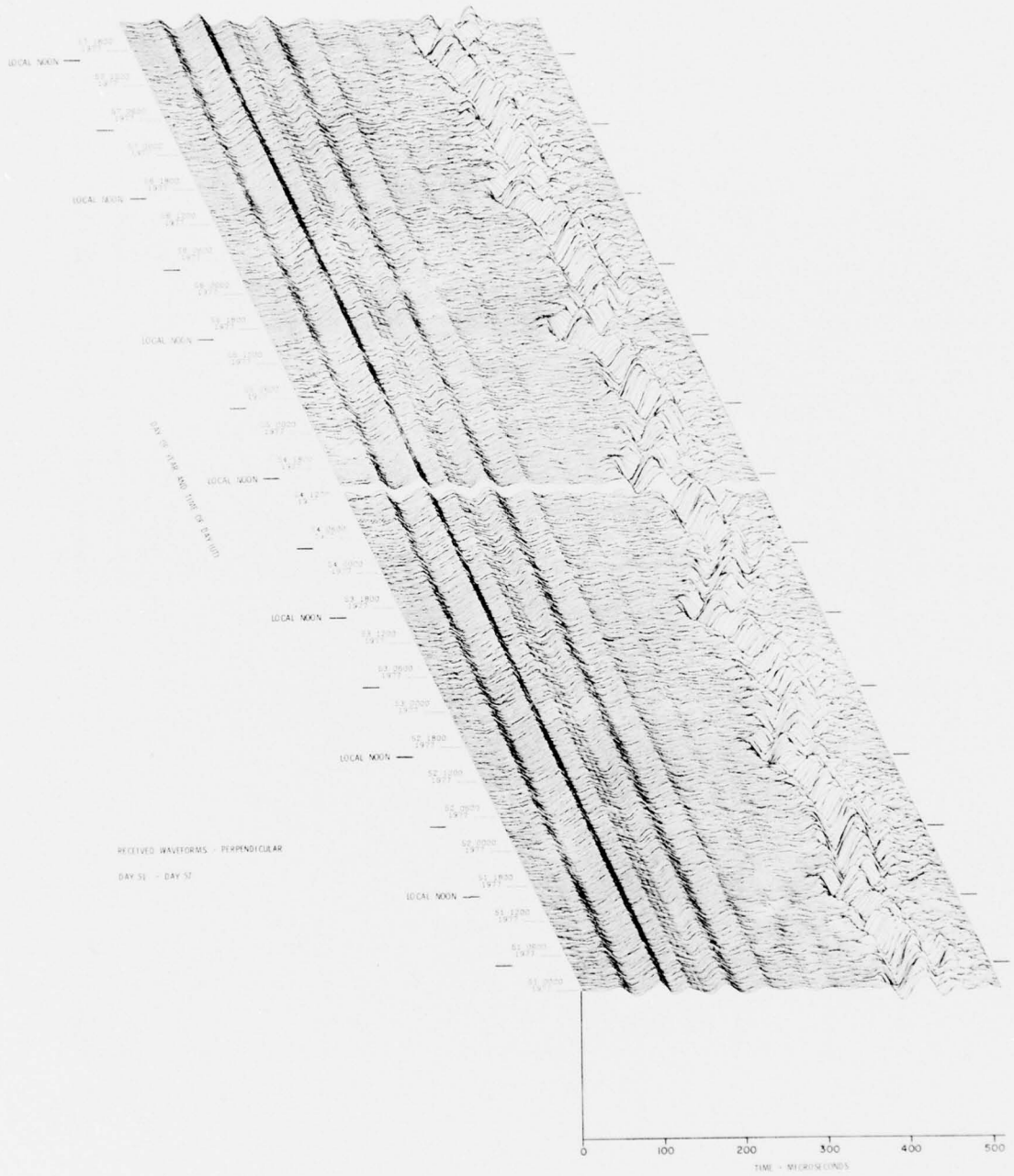

Figure 10. VLF/LF Reflectivity Data for the Polar Ionosphere, DAY 51 (20 Feb) – DAY 57 (26 Feb) 1977 (Cont). Part S, ⊥Waveform Display

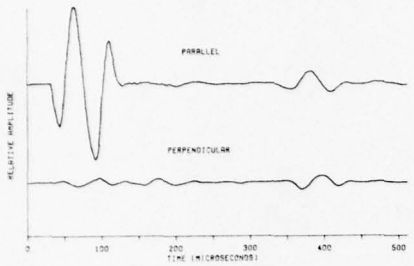

A. RECEIVED WAVEFORMS - 1600GMT, DAY 61

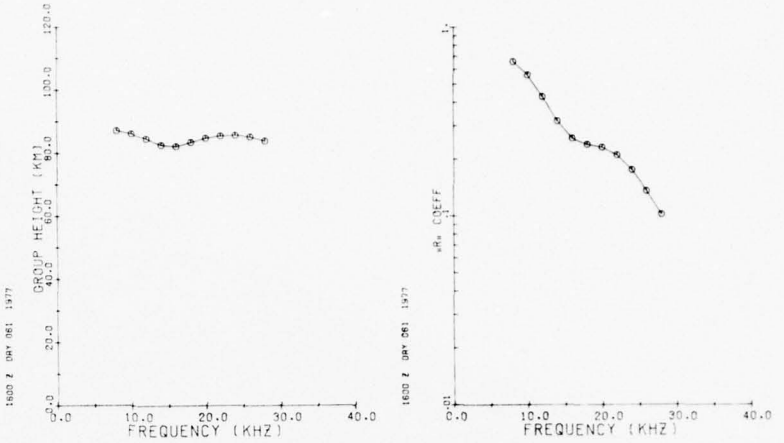

C. GROUP MIRROR REFLECTION HEIGHTS AND ASSOCIATED $_{\parallel}R_{\parallel}$ REFLECTION COEFFICIENTS FROM PARALLEL SKYWAVE DATA

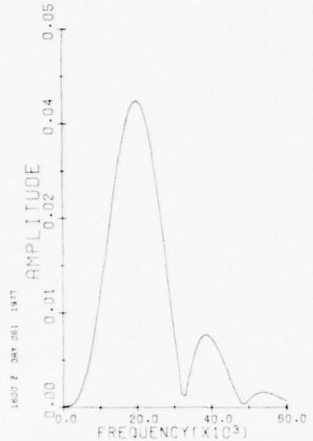

B. FOURIER AMPLITUDE SPECTRUM OF GROUNDWAVE PULSE

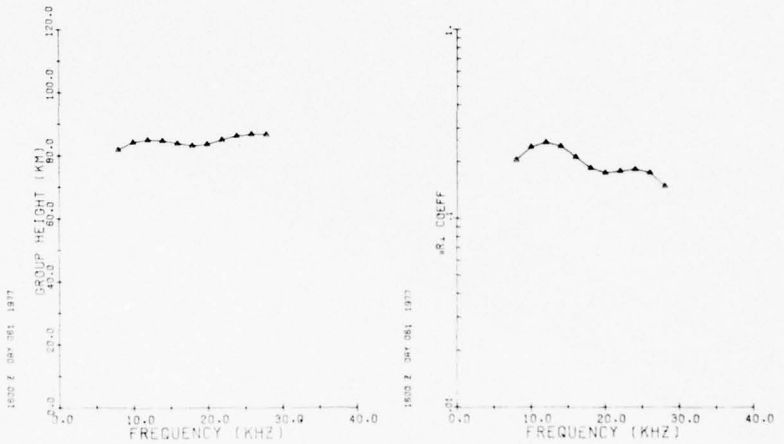

D. GROUP MIRROR REFLECTION HEIGHTS AND ASSOCIATED $_{\parallel}R_{\perp}$ REFLECTION COEFFICIENTS FROM PERPENDICULAR SKYWAVE DATA

Figure 11. VLF/LF Reflectivity Data for the Polar Ionosphere, DAY 58 (27 Feb) – DAY 64 (5 Mar) 1977

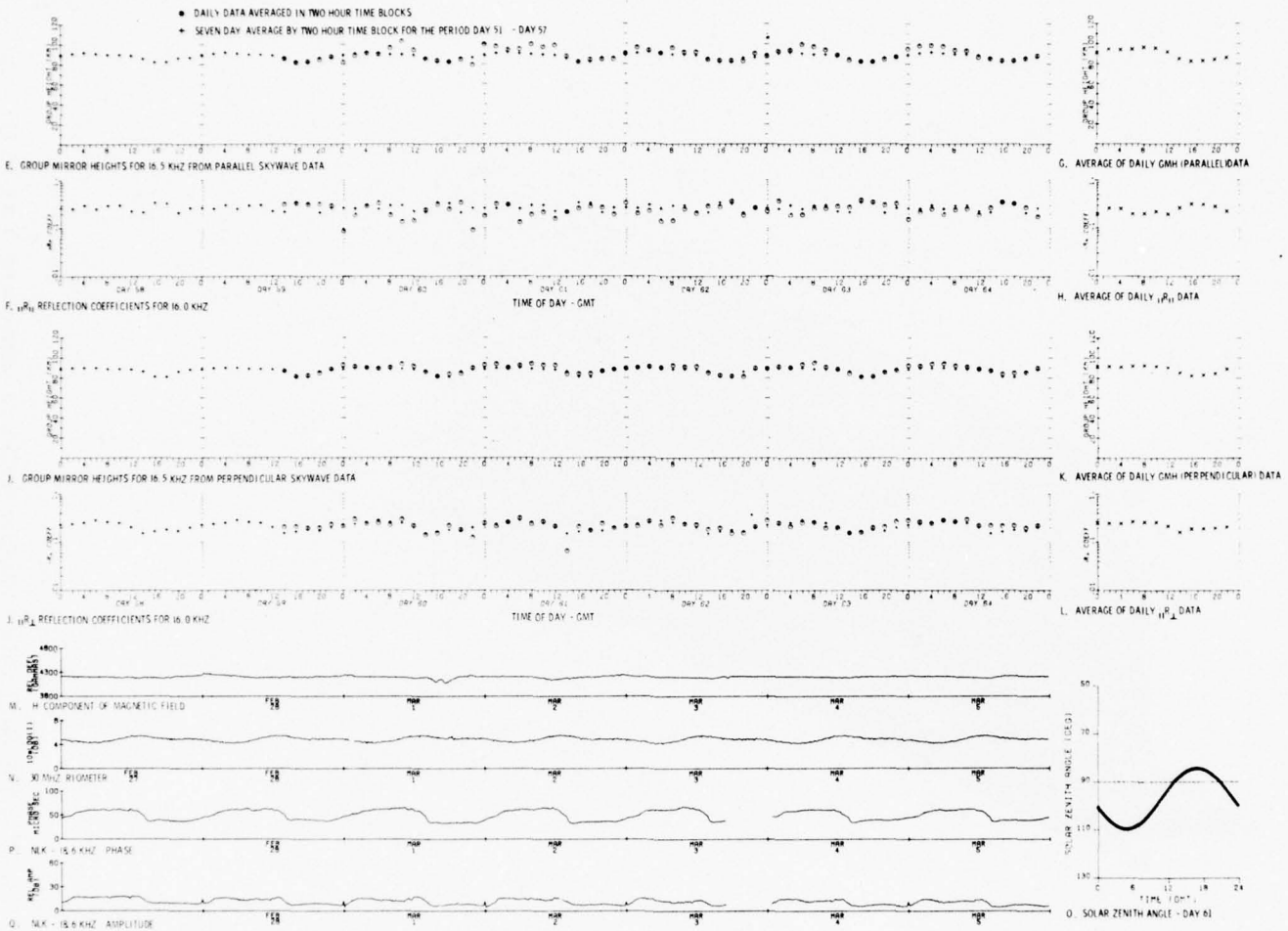

Figure 11. VLF/LF Reflectivity Data for the Polar Ionosphere, DAY 58 (27 Feb) – DAY 64 (5 Mar) 1977 (Cont)

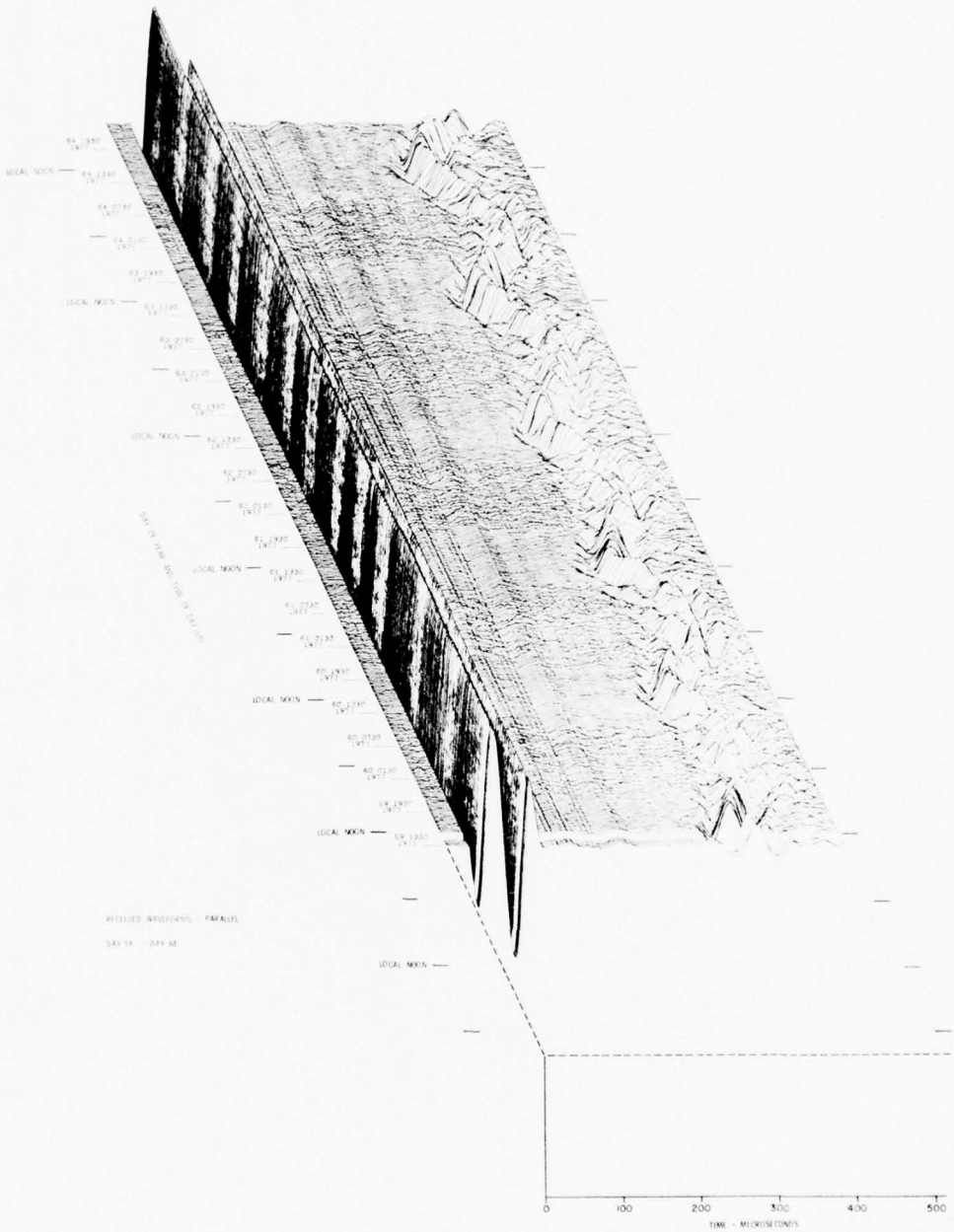

Figure 11. VLF/LF Reflectivity Data for the Polar Ionosphere, DAY 58 (27 Feb) – DAY 64 (5 Mar) 1977 (Cont). Part R, ||Waveform Display

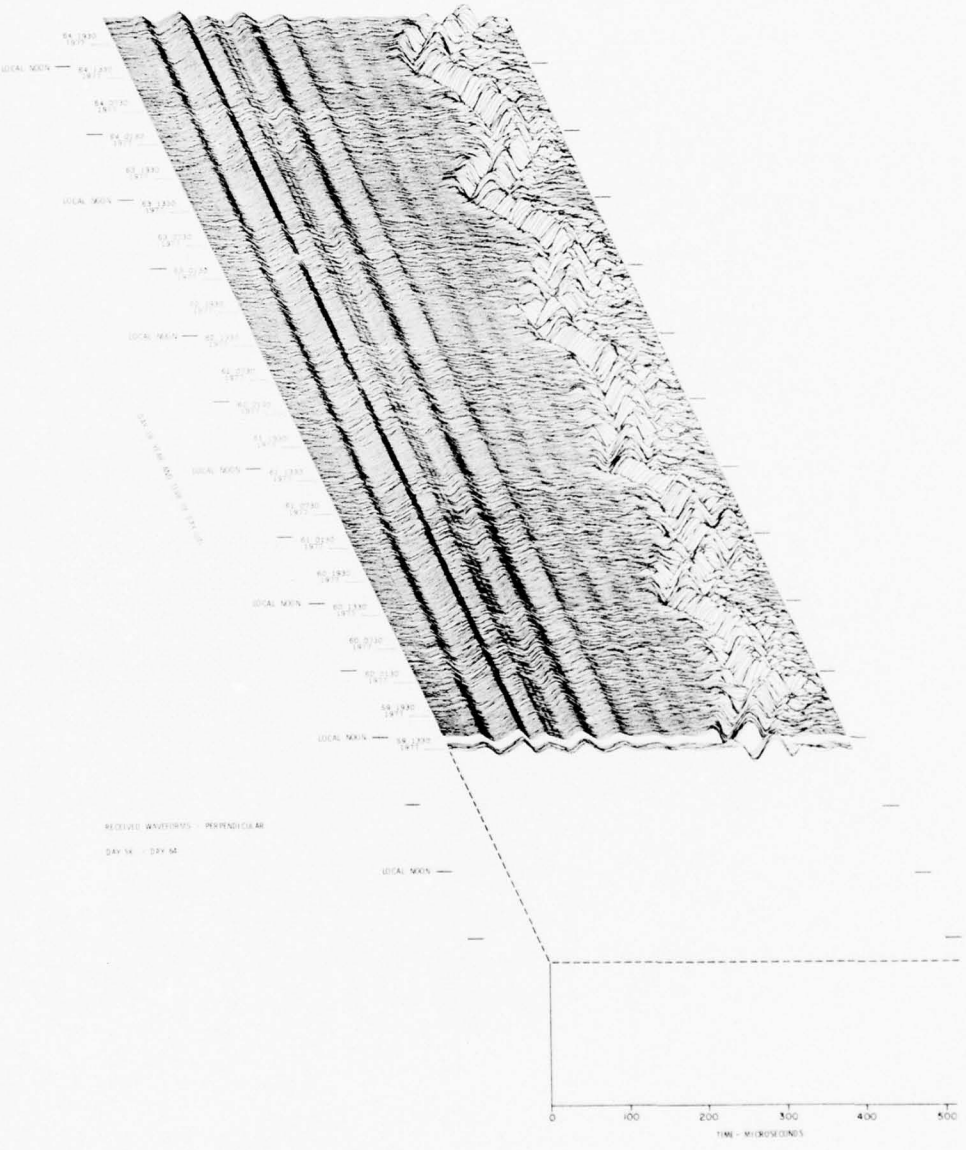

Figure 11. VLF/LF Reflectivity Data for the Polar Ionosphere, DAY 58 (27 Feb) – DAY 64 (5 Mar) 1977 (Cont). Part S, ⊥ Waveform Display

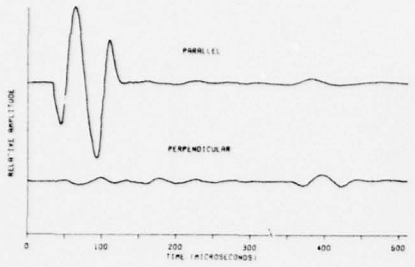

A. RECEIVED WAVEFORMS - 1600GMT, DAY 68

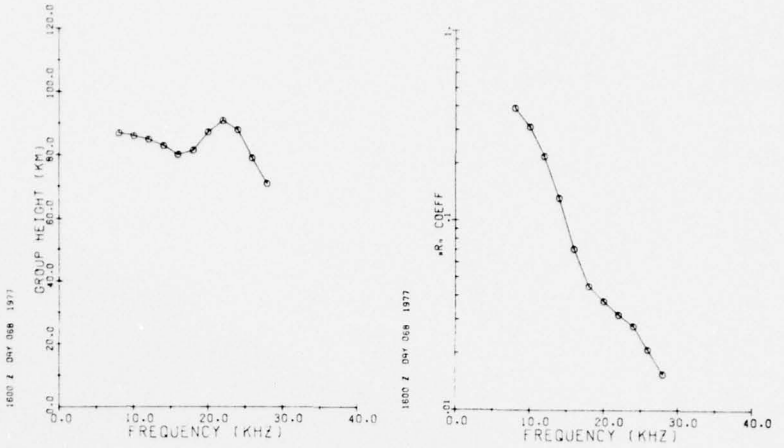

C. GROUP MIRROR REFLECTION HEIGHTS AND ASSOCIATED $_{\parallel}R_{\parallel}$ REFLECTION COEFFICIENTS FROM PARALLEL SKYWAVE DATA

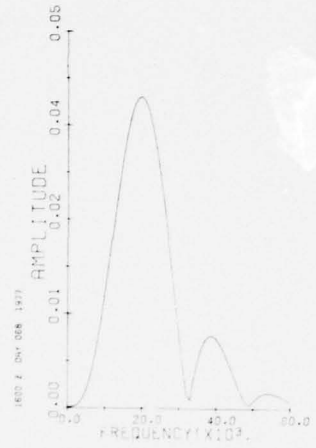

B. FOURIER AMPLITUDE SPECTRUM OF GROUNDWAVE PULSE

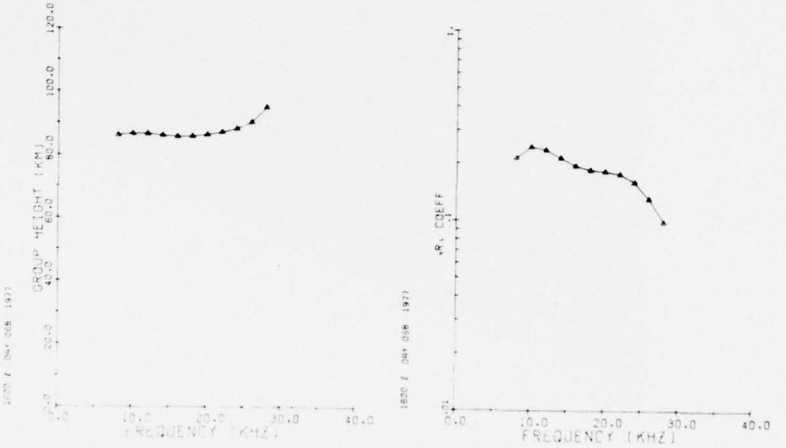

D. GROUP MIRROR REFLECTION HEIGHTS AND ASSOCIATED $_{\perp}R_{\perp}$ REFLECTION COEFFICIENTS FROM PERPENDICULAR SKYWAVE DATA

Figure 12. VLF/LF Reflectivity Data for the Polar Ionosphere, DAY 65 (6 Mar) – DAY 71 (12 Mar) 1977

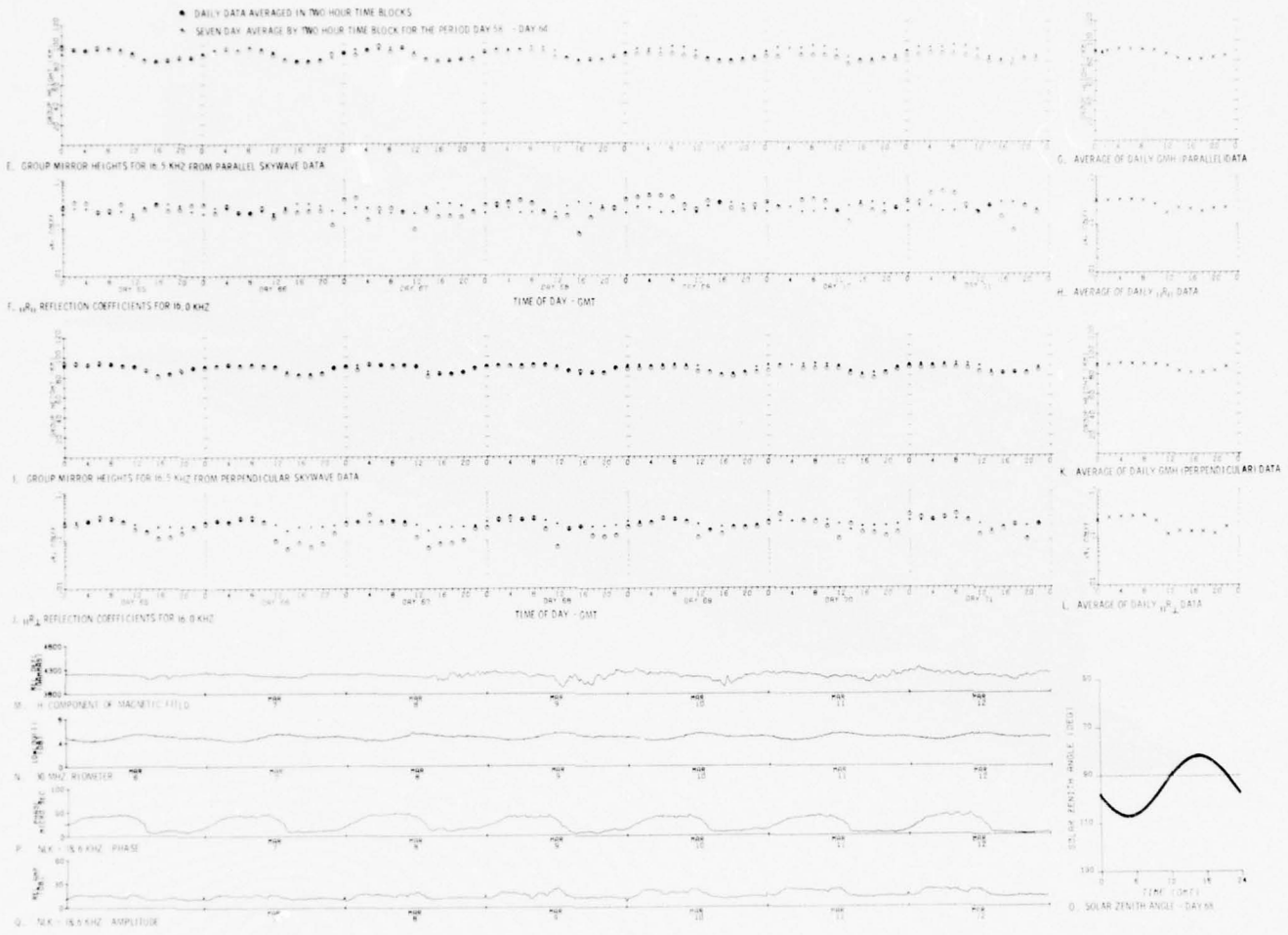

Figure 12. VLF/LF Reflectivity Data for the Polar Ionosphere, DAY 65 (6 Mar) – DAY 71 (12 Mar) 1977 (Cont)

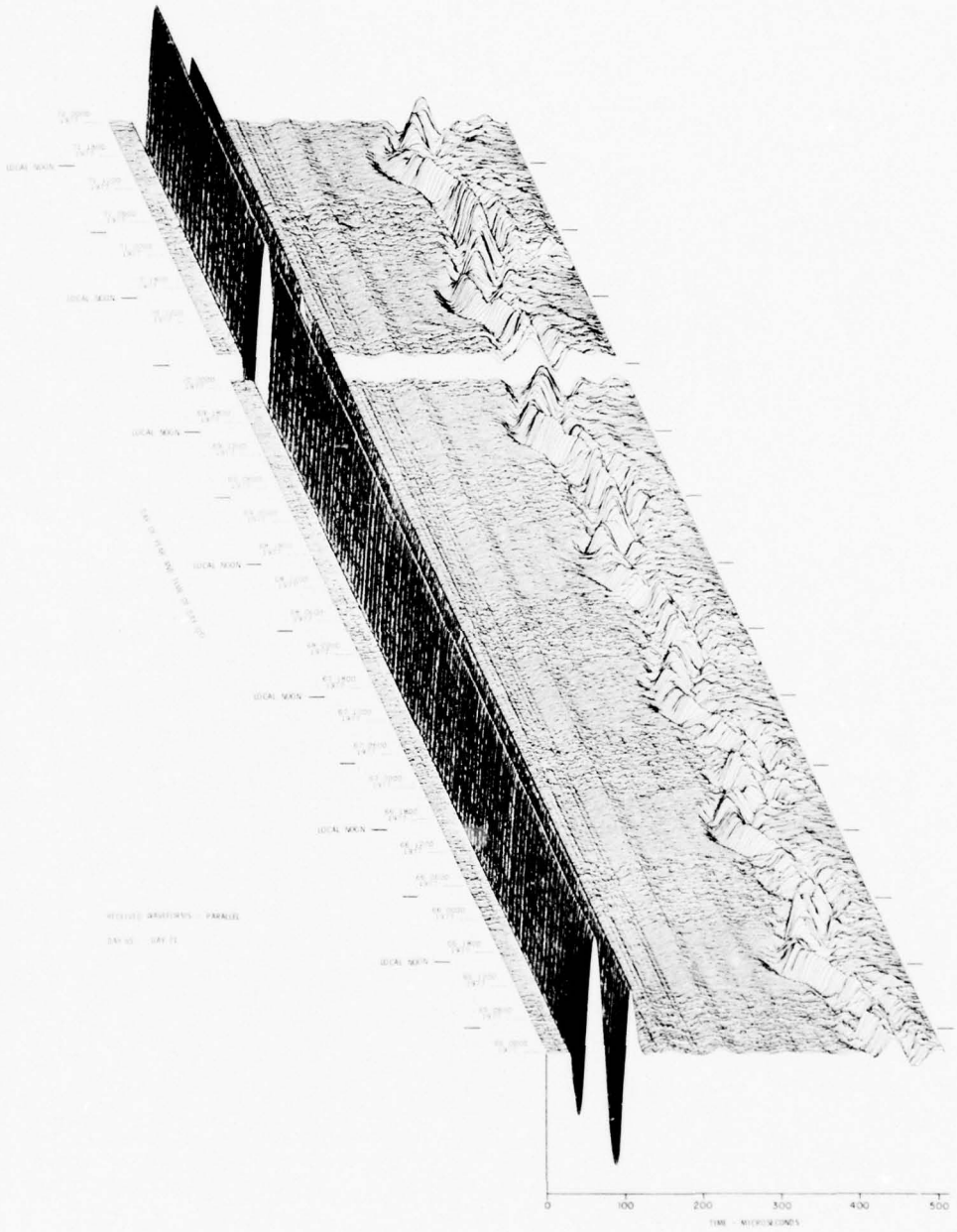

Figure 12. VLF/LF Reflectivity Data for the Polar Ionosphere, DAY 65 (6 Mar) – DAY 71 (12 Mar) 1977 (Cont). Part R, ||Waveform Display

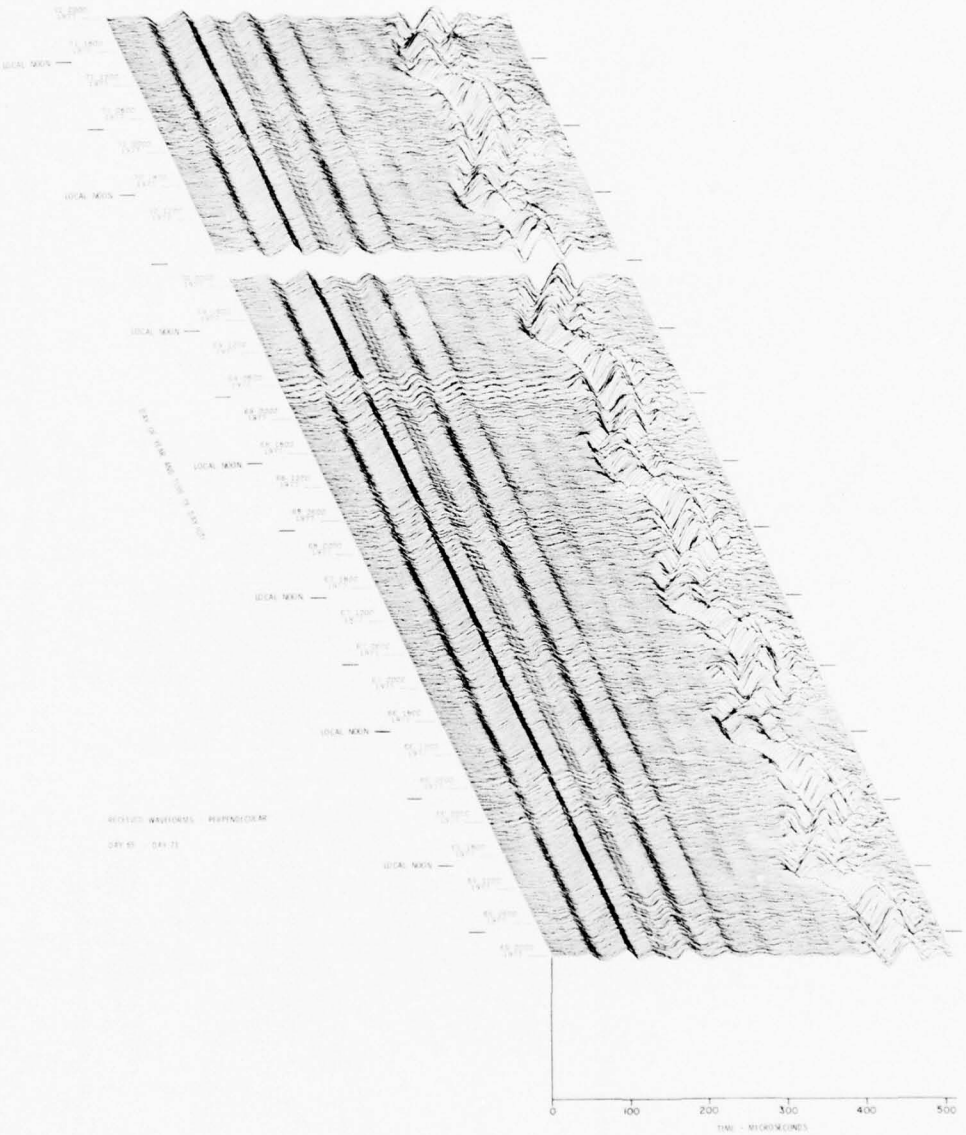

Figure 12. VLF/LF Reflectivity Data for the Polar Ionosphere, DAY 65 (6 Mar) – DAY 71 (12 Mar) 1977 (Cont). Part S, ⊥ Waveform Display

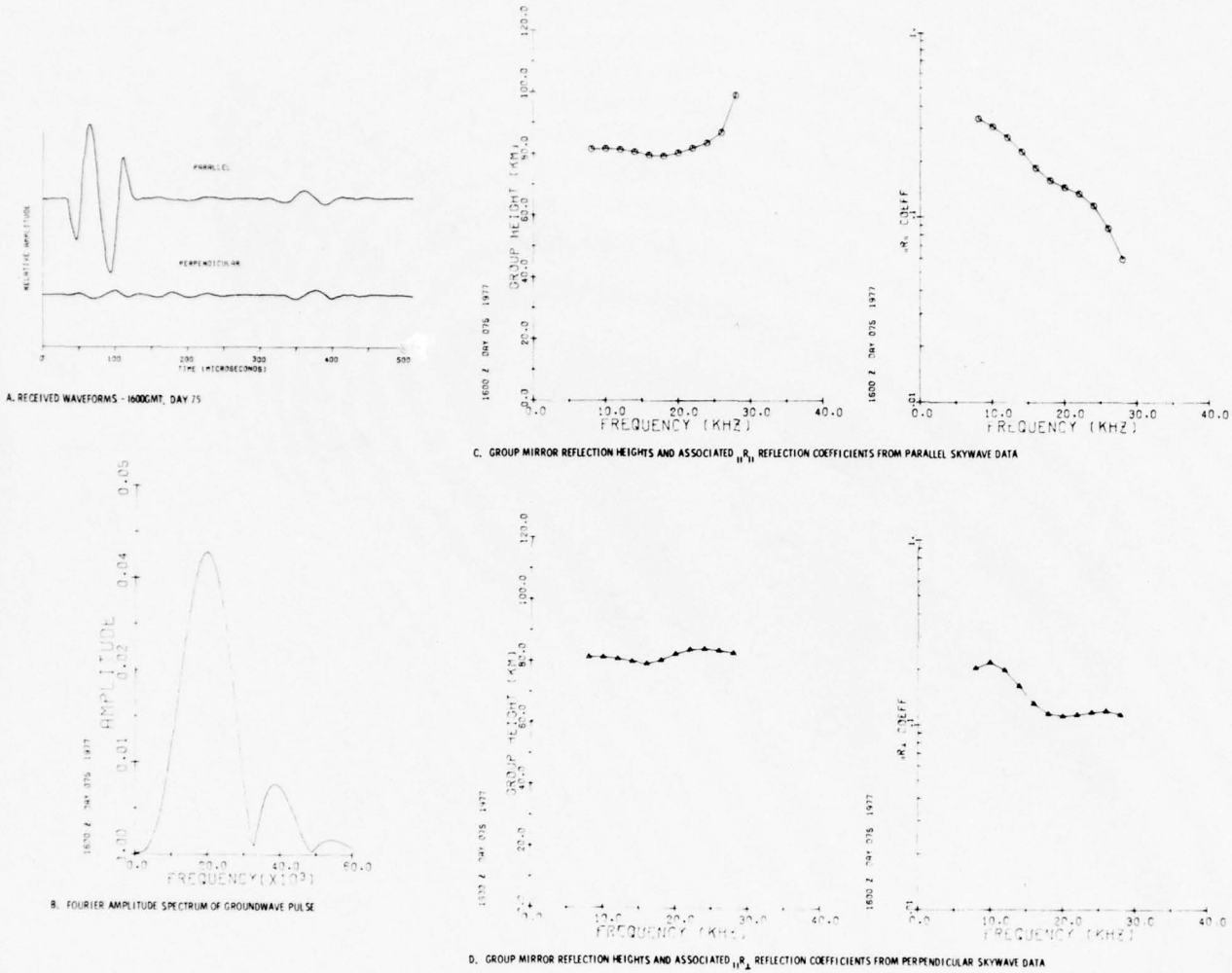

Figure 13. VLF/LF Reflectivity Data for the Polar Ionosphere, DAY 72 (13 Mar) — DAY 78 (19 Mar) 1977

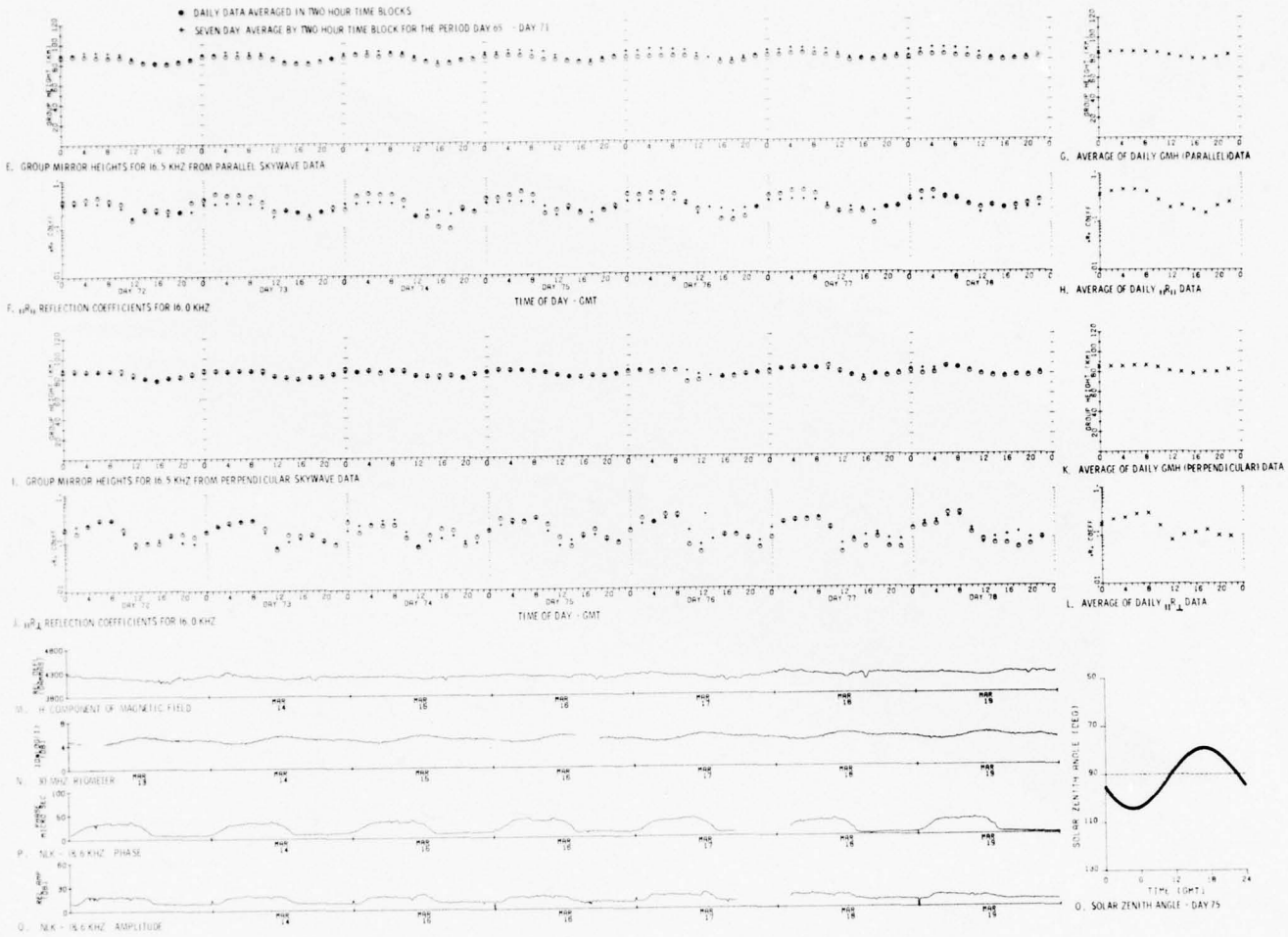

Figure 13. VLF/LF Reflectivity Data for the Polar Ionosphere, DAY 72 (13 Mar) – DAY 78 (19 Mar) 1977 (Cont)

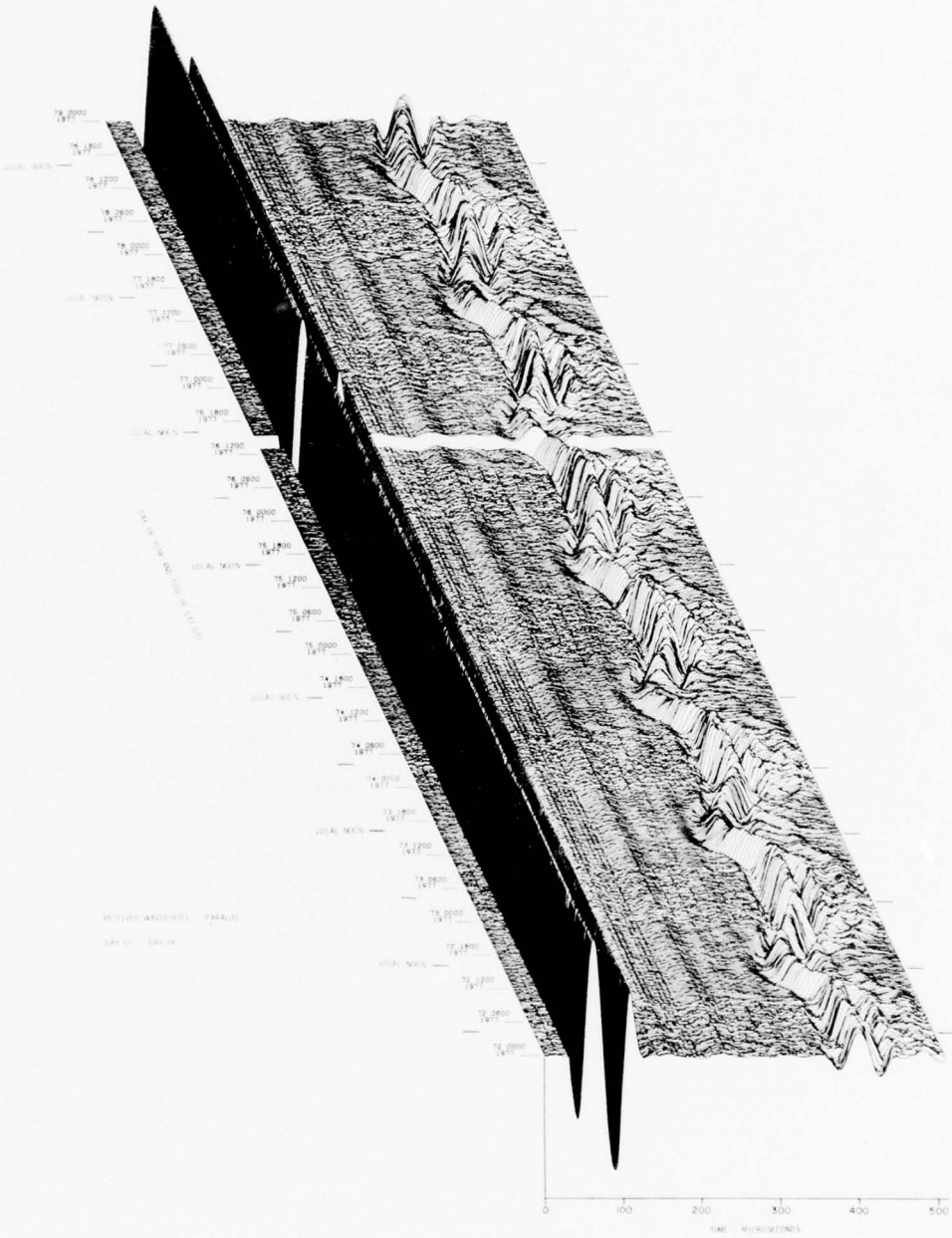

Figure 13. VLF/LF Reflectivity Data for the Polar Ionosphere, DAY 72 (13 Mar) – DAY 78 (19 Mar) 1977 (Cont). Part R, ||Waveform Display

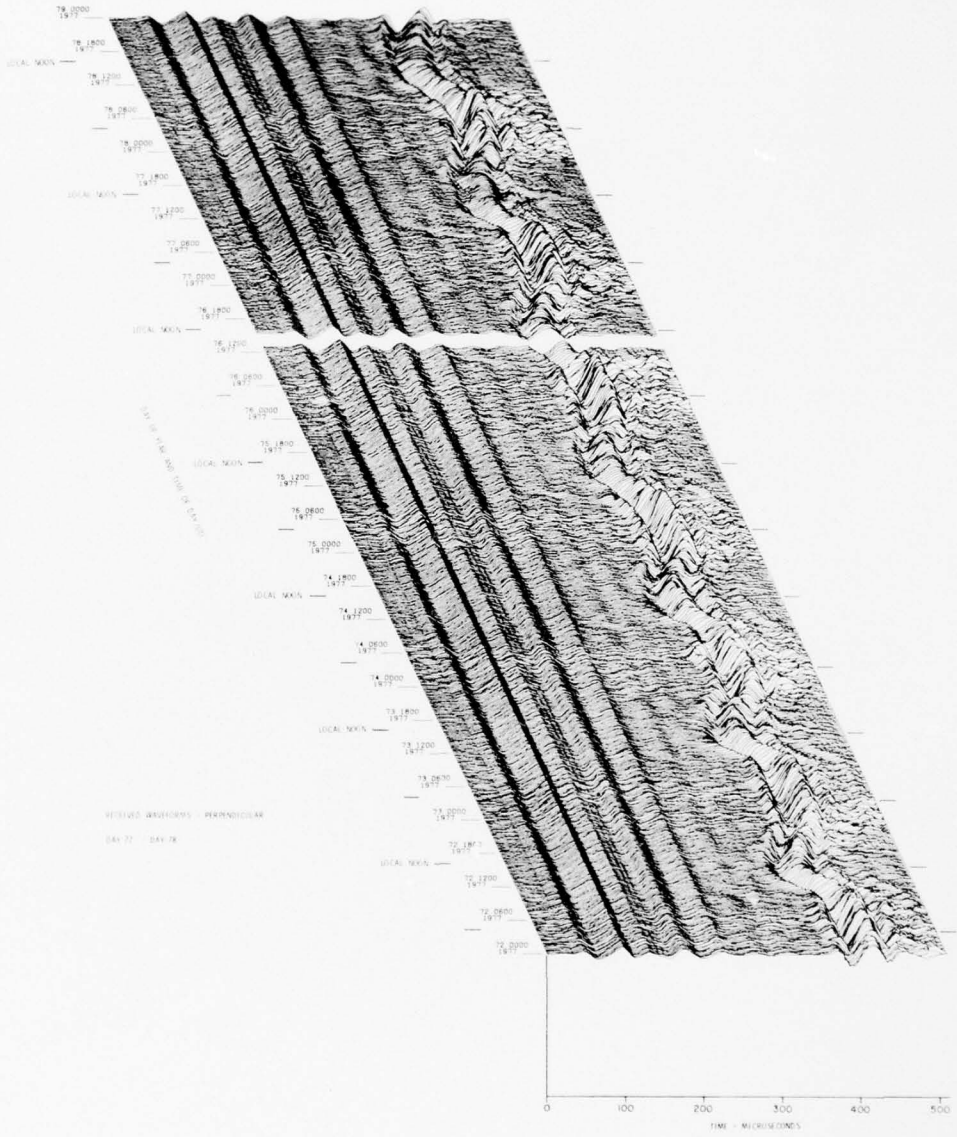

Figure 13. VLF/LF Reflectivity Data for the Polar Ionosphere, DAY 72 (13 Mar) – DAY 78 (19 Mar) 1977 (Cont). Part S, ⊥Waveform Display

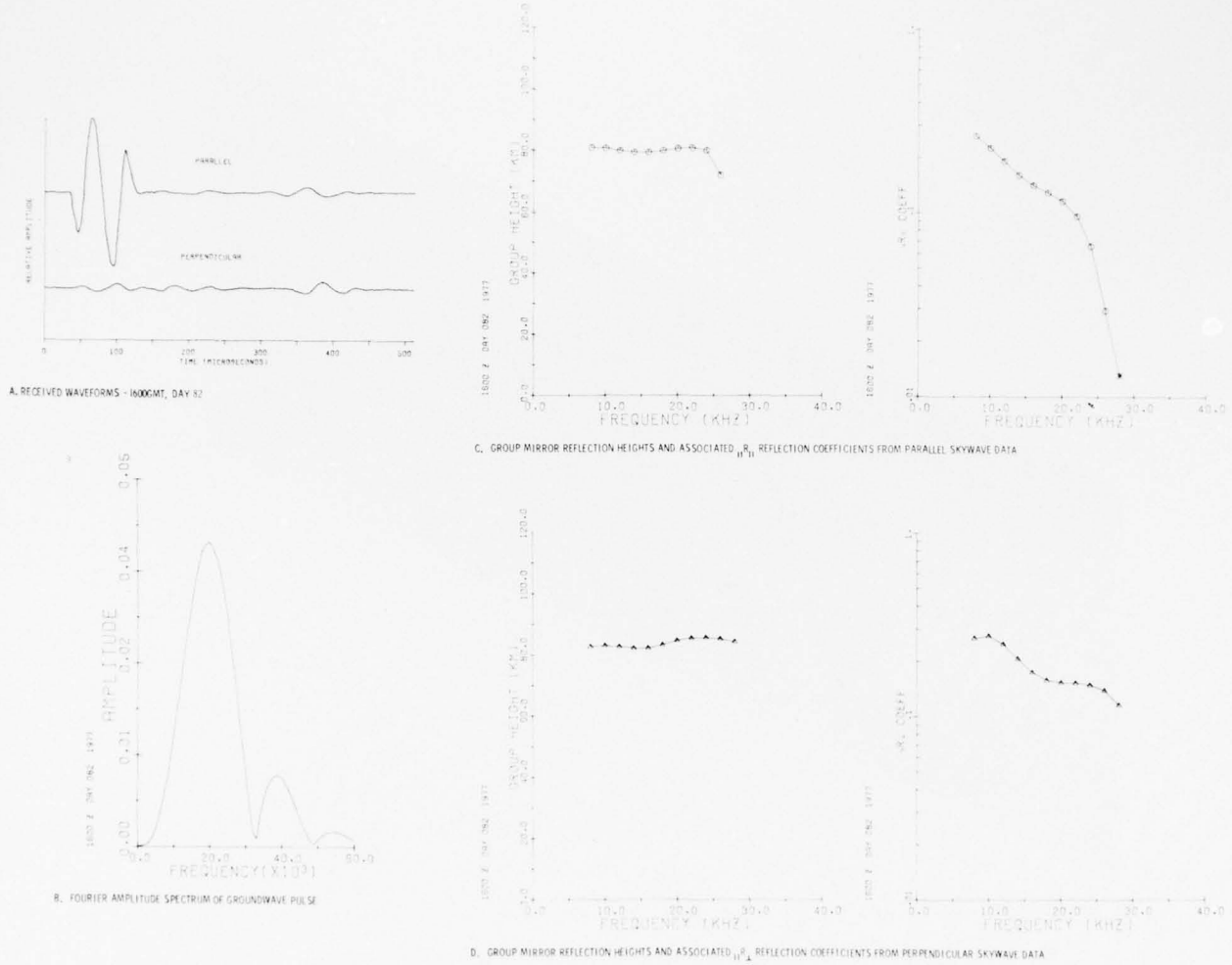

Figure 14. VLF/LF Reflectivity Data for the Polar Ionosphere, DAY 79 (20 Mar) – DAY 85 (26 Mar) 1977

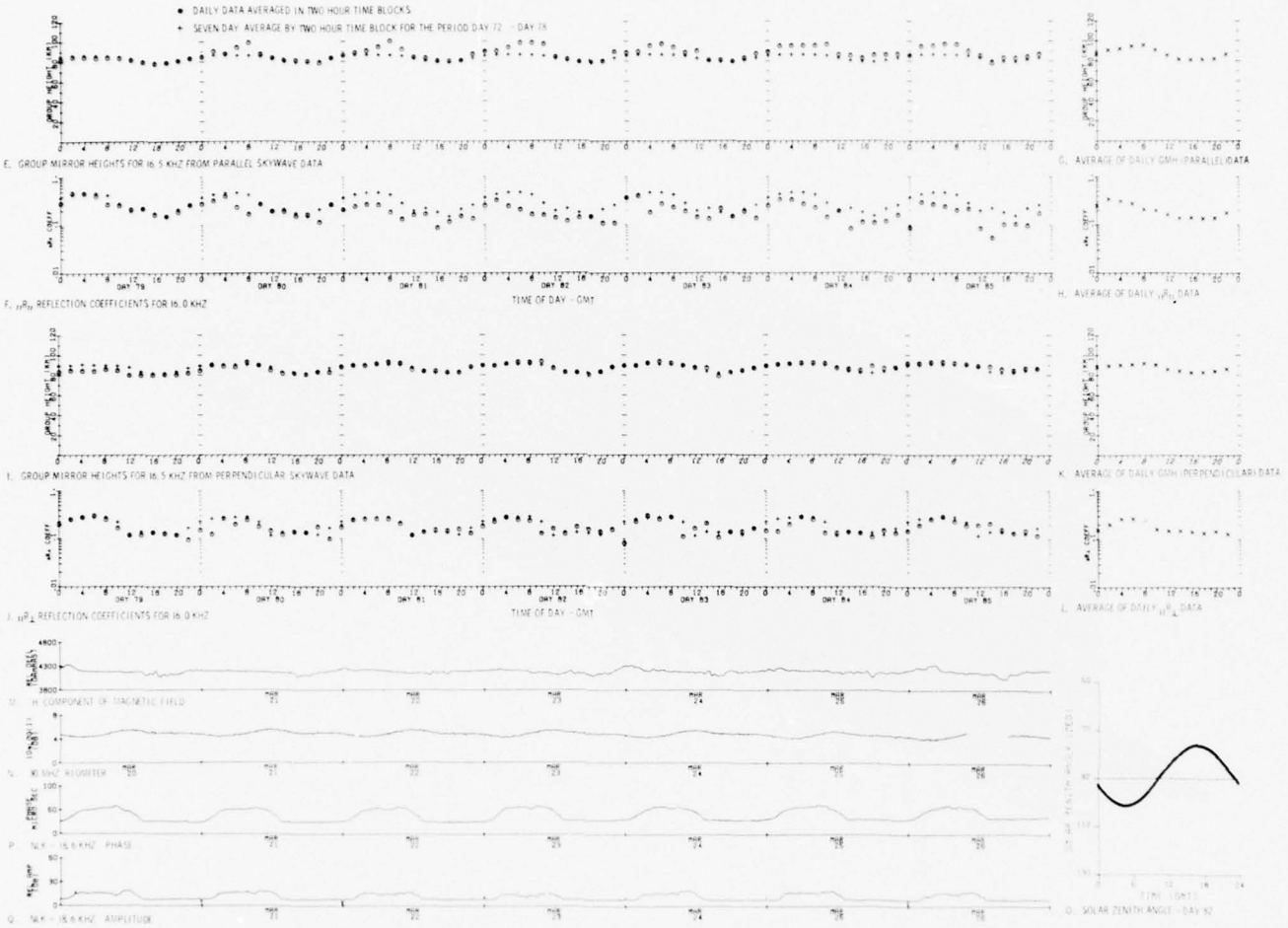

Figure 14. VLF/LF Reflectivity Data for the Polar Ionosphere, DAY 79 (20 Mar) – DAY 85 (26 Mar) 1977 (Cont)

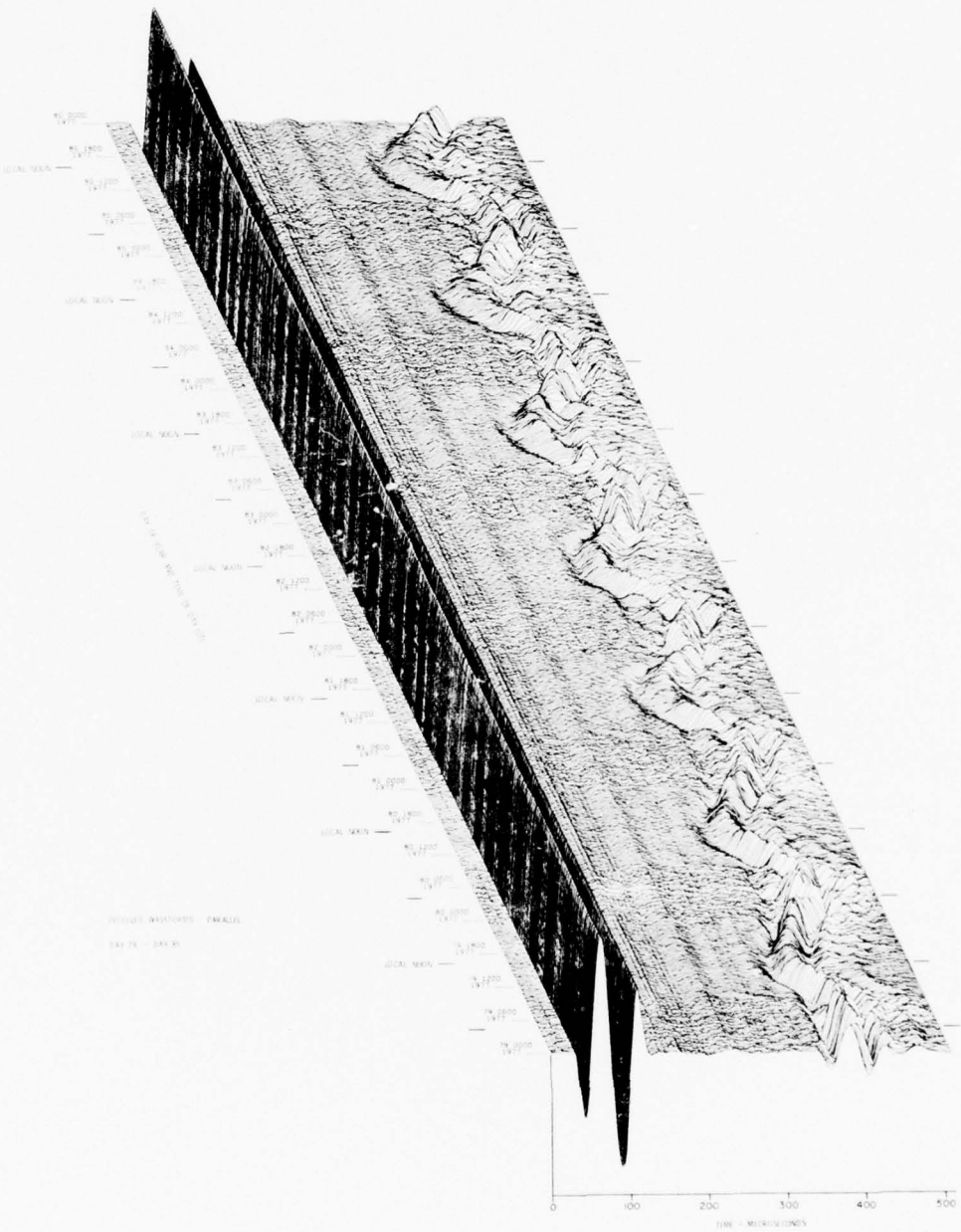

Figure 14. VLF/LF Reflectivity Data for the Polar Ionosphere, DAY 79 (20 Mar) – DAY 85 (26 Mar) 1977 (Cont). Part R, ||Waveform Display

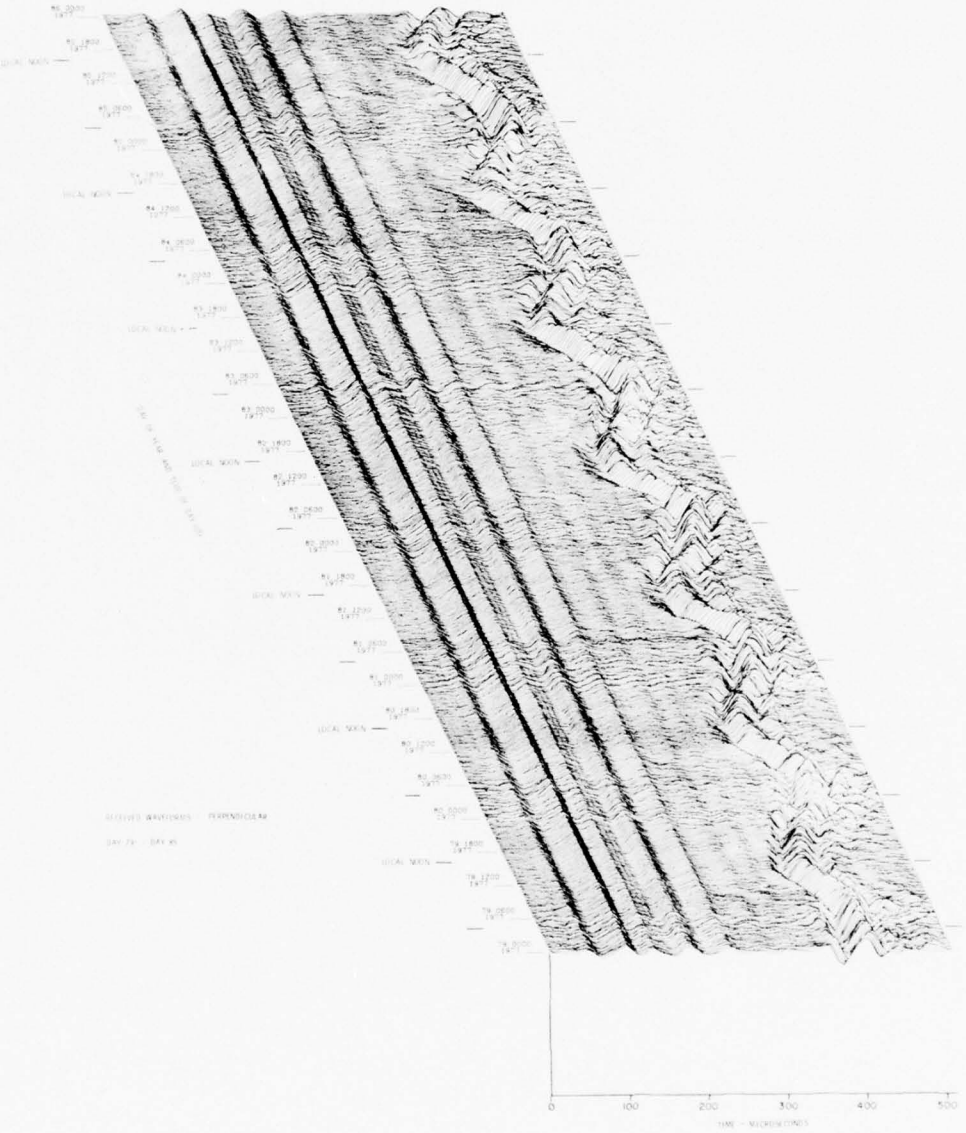

Figure 14. VLF/LF Reflectivity Data for the Polar Ionosphere, DAY 79 (20 Mar) – DAY 85 (26 Mar) 1977 (Cont). Part S, ⊥Waveform Display

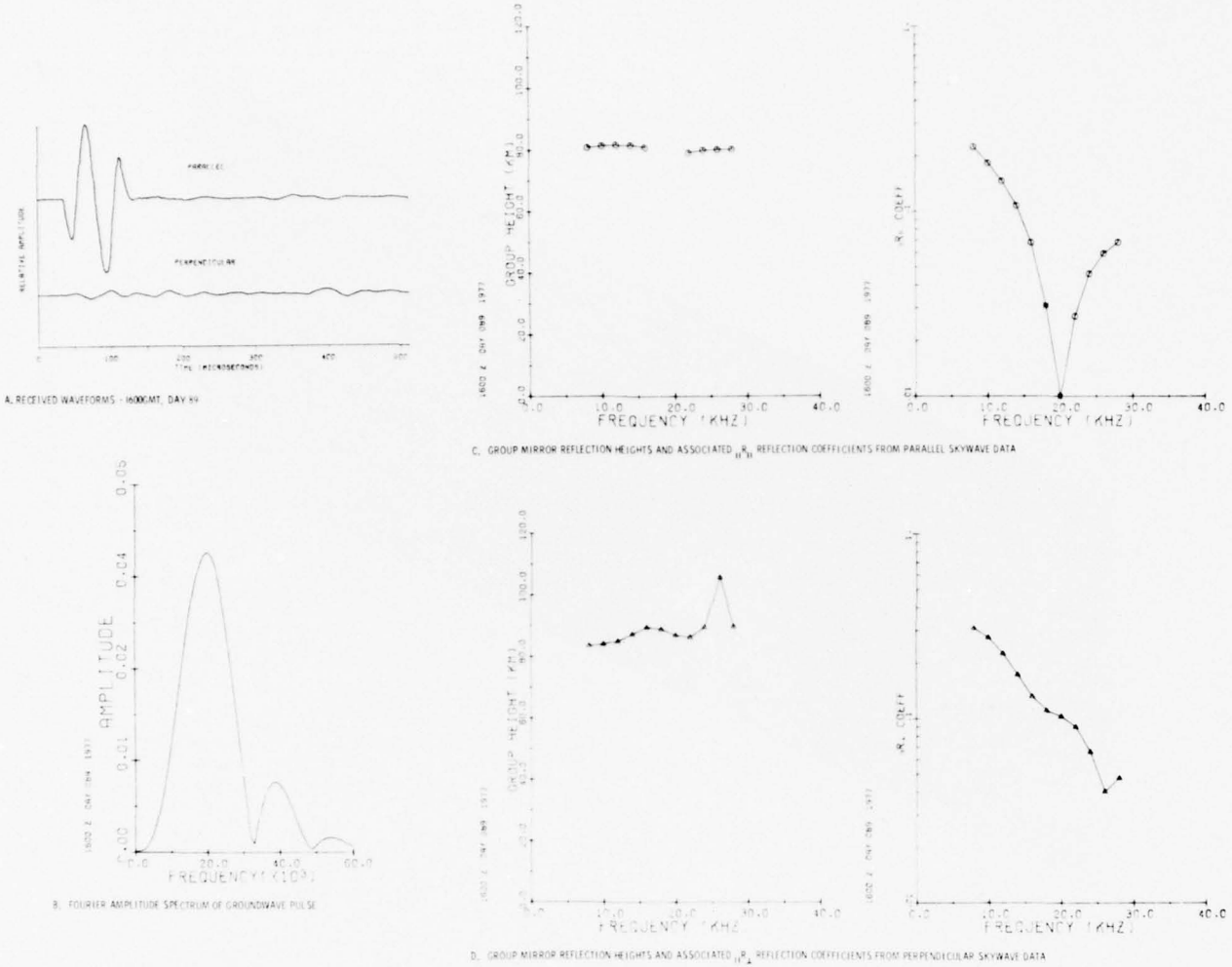

Figure 15. VLF/LF Reflectivity Data for the Polar Ionosphere, DAY 86 (27 Mar) – DAY 92 (2 Apr) 1977

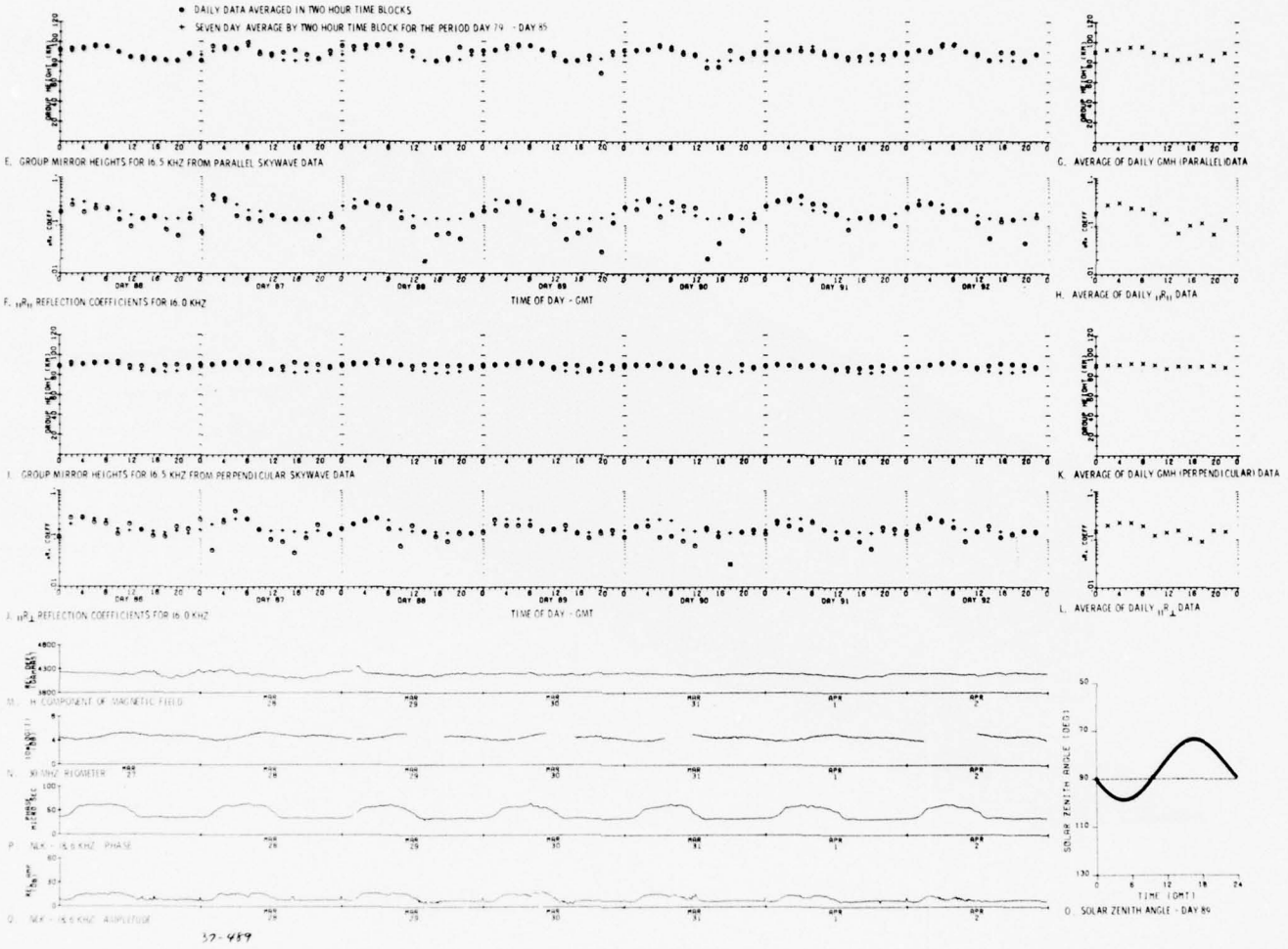

Figure 15. VLF/LF Reflectivity Data for the Polar Ionosphere, DAY 86 (27 Mar) – DAY 92 (2 Apr) 1977 (Cont)

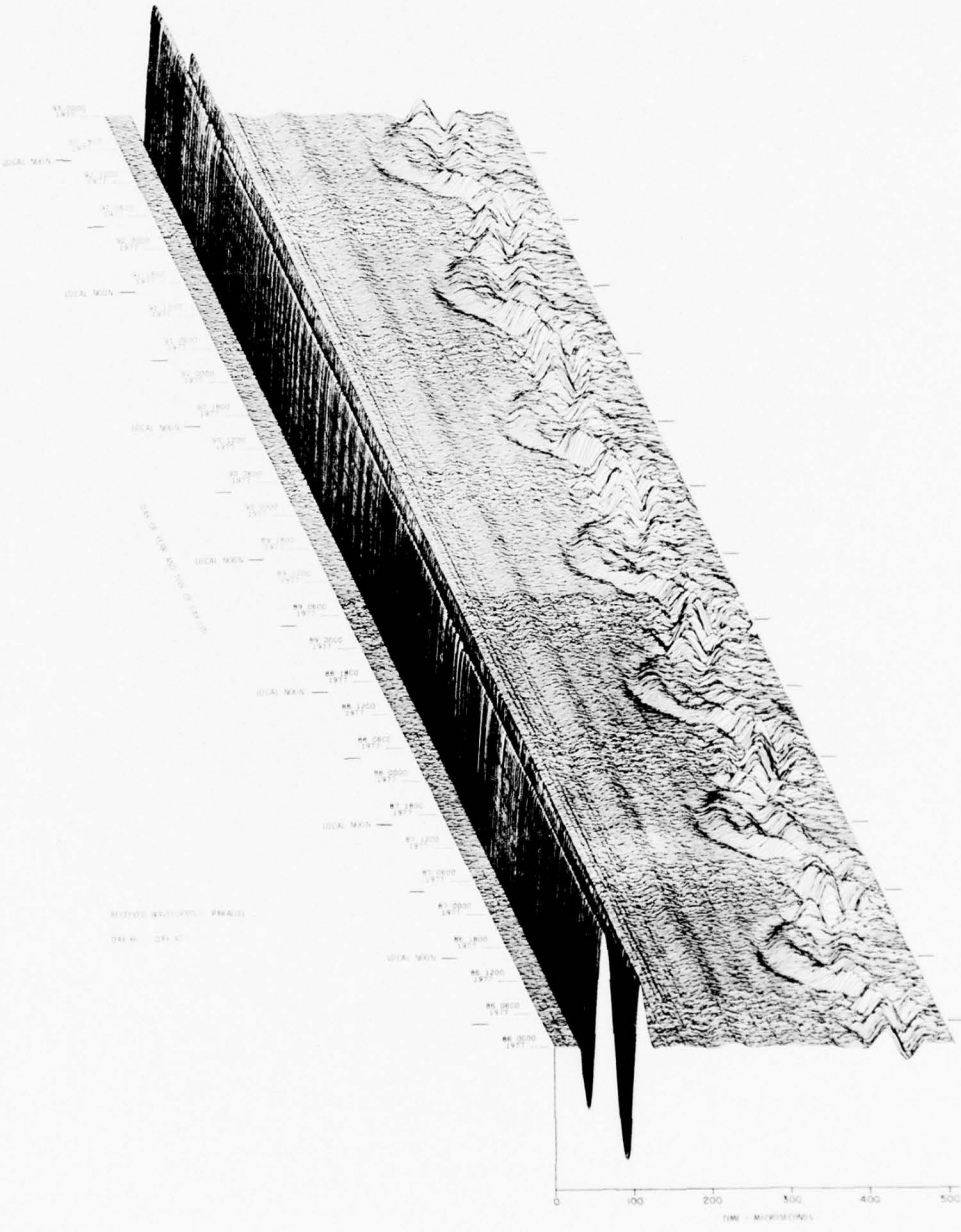

Figure 15. VLF/LF Reflectivity Data for the Polar Ionosphere, DAY 86 (27 Mar) – DAY 92 (2 Apr) 1977 (Cont). Part R, || Waveform Display

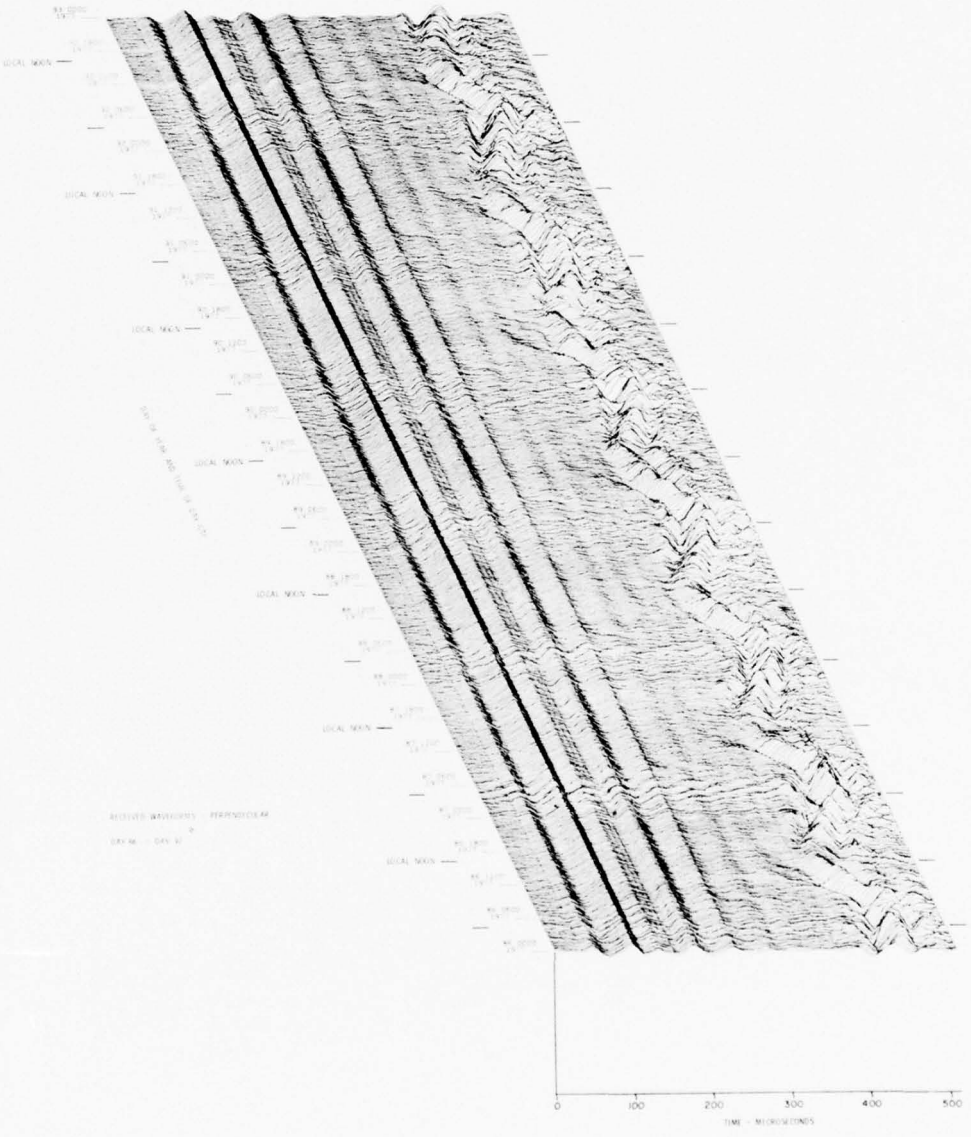

Figure 15. VLF/LF Reflectivity Data for the Polar Ionosphere, DAY 86 (27 Mar) – DAY 92 (2 Apr) 1977 (Cont). Part S, ⊥Waveform Display

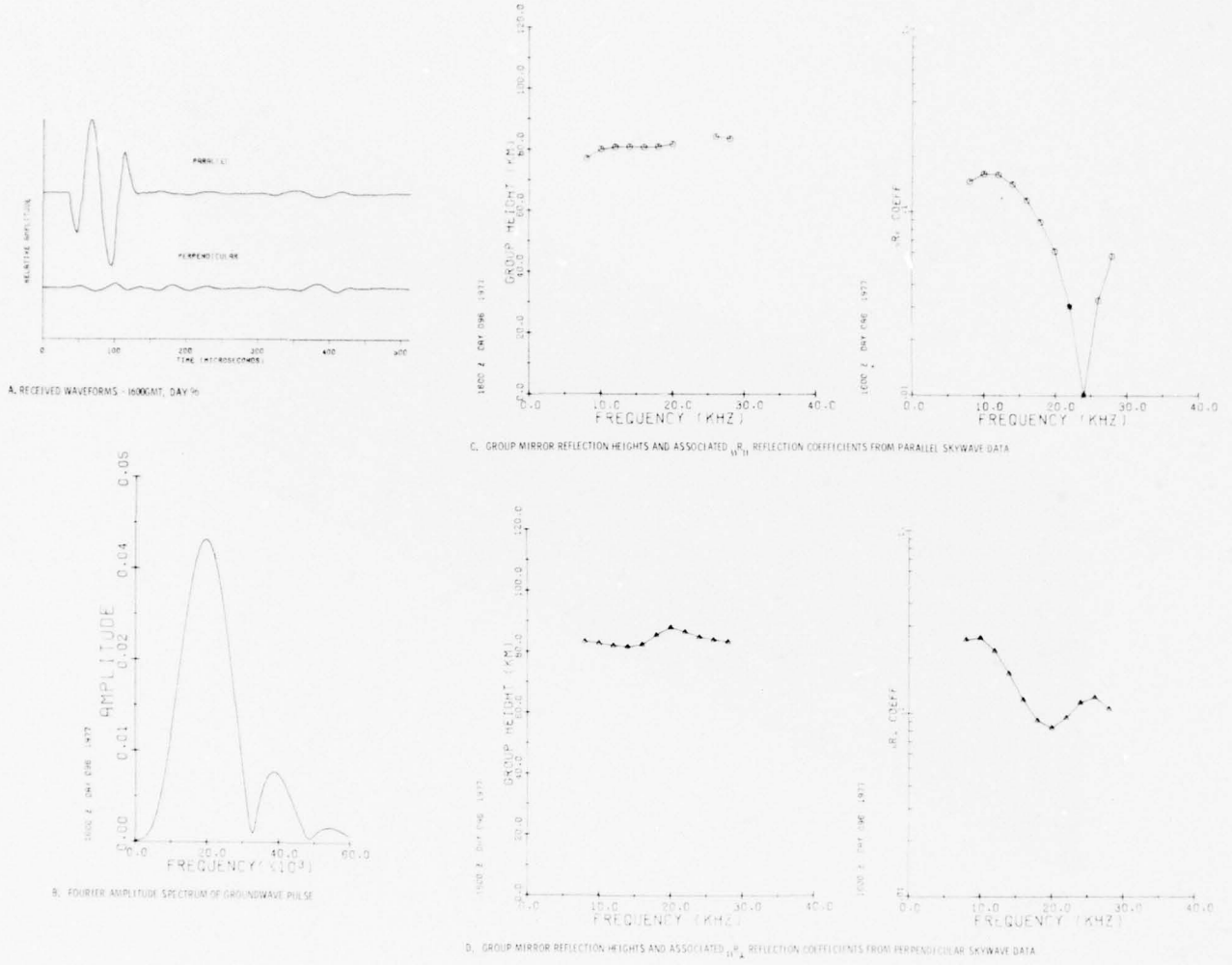

Figure 16. VLF/LF Reflectivity Data for the Polar Ionosphere, DAY 93 (3 Apr) – DAY 99 (9 Apr) 1977

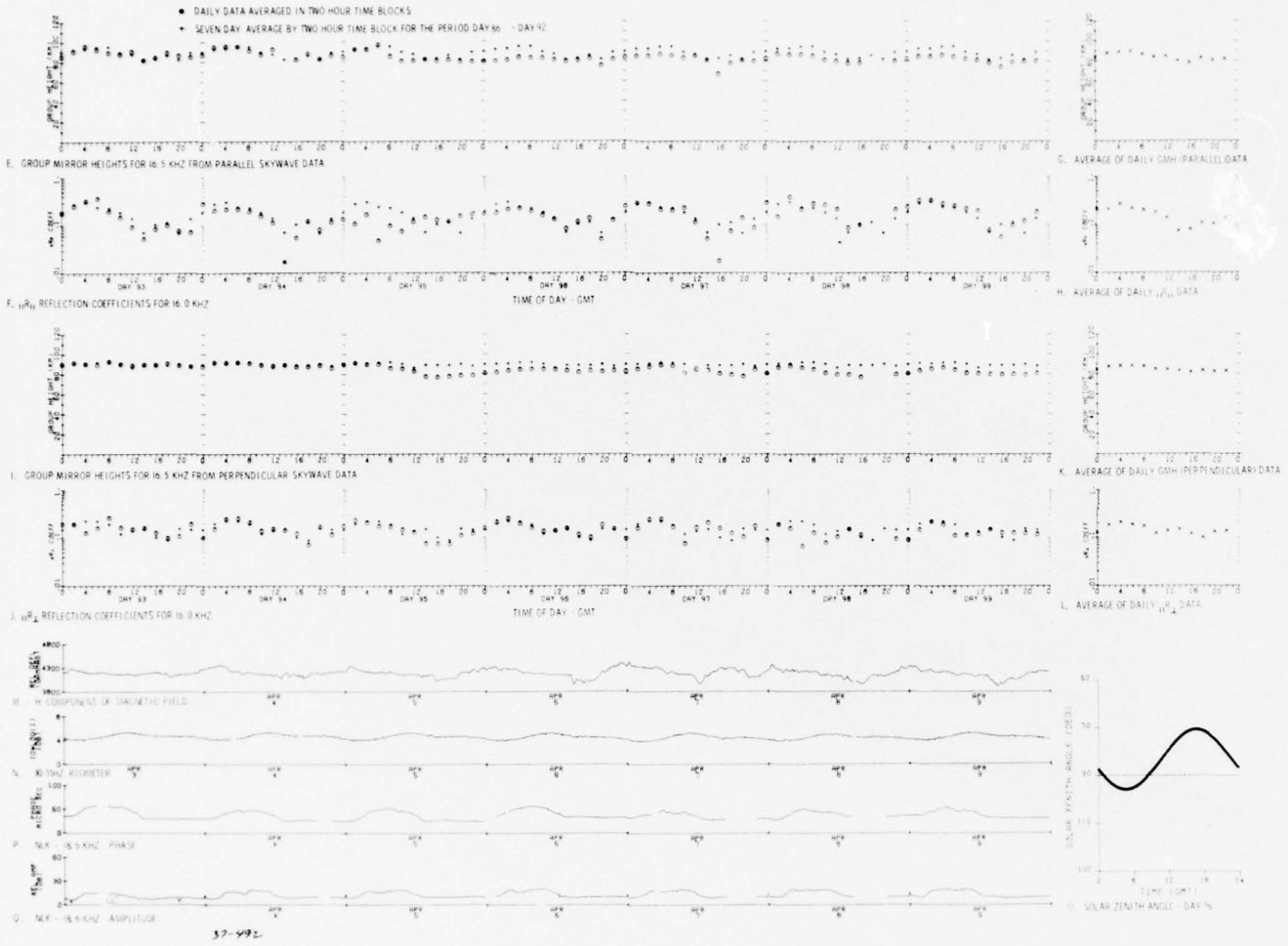

Figure 16. VLF/LF Reflectivity Data for the Polar Ionosphere, DAY 93 (3 Apr) – DAY 99 (9 Apr) 1977 (Cont)

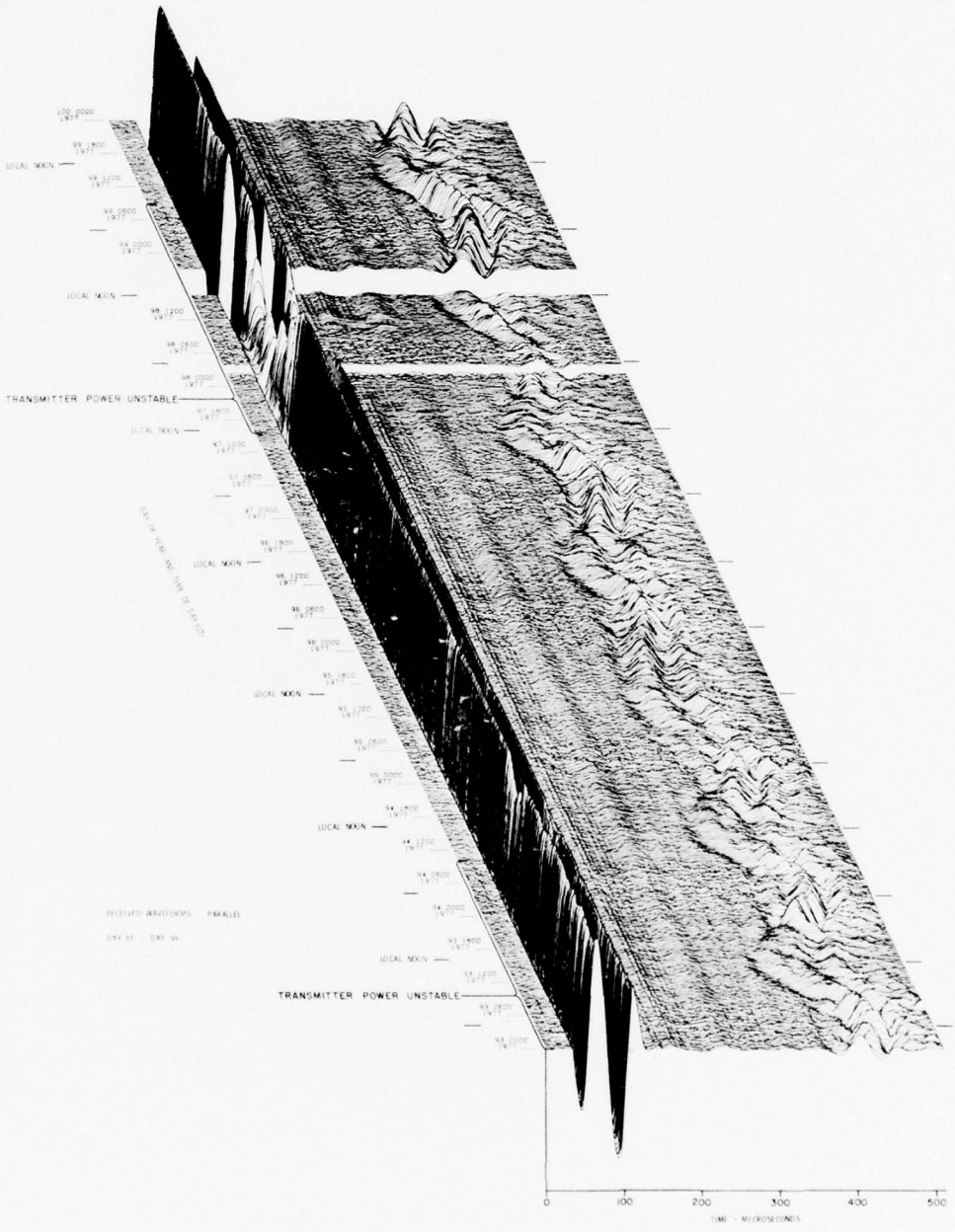

Figure 16. VLF/LF Reflectivity Data for the Polar Ionosphere, DAY 93 (3 Apr) — DAY 99 (9 Apr) 1977 (Cont). Part R, || Waveform Display

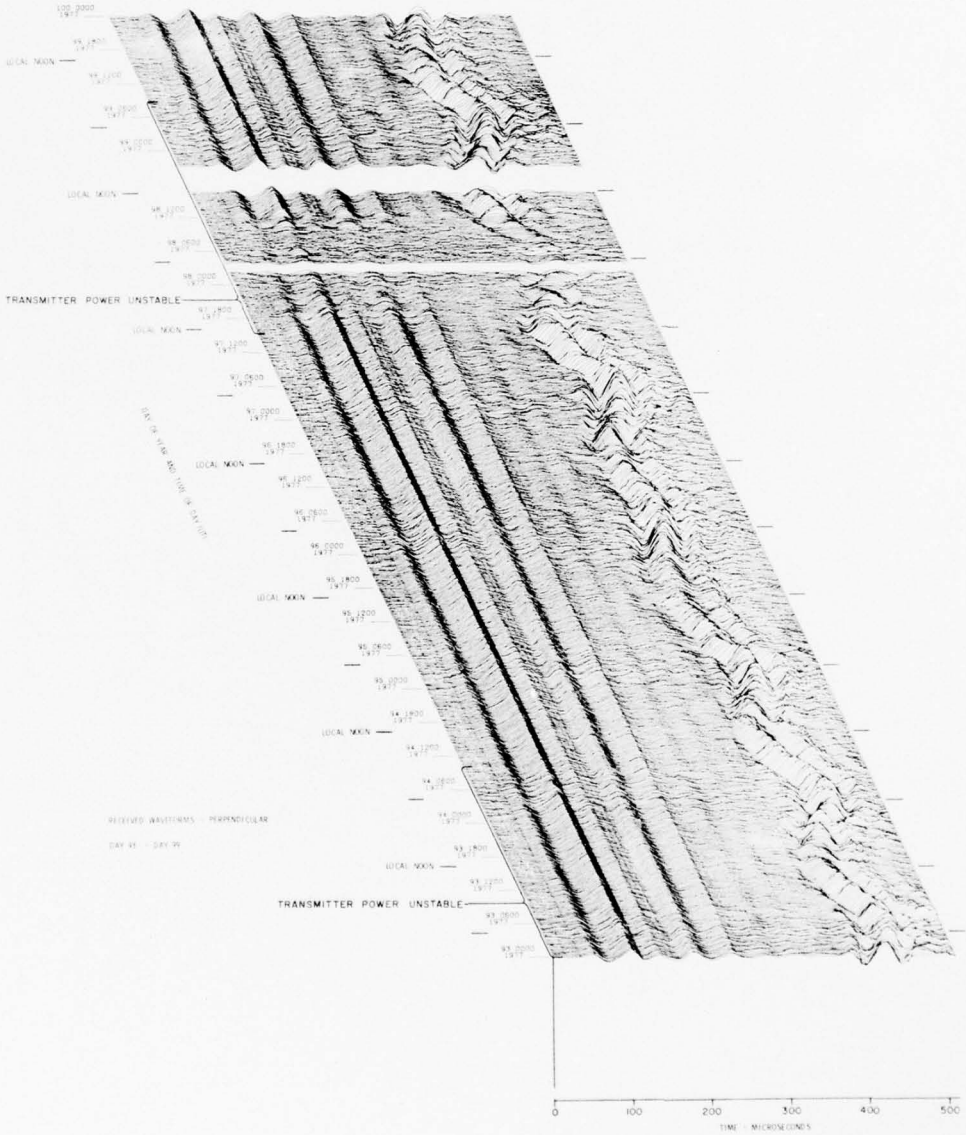

Figure 16. VLF/LF Reflectivity Data for the Polar Ionosphere, DAY 93 (3 Apr) — DAY 99 (9 Apr) 1977 (Cont). Part S, ⊥Waveform Display

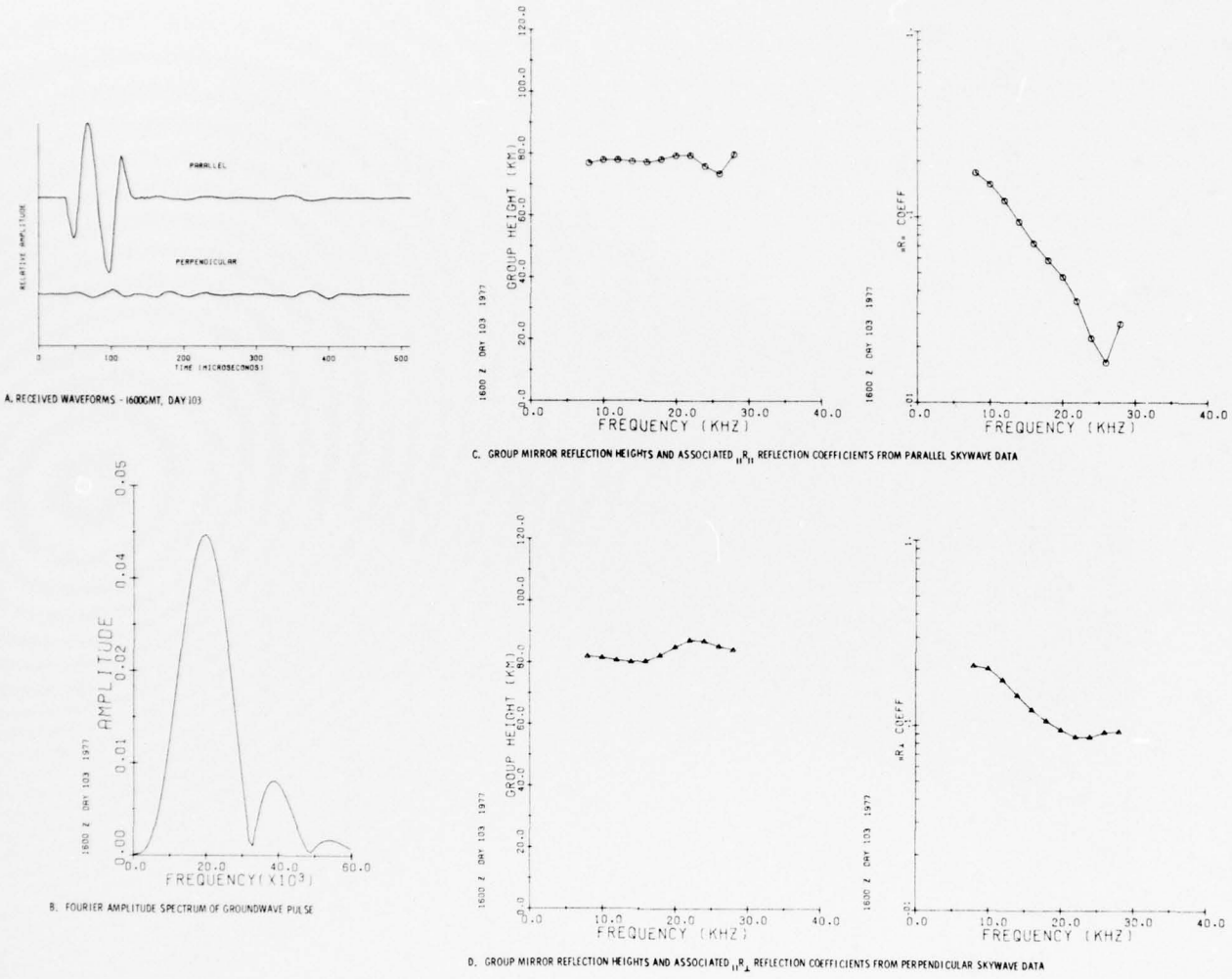

Figure 17. VLF/LF Reflectivity Data for the Polar Ionosphere, DAY 100 (10 Apr) — DAY 106 (16 Apr) 1977

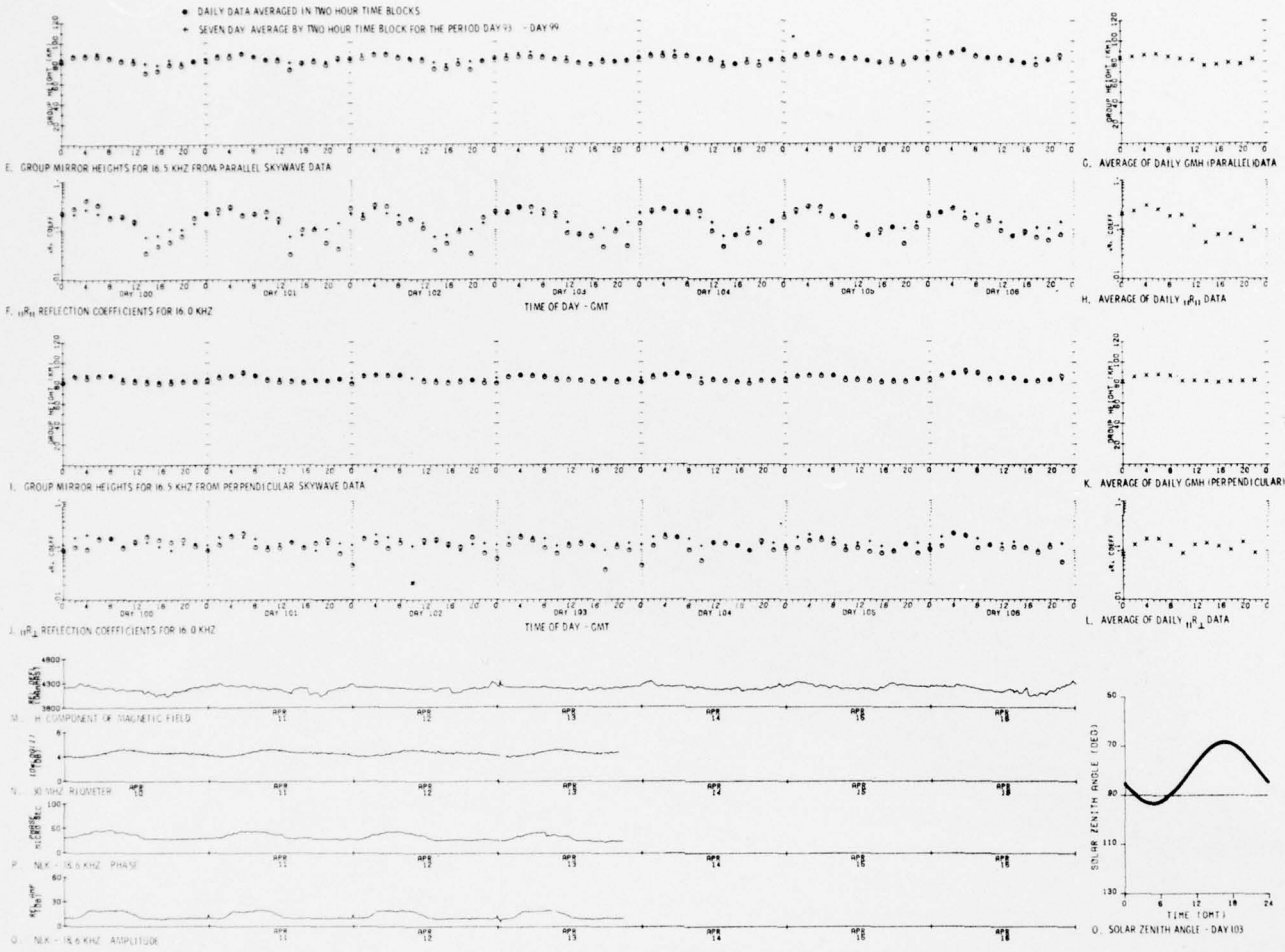

Figure 17. VLF/LF Reflectivity Data for the Polar Ionosphere, DAY 100 (10 Apr) – DAY 106 (16 Apr) 1977 (Cont)

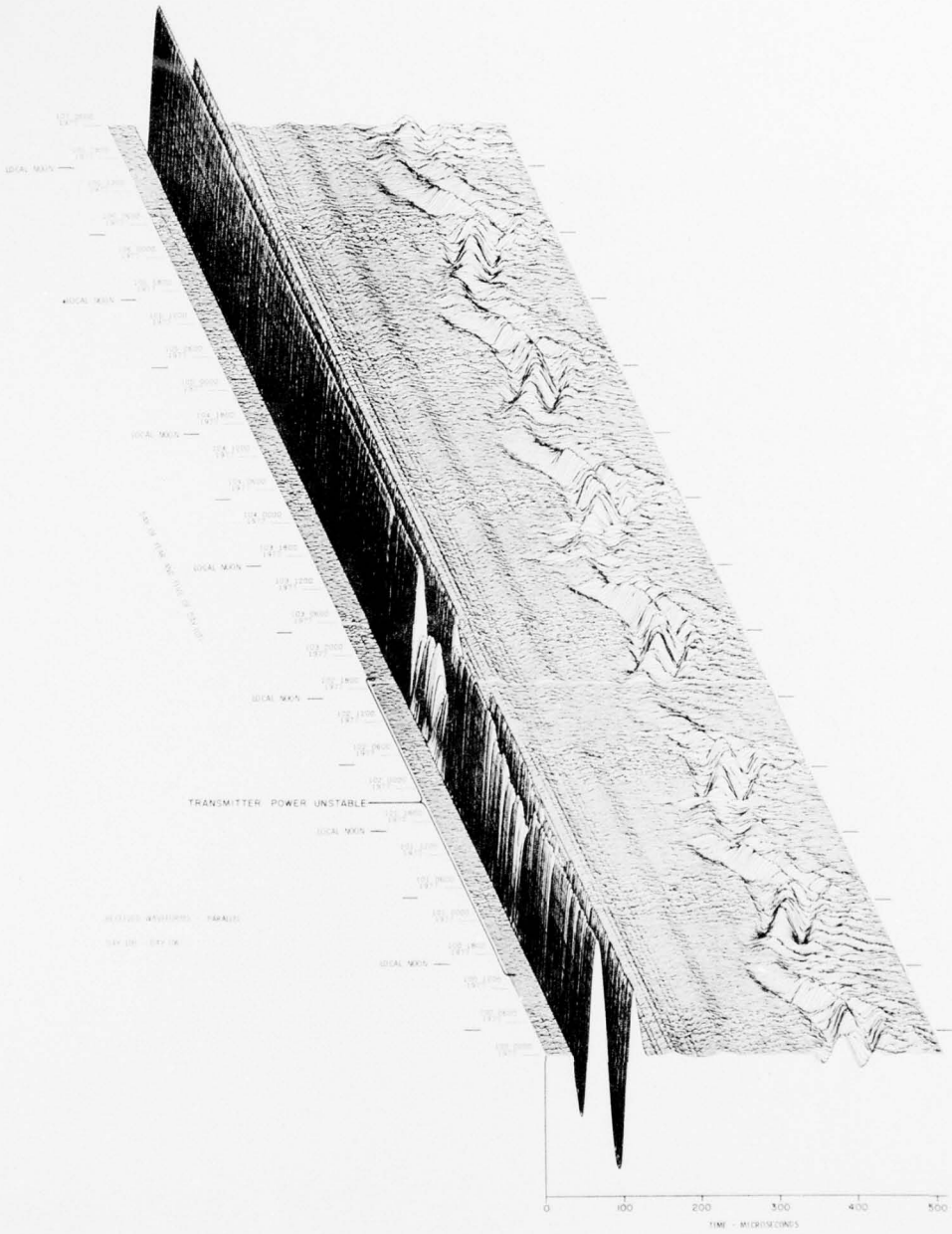

Figure 17. VLF/LF Reflectivity Data for the Polar Ionosphere, DAY 100 (10 Apr) – DAY 106 (16 Apr) 1977 (Cont). Part R, ||Waveform Display

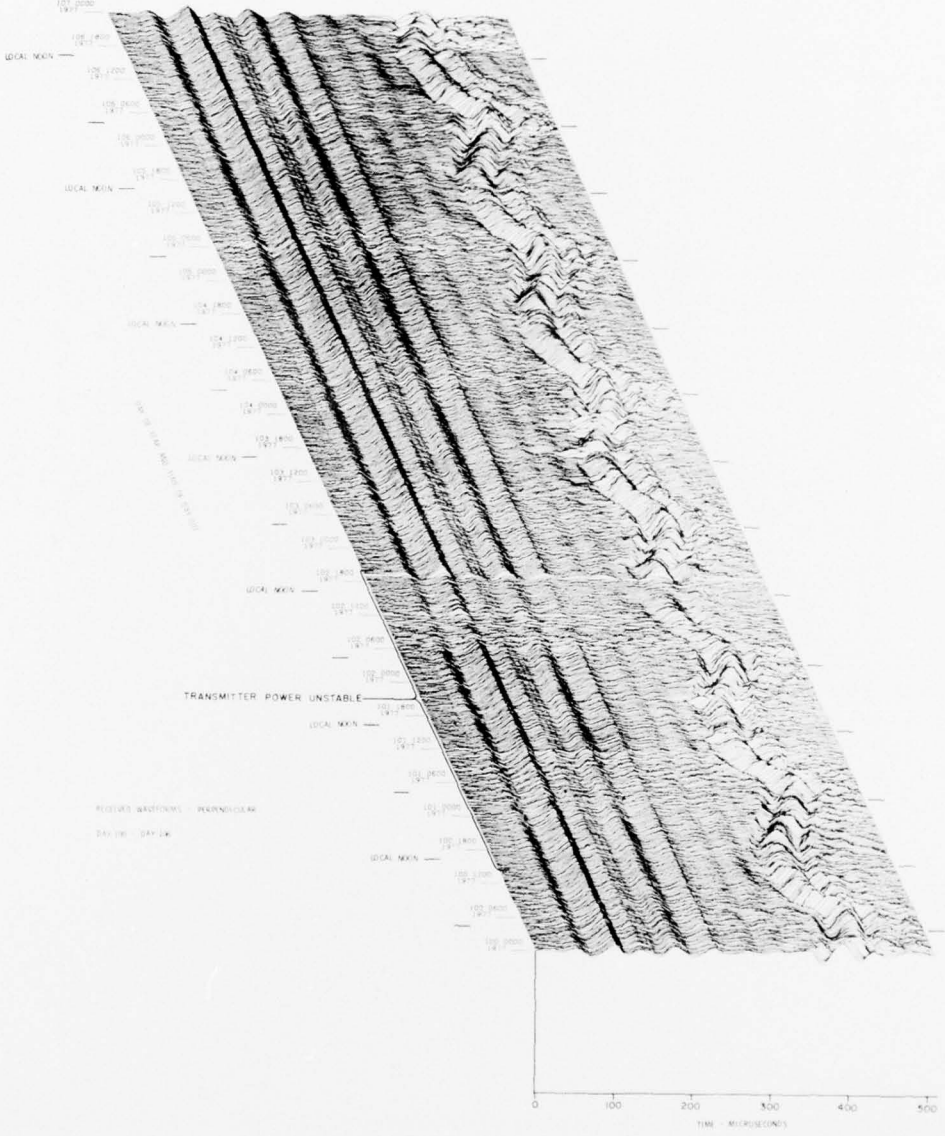

Figure 17. VLF/LF Reflectivity Data for the Polar Ionosphere, DAY 100 (10 Apr) – DAY 106 (16 Apr) 1977 (Cont). Part S, ⊥Waveform Display

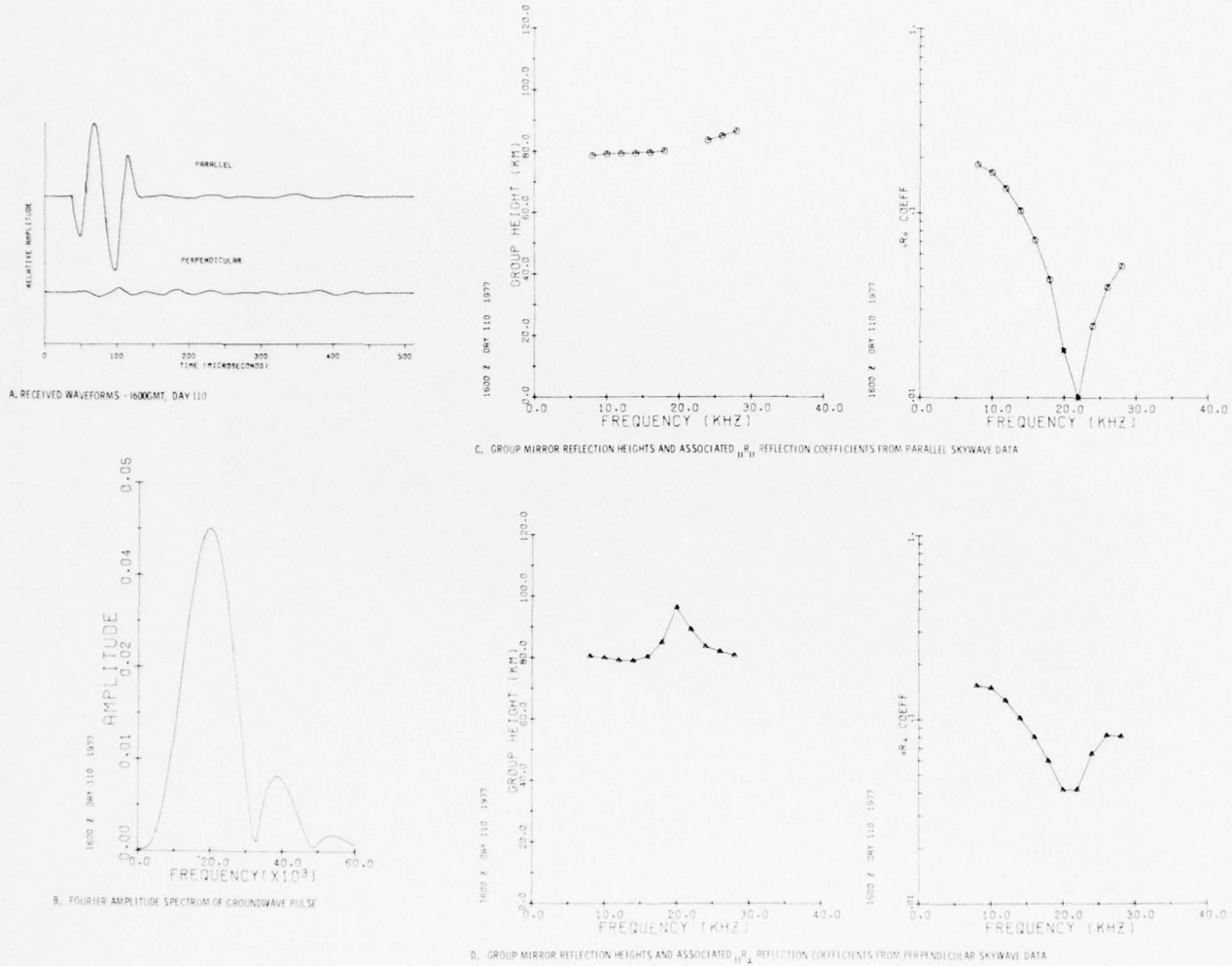

Figure 18. VLF/LF Reflectivity Data for the Polar Ionosphere, DAY 107 (17 Apr) – DAY 113 (23 Apr) 1977

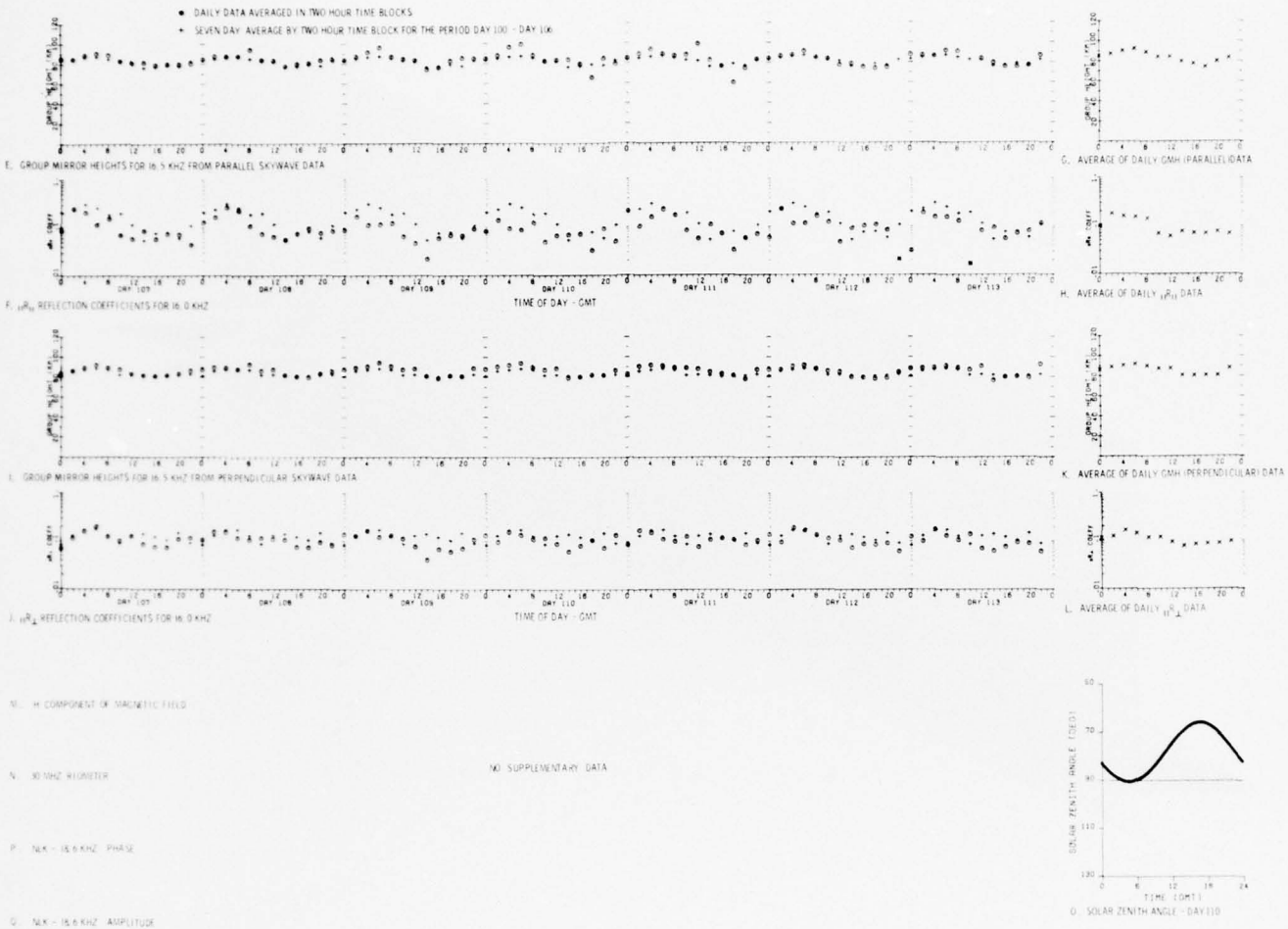

Figure 18. VLF/LF Reflectivity Data for the Polar Ionosphere, DAY 107 (17 Apr) – DAY 113 (23 Apr) 1977 (Cont)

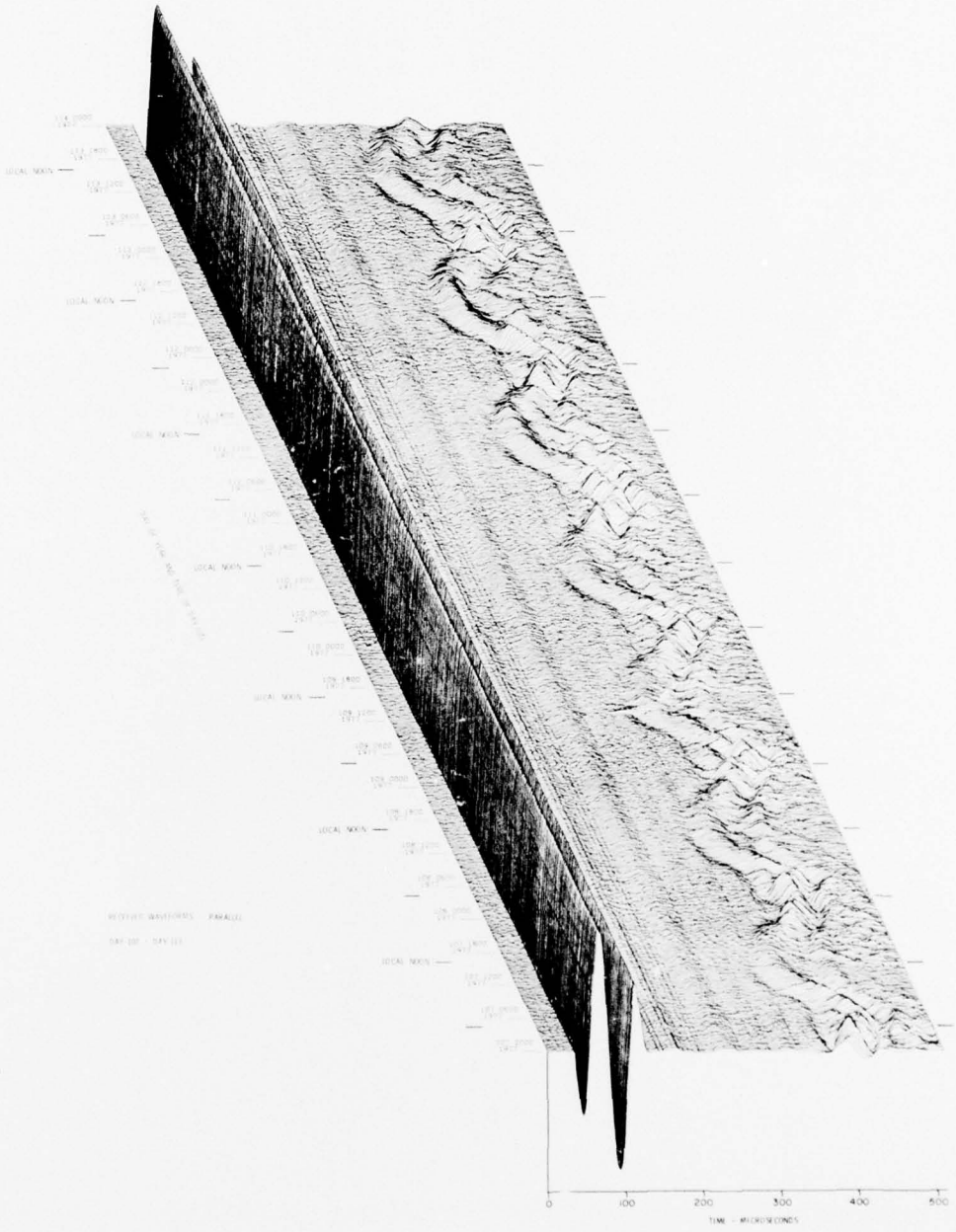

Figure 18. VLF/LF Reflectivity Data for the Polar Ionosphere, DAY 107 (17 Apr) — DAY 113 (23 Apr) 1977 (Cont). Part R, ∥ Waveform Display

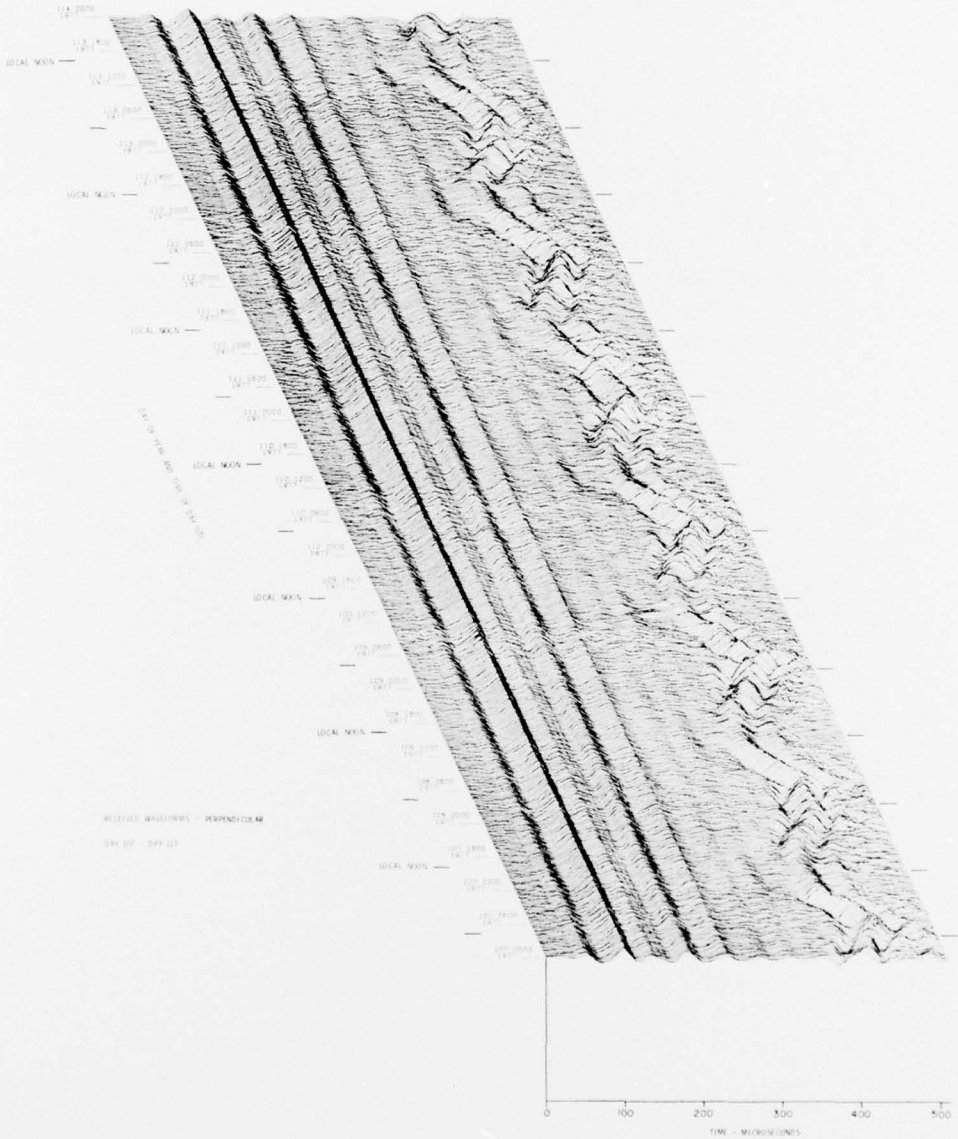

Figure 18. VLF/LF Reflectivity Data for the Polar Ionosphere, DAY 107 (17 Apr) – DAY 113 (23 Apr) 1977 (Cont). Part S, ⊥ Waveform Display

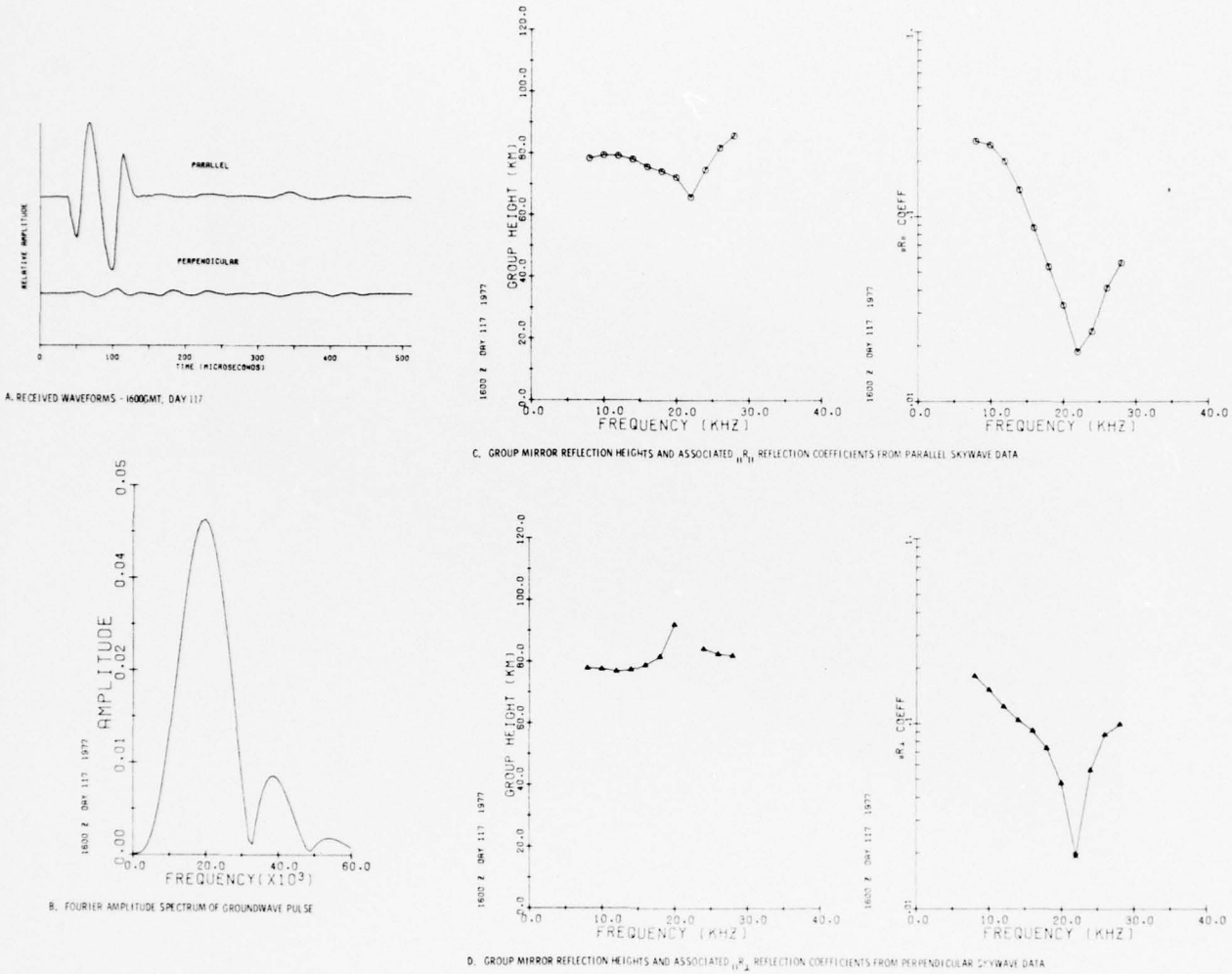

Figure 19. VLF/LF Reflectivity Data for the Polar Ionosphere, DAY 114 (24 Apr) – DAY 120 (30 Apr) 1977

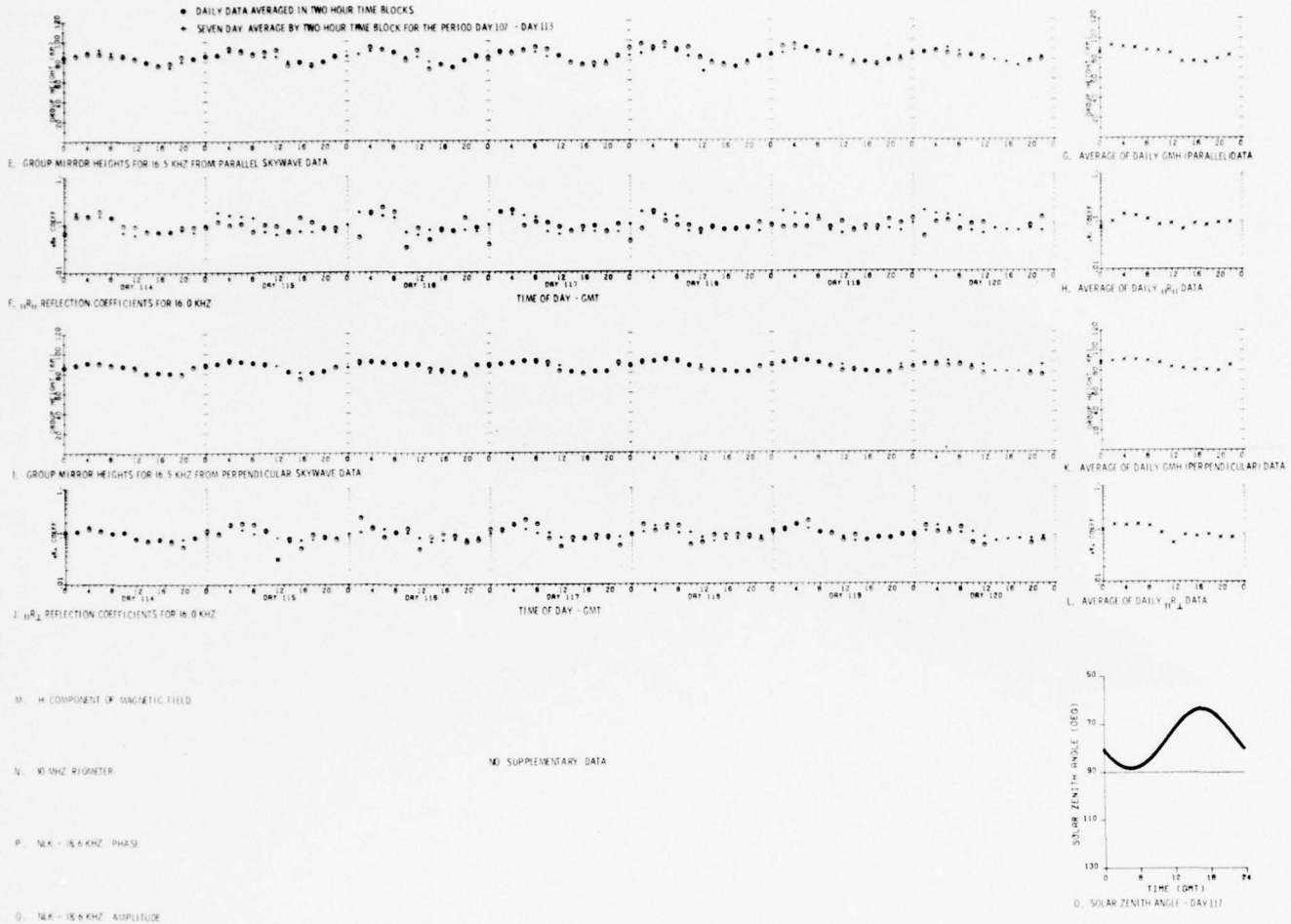

Figure 19. VLF/LF Reflectivity Data for the Polar Ionosphere, DAY 114 (24 Apr) – DAY 120 (30 Apr) 1977 (Cont)

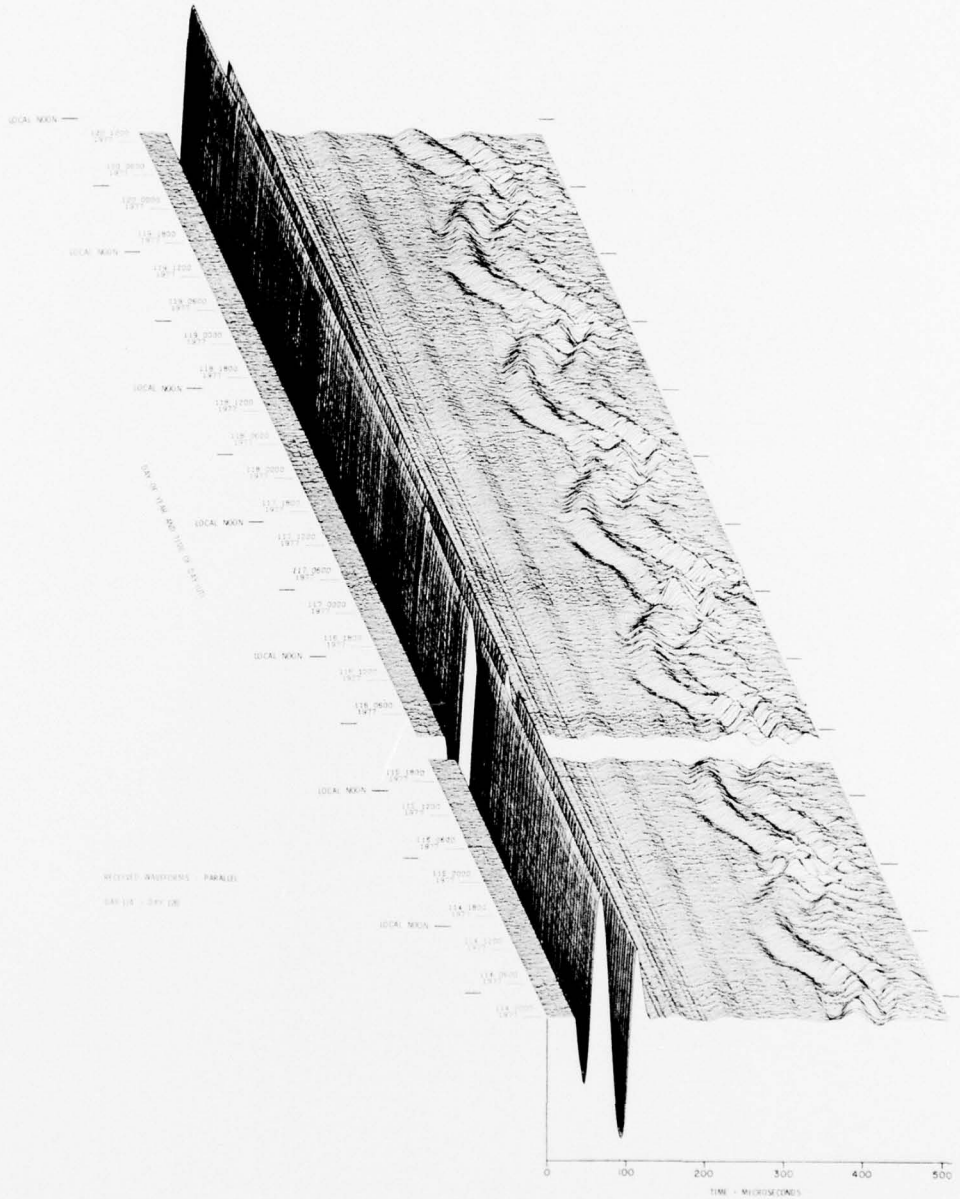

Figure 19. VLF/LF Reflectivity Data for the Polar Ionosphere, DAY 114 (24 Apr) — DAY 120 (30 Apr) 1977 (Cont). Part R, || Waveform Display

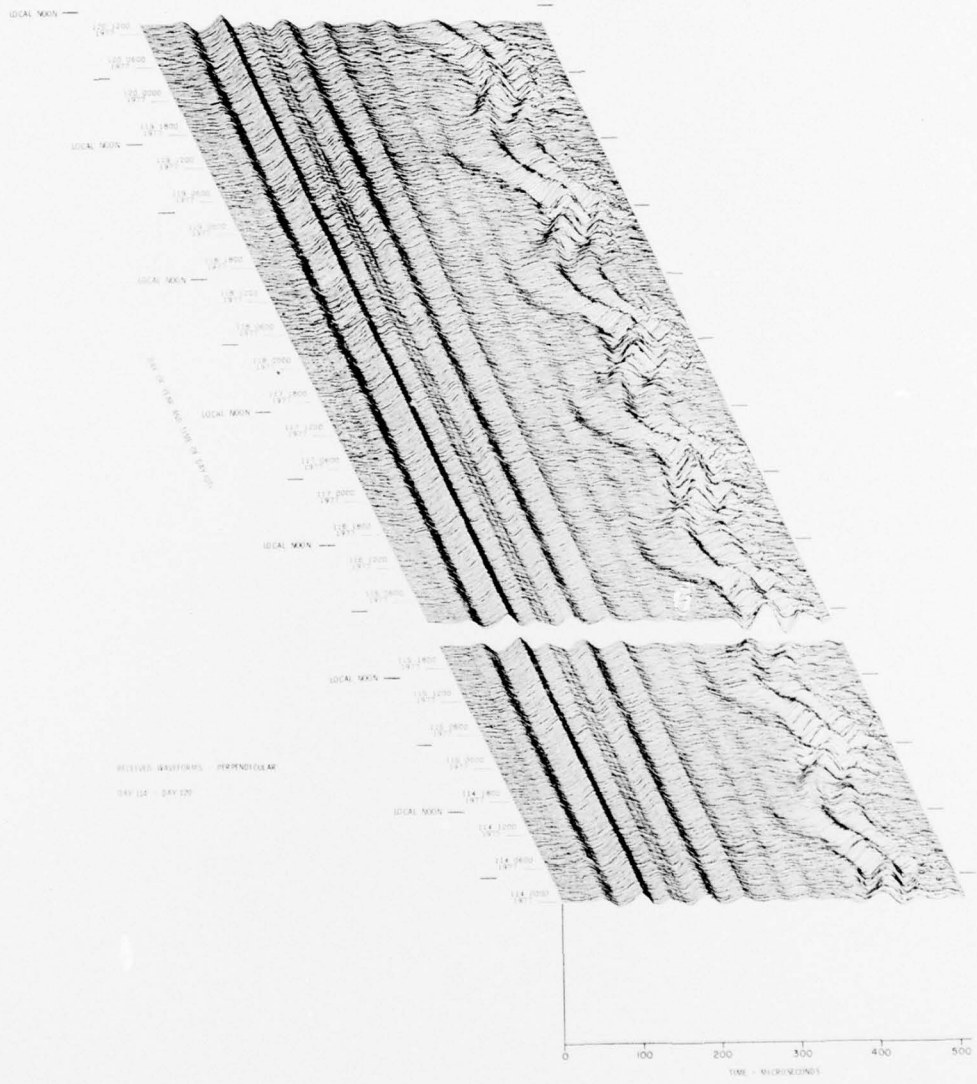

Figure 19. VLF/LF Reflectivity Data for the Polar Ionosphere, DAY 114 (24 Apr) – DAY 120 (30 Apr) 1977 (Cont). Part S, ⊥ Waveform Display

References

1. Lewis, E.A., Rasmussen, J.E., and Kossey, P.A. (1973) Measurements of ionospheric reflectivity from 6 to 35 kHz, J. Geophys. Res. 78:19.

2. Kossey, P.A., Rasmussen, J.E., and Lewis, E.A. (1974) VLF pulse ionosounder measurements of the reflection properties of the lower ionosphere, Akademie Verlaq, COSPAR, July.

3. Wait, J.R., and Howe, H.H. (1956) Amplitude and Phase Curves for Ground-Wave Propagation in the Band 200 Cycles per Second to 500 Kilocycles, Nat. Bur. Stand. U.S. Circ. No. 574.

4. Budden, K.G. (1961) Radio Waves in the Ionosphere, p. 85, Cambridge University Press, London.

5. Rasmussen, J.E., McLain, R.J., Capt, USAF, and Turtle, J.P. (1976) VLF/LF Reflectivity of the Polar Ionosphere, 19 January – 2 March 1975, AFCRL-TR-76-0045.

6. Rasmussen, J.E., McLain, R.J., Capt, USAF, and Turtle, J.P. (1976) VLF/LF Reflectivity of the Polar Ionosphere, 2 March – 3 May 1975, RADC-TR-76-146.

7. Rasmussen, J.E., McLain, R.J., Capt, USAF, Turtle, J.P., and Klemetti, W.I. (1976) VLF/LF Reflectivity of the Polar Ionosphere, 4 May – 5 July 1975, RADC-TR-76-270.

8. Rasmussen, J.E., McLain, R.J., Capt, USAF, Turtle, J.P., and Klemetti, W.I. (1976) VLF/LF Reflectivity of the Polar Ionosphere, 20 July – 20 September 1975, RADC-TR-76-327.

9. Rasmussen, J.E., McLain, R.J., Capt, USAF, Turtle, J.P., and Klemetti, W.I. (1976) VLF/LF Reflectivity of the Polar Ionosphere, 21 September 1975 – 3 January 1976, RADC-TR-76-378.

10. Rasmussen, J.E., Turtle, J.P., Pagliarulo, R.P., and Klemetti, W.I. (1977) VLF/LF Reflectivity of the Polar Ionosphere, 4 January – 3 July 1976, RADC-TR-77-68.

11. Rasmussen, J.E., Turtle, J.P., Pagliarulo, R.P., and Klemetti, W.I. (1977) VLF/LF Reflectivity of the Polar Ionosphere, 1 August 1976 – 1 January 1977, RADC-TR-77-141.

METRIC SYSTEM

BASE UNITS:

Quantity	Unit	SI Symbol	Formula
length	metre	m	..
mass	kilogram	kg	..
time	second	s	..
electric current	ampere	A	...
thermodynamic temperature	kelvin	K	...
amount of substance	mole	mol	...
luminous intensity	candela	cd	...

SUPPLEMENTARY UNITS:

plane angle	radian	rad	...
solid angle	steradian	sr	...

DERIVED UNITS:

Acceleration	metre per second squared	...	m/s
activity (of a radioactive source)	disintegration per second	...	(disintegration)/s
angular acceleration	radian per second squared	...	rad/s
angular velocity	radian per second	...	rad/s
area	square metre	...	m
density	kilogram per cubic metre	...	kg/m
electric capacitance	farad	F	A·s/V
electrical conductance	siemens	S	A/V
electric field strength	volt per metre	...	V/m
electric inductance	henry	H	V·s/A
electric potential difference	volt	V	W/A
electric resistance	ohm		V/A
electromotive force	volt	V	W/A
energy	joule	J	N·m
entropy	joule per kelvin	...	J/K
force	newton	N	kg·m/s
frequency	hertz	Hz	(cycle)/s
illuminance	lux	lx	lm/m
luminance	candela per square metre	...	cd/m
luminous flux	lumen	lm	cd·sr
magnetic field strength	ampere per metre	...	A/m
magnetic flux	weber	Wb	V·s
magnetic flux density	tesla	T	Wb/m
magnetomotive force	ampere	A	...
power	watt	W	J/s
pressure	pascal	Pa	N/m
quantity of electricity	coulomb	C	A·s
quantity of heat	joule	J	N·m
radiant intensity	watt per steradian	...	W/sr
specific heat	joule per kilogram-kelvin	...	J/kg·K
stress	pascal	Pa	N/m
thermal conductivity	watt per metre-kelvin	...	W/m·K
velocity	metre per second	...	m/s
viscosity, dynamic	pascal-second	...	Pa·s
viscosity, kinematic	square metre per second	...	m/s
voltage	volt	V	W/A
volume	cubic metre	...	m
wavenumber	reciprocal metre	...	(wave)/m
work	joule	J	N·m

SI PREFIXES:

Multiplication Factors	Prefix	SI Symbol
1 000 000 000 000 = 10^{12}	tera	T
1 000 000 000 = 10^{9}	giga	G
1 000 000 = 10^{6}	mega	M
1 000 = 10^{3}	kilo	k
100 = 10^{2}	hecto*	h
10 = 10^{1}	deka*	da
0.1 = 10^{-1}	deci*	d
0.01 = 10^{-2}	centi*	c
0.001 = 10^{-3}	milli	m
0.000 001 = 10^{-6}	micro	μ
0.000 000 001 = 10^{-9}	nano	n
0.000 000 000 001 = 10^{-12}	pico	p
0.000 000 000 000 001 = 10^{-15}	femto	f
0.000 000 000 000 000 001 = 10^{-18}	atto	a

* To be avoided where possible.